# Model Risk for Barrier Options When Priced Under Different Lévy Dynamics

by

Chidinma Mbakwe

Thesis presented in partial fulfilment
of the requirements for the degree of
Master of Science
at Stellenbosch University

Supervisor: Dr. Peter Ouwehand

December 2011

# Declaration

I, the undersigned, hereby declare that the work contained in this thesis is my own original work and has not previously, in its entirety or in part, been submitted at any university for a degree.

---------- ----------

Chidinma Mbakwe Date

**Abstract**

Barrier options are options whose payoff depends on whether or not the underlying asset price hits a certain level – the barrier – during the life of the option. Closed–form solutions for the prices of these path–dependent options are available in the Black–Scholes framework. It is well–known, however, that the Black–Scholes model does not price even the so–called vanilla options correctly. There are a number of popular asset price models based on exponential Lévy dynamics which are all able to capture the volatility smile, i.e. reproduce market–observed prices of vanilla options.

This thesis investigates the potential model risk associated with the pricing of barrier options in several exponential Lévy models. First, the Variance Gamma, Normal Inverse Gaussian and CGMY models are calibrated to market–observed vanilla option prices. Barrier option prices are then evaluated in these models using Monte Carlo methods. The prices obtained are then compared to each other, as well as the Black–Scholes prices. It is observed that the different exponential Lévy models yield barrier option prices which are quite close to each other, though quite different from the Black–Scholes prices. This suggests that the associated model risk is low.

# Opsomming

Versperring opsies is opsies met 'n afbetaling wat afhanklik is daarvan of die onderliggende bateprys 'n bepaalde vlak – die versperring – bereik gedurende die lewe van die opsie, of nie. Formules vir die pryse van sulke opsies is beskikbaar binne die Black–Scholes raamwerk. Dit is egter welbekend dat die Black–Scholes model nie in staat is om selfs die sogenaamde vanilla opsies se pryse korrek te bepaal nie. Daar bestaan 'n aantal populêre bateprysmodelle gebaseer op eksponensiële Lévy–dinamika, wat almal in staat is om die mark–waarneembare vanilla opsie pryse te herproduseer.

Hierdie tesis ondersoek die potensiële modelrisiko geassosieer met die prysbepaling van versperring opsies in verskeie eksponeniële Lévy–modelle. Eers word die *Variance Gamma–, Normal Inverse Gaussian–* en *CGMY*–modelle gekalibreer op mark–waarneembare vanilla opsiepryse. Die pryse van versperring opsies in hierdie modelle word dan bepaal deur middel van Monte Carlo metodes. Hierdie pryse word dan met mekaar vergelyk, asook met die Black–Scholespryse. Dit word waargeneem dat die versperring opsiepryse in die verskillende eksponensiële Lévymodelle redelik na aan mekaar is, maar redelik verskil van die Black–Scholespryse. Dit suggereer dat die geassosieerde modelrisiko laag is.

# Dedication

To my parents
(Rev. and Mrs Ben Agbawodikeizu)
and
My Husband
(Mr. Ikenna Mbakwe)

# Acknowledgments

Firstly, I wish to express my profound gratitude to the Most High God who has indeed been and still is, my source of inspiration. He has been my help in ages past and my hope for years to come.

I would also want to appreciate my supervisor, Dr Peter Ouwehand for his support, advice and encouragement through out the course of this work. I am so grateful to have worked with you and have indeed learnt a lot from you. Thanks so much for giving me the wings to fly across and beyond the challenges I faced through out the period of this work. To the best parents and siblings, I remain humbled by your care, love and prayers. You all are simply the very best. To my 'Walking Diamond', thanks for loving me the way you do. Leaning on your shoulders at those times it looked so challenging was the best comfort ever.

To my colleaques, Trust and Jean Claude, I am so grateful for the ideas shared and the assistance you rendered at different points. Mary, Vicky, Josephine, Banky, Esther and all my friends who in one way or the other contributed to the success of this work, I remain ever grateful.

This research work was supported by African Institute for Mathematical Sciences (AIMS) and the Department of Mathematical Sciences at the University of Stellenbosch.

# Contents

**1 Introduction** **1**

1.1 Barrier Options . . . . . 2

1.2 Non-Gaussian Characteristics of Log Returns . . . . . 4

1.2.1 Non-Gaussian Property . . . . . 5

1.3 Review of the Literature . . . . . 7

1.4 Outline of the Dissertation . . . . . 11

**2 Lévy Processes** **12**

2.1 Definition of Lévy Processes . . . . . 13

2.2 Analysis of Jump Measures and Major Results . . . . . 17

2.3 Subordinators . . . . . 23

2.4 Construction of Lévy Processes . . . . . 24

2.4.1 Brownian Subordination . . . . . 24

2.4.2 Specifying the Probability Density . . . . . 25

2.4.3 Specifying the Lévy Measure . . . . . 26

**3 Models Driven by Lévy Dynamics 27**

3.1 The Variance Gamma Model . . . . . 28

3.2 The Normal Inverse Gaussian Model . . . . . 30

3.3 The CGMY Model . . . . . 33

3.4 Simulation of Lévy Processes . . . . . 35

3.4.1 Simulation of the Variance Gamma Process . . . . . 35

3.4.2 Simulation of the Normal Inverse Gaussian Process . . . . . 36

3.4.3 Simulation of the CGMY process . . . . . 37

3.5 Density Estimation of Historic Data . . . . . 41

3.5.1 Empirical Density . . . . . 41

3.5.2 Model Density . . . . . 42

3.5.3 Kolmogorov-Smirnov Test . . . . . 43

**4 Model Calibration 49**

4.1 Methods of Calibration . . . . . 50

4.1.1 Generalized Method of Moments (GMM) . . . . . 50

4.1.2 Maximum Likelihood Estimation (MLE) . . . . . 51

4.1.3 Least-Squares Estimation (LSE) . . . . . 52

4.2 The Lévy Market Model: The Pricing Framework . . . . . 53

4.2.1 Equivalent Martingale Measure (EMM) . . . . . 53

4.2.2 Pricing Formula for European Options . . . . . 55

4.3 FFT Option Pricing Technique . . . . . 56

**5 Calibration to Option Prices** **60**

5.1 The Estimation Procedure . . . . . 60

5.1.1 Results of Estimation . . . . . 62

5.1.2 Vanilla Price Comparison . . . . . 64

5.2 Implied Volatility Surface . . . . . 72

5.3 Simulation of the Stock Price Process . . . . . 75

**6 The Pricing of Barrier Options** **79**

6.1 The Concept of Monte Carlo Simulation . . . . . 80

6.2 Pricing in the Black-Scholes Framework . . . . . 81

6.3 Numerical Results . . . . . 82

**7 Conclusion** **92**

**Appendices** **95**

**A Call Option Prices** **95**

A.1 INTC Call Option Prices . . . . . 95

A.2 S&P 500 Call Option Prices . . . . . 96

**References** **97**

# List of Figures

3.1 Typical trajectories of the variance gamma process. All trajectories were simulated with $\sigma = 0.3$ and $\theta = 0.05$. The varying parameter $\nu$ is 0.22, 0.022, 0.002, and 0.00022 for (a), (b), (c) and (d) respectively. These parameters were chosen at random. . . . . 31

3.2 Simulated trajectories of the NIG process with $\sigma = 0.3$, $\theta = 0.1$ and $\kappa = 0.05,\ 0.9$ respectively. These trajectories were simulated using Algorithm 3.4.3. . . . . 33

3.3 Simulated trajectory of the variance gamma process . . . . . 36

3.4 Simulated trajectory of the NIG process . . . . . 38

3.5 Simulated trajectory of the CGMY process with $C = 0.50,\ G = 0.90,\ M = 7.15$ and the $Y$ parameter varied. . . . . 40

3.6 VG density plots for DELL data . . . . . 43

3.7 VG density plots for IBM data . . . . . 44

3.8 VG density plots for INTC data . . . . . 44

3.9 VG density plots for S&P 500 index data . . . . . 45

3.10 Density plots for the NIG Model . . . . . 46

3.11 Density plots for the CGMY Model . . . . . 47

5.1 CGMY calibration of INTC options (circles are market prices, pluses are model prices). . . . . 65

5.2 CGMY calibration of S&P 500 options (circles are market prices, pluses are model prices). . . . . 66

5.3 NIG calibration of INTC options (circles are market prices, pluses are model prices). . . . . 67

5.4 NIG calibration of S&P 500 options (circles are market prices, pluses are model prices). . . . . 68

5.5 VG calibration of INTC options (circles are market prices, pluses are model prices). . . . . 69

5.6 VG calibration of S&P 500 options (circles are market prices, pluses are model prices). . . . . 70

5.7 Comparison of market prices of options to those obtained from the models through the different calibration procedures via FFT. This is carried out on the October 2010 and December 2002 maturities, for the INTC and S&P 500 data sets . . . . . 71

5.8 Implied volatility surface for the INTC call options data. . . . . 73

5.9 Implied volatility surface for the S&P 500 call options data. . . . . 74

5.10 Simulation of VG trajectories and stock price process using parameters obtained from the global set of parameters. . . . . 76

5.11 Simulation of NIG trajectories and stock price process using parameters obtained from the global set of parameters. . . . . 77

5.12 Simulation of CGMY trajectories and stock price process using parameters obtained from the global set of parameters. . . . . 78

6.1 Up-and-in call option prices for the VG model computed using the four parameter sets. This is compared to those of the Black-Scholes model and the vanilla market prices. . . . . 85

6.2 Up-and-in call option prices for the NIG model computed using the four parameter sets. This is compared to those of the Black-Scholes model and the vanilla market prices. . . . . 85

6.3 Up-and-in call option prices for the CGMY model computed using the four parameter sets. This is compared to those of the Black-Scholes model and the vanilla market prices. . . . . 86

6.4 Up-and-in call option prices for all the models computed using the global parameter sets. This is compared to those of the Black-Scholes model and the vanilla market prices. . . . . 87

6.5 Up-and-in call option prices for all the models computed using the single parameter sets. This is compared to those of the Black-Scholes model and the vanilla market prices. . . . . 88

6.6 'Up' barrier call option prices for the VG model computed using the global parameter sets. These are compared to those of the Black-Scholes model. The barrier is varied by 0.5 to 1.5 of the spot price in each case. . . . . 89

6.7 'Up' barrier call option prices for the NIG model computed using the global parameter sets. These are compared to those of the Black-Scholes model. The barrier is varied by 0.5 to 1.5 of the spot price in each case. . . . . 89

6.8 'Up' barrier call option prices for the CGMY model computed using the global parameter sets. These are compared to those of the Black-Scholes model. The barrier is varied by 0.5 to 1.5 of the spot price in each case. . . 90

6.9 Up-and-in barrier call option prices for all the models computed using the global parameter sets. These are compared to those of the Black-Scholes model. The barrier is varied by 0.5 to 1.5 of the spot price in each case. . . 90

6.10 Up-and-out barrier call option prices for all the models computed using the global parameter sets. These are compared to those of the Black-Scholes model. The barrier is varied by 0.5 to 1.5 of the spot price in each case. . . 91

# List of Tables

1.1 Mean, standard deviation, skewness and kurtosis of the log returns of major securities. . . . . 5

1.2 Excess kurtosis of major securities . . . . . 7

3.1 Kolmogorov-Smirnov test for normality of log returns . . . . . 48

3.2 Kolmogorov-Smirnov test for comparing distributions of daily log returns for the NIG Model . . . . . 48

4.1 The m parameter for the mean-correcting EMM . . . . . 54

5.1 Risk-neutral parameter sets for the INTC options. . . . . 63

5.2 Risk-neutral parameter sets for the S&P 500 options. . . . . 64

6.1 Up-and-in call option prices using the parameters obtained from calibrating the INTC data. . . . . 83

6.2 Up-and-in call option prices using the parameters obtained from calibrating the S&P 500 index data. . . . . 84

6.3 INTC 'Up' call option prices for varying barrier levels. The barrier is varied by 0.5 to 1.5 of the spot price in each case. . . . . 87

6.4 S&P 500 index 'Up' call option for varying barrier levels. The barrier is varied by 0.5 to 1.5 of the spot price in each case. . . . . 88

A.1 The data set for INTC plain vanilla call option prices . . . . . 95

A.2 The data set for S&P 500 plain vanilla call option prices . . . . . 96

# Chapter 1

# Introduction

Options are financial contracts that give the holder the right to buy or sell a given number of shares at a given price and at a particular time. They can either be described as call or put options[1]. It is worth noting that the right given to the holder is not an obligation as he/she may decide to either exercise or leave the option to expire worthless. Barrier options are options whose payoff depends on whether the price of the underlying asset crosses a certain level (the barrier) during the life of the option (before maturity). These are our main area of focus and have been in existence since before the establishment of the Chicago Board of Options Exchange (CBOE) in 1973,the oldest organized option exchange in the world [69]. Despite how long these options have been in existence, they were not traded on organized exchanges until 1991 when they were first traded on CBOE and then by the American Stock Exchange [69].

Barrier options are examples of exotic options [2], and can be seen as special-purpose options as they are geared towards serving a special need which their vanilla counterparts do not satisfy. Other examples of exotic options include Asian options whose payoffs depend on some average, lookback options whose payoffs depend on the maximum or minimum of the underlying asset's price over the life of the option, basket options whose payoffs depend on more than one asset, spread options, rainbow options and quanto options ([95] and [82]). Many of these options are either directly or indirectly related in one way or the other to

[1] A call option gives the holder the right to buy while a put option gives the holder the right to sell.

[2] An exotic option is a financial derivative which has more complex features than the commonly traded options (vanilla options).

vanilla options. The relation between barrier options and vanilla options will be discussed later in this chapter.

The pricing of barrier options involves risks that are usually not easy to perceive distinctly and can lead to unexpected losses. This is mainly due to the nature of the options as will be seen later in this chapter. This dissertation is set to study the model risk associated with the pricing of barrier options using models that are driven by Lévy dynamics. In order to achieve this, we shall set out to do the following:

- Justify our choice of models driven by Lévy dynamics;
- Investigate how easily these processes can be simulated;
- Check the abilities of these models to fit vanilla option prices;
- Check how efficiently these models can be calibrated;
- Analyze and compare the prices of barrier options obtained using these models.

With these objectives in mind, we begin by presenting an overview of what barrier options entail. Our study will be based on the most basic types of barrier option - the single barrier option. This is the focus of the next section.

## 1.1 Barrier Options

Barrier options are path-dependent options that are either activated or cancelled if the underlying instrument reaches a certain level (barrier) during the life of the option, regardless of the point at which the underlying asset is trading at maturity. Their payoffs are dependent on the realized asset path via its level, as certain aspects of the contract are triggered if the asset price becomes too high or too low. Single-barrier options can be classified as "knock-out" and "knock-in" barrier options. Knock-out (up-and-out and down-and-out) options are options which are alive while the underlying asset has not hit the given barrier level, while knock-in (up-and-in and down-and-in) options come alive with the underlying asset hitting the given barrier level. If the barrier is above the initial asset price, it is an "up" option and when the barrier is below the initial asset value, we have a "down"

option. It is worth noting that sometimes a rebate (partial refund) is paid if the barrier is reached for 'out' barrier as cushioning the blows of losing the payoff. This rebate can be paid immediately the barrier is triggered or at expiry. Barrier options are cheaper than the corresponding European options. A trader who has precise views about the direction of the market and desires the payoff from a call option can use an up-and-out call option instead. If his views are correct and the barrier is not triggered, he gets the payoff he wanted. The closer that barrier is to the current asset price, the greater the likelihood of the option to be knocked out and hence, the cheaper the contract [93]. Similarly, 'in' options are bought by traders who believe that the barrier level will be triggered.

Considering contracts of duration $T$, let $S_T$ be the price of an option at time $T$ and $K$ the strike price of the option. The payoff of a European call option is given by

$$C_T = \exp(-rT)\,\mathbb{E}_Q[(S_T - K)^+]\,,$$

where $r$ is the risk-free interest rate. For the European put option, the payoff is given by

$$P_T = \exp(-rT)\,\mathbb{E}_Q[(K - S_T)^+]\,.$$

We denote the maximum and minimum of a process $Y = \{Y_t, 0 \leq t \leq T\}$ by

$$M_t^Y = \sup\{Y_u; 0 \leq u \leq t\} \quad \text{and} \quad m_t^Y = \inf\{Y_u; 0 \leq u \leq t\}, \qquad 0 \leq t \leq T$$

respectively, and the indicator function by $1(A)$, which has a value of 1 if the event $A$ occurs and zero otherwise. We focus on call options for single-barrier options. The following applies:

- The down-and-out barrier call (DOC) becomes worthless when its minimum crosses some low barrier $L$, and retains the structure of a European call with strike $K$ otherwise. Its payoff is given by:

$$DOC = \exp(-rt)\ E_Q[(S_T - K)^+\ 1(m_T^S > L)]\ .$$

- The down-and-in barrier call (DIC) is a normal European call with strike $K$, if its minimum crosses some low barrier $L$. This option is worthless if this barrier was never reached during the life-time of the option. Its payoff is given by:

$$DIC = \exp(-rt)\ E_Q[(S_T - K)^+\ 1(m_T^S \leq L)]\ .$$

- The up-and-out barrier call (UOC) becomes worthless when its maximum crosses some high barrier $L$. Otherwise, it retains the structure of a European call with strike $K$. Its payoff is given by:

$$UOC = \exp(-rt)\ E_Q[(S_T - K)^+\ 1(M_T^S < L)]\ .$$

- The up-and-in barrier call (UIC) is worthless unless its maximum crosses some high barrier $L$, in which case it retains the structure of a European call with strike $K$. Its payoff is given by:

$$UIC = \exp(-rt)\ E_Q[(S_T - K)^+\ 1(M_T^S \geq L)]\ .$$

Note that we have the following in-out parity relations.

$$\begin{aligned} DOC + DIC &= \exp\{-rT\}\mathbb{E}_Q[(S_T - K)^+ (1(m_T^S < L) + 1(m_T^S \geq L))]\ , \\ &= \exp\{-rT\}\mathbb{E}_Q[(S_T - K)^+]\ , \\ &= C_T\ , \\ UOC + UIC &= \exp\{-rT\}\mathbb{E}_Q[(S_T - K)^+ (1(M_T^S > L) + 1(M_T^S \leq L))]\ , \\ &= \exp\{-rT\}\mathbb{E}_Q[(S_T - K)^+]\ , \\ &= C_T\ . \end{aligned}$$

For their put counterparts, if we replace $(S_T - K)^+$ with $(K - S_T)^+$, we can along the same lines define their prices. Apart from the single-barrier options which are our focus, there also exist other types of barrier options. Amongst them are double-barrier options, partial barrier options, reset barrier options, roll-up and roll-down options. Further details on barrier options can be found in [93], [81], [47], [49], and [83].

## 1.2 Non-Gaussian Characteristics of Log Returns

The valuation of barrier options is one of great interest due to their path-dependent nature. Cheng [26] provides an overview of several methods used for this, with corresponding literature. Much research on this topic is set within the Black-Scholes framework ([67], [75], [17], [21]) and we must ask ourselves, "Why are we not pricing barrier options in the

Black-Scholes framework"? Despite the popularity of this framework (as a result of the ease with which it can be implemented, and the availability of analytical formulas for the pricing of several options), it is well known to have severe limitations when compared to what is required in practice. These limitations include amongst others, that it assumes that the risk-free rate and the stock's volatility are constant, and involves cost-less and continuous trading. Another major assumption is that stock returns are normally distributed, this is not borne out by financial data. We shall carry out an analysis on some major securities and show that they exhibit a non-Gaussian character. Other studies that have been carried out on the empirical properties of asset returns can be found in [20], [60], [27], and [29]. The data set used in this section contains daily/weekly log returns of stocks with ticker names DELL, IBM, INTC and on a major index which is the weighted average of the main 500 American stocks, S&P 500 Index over the period Aug. 17, 1988 to Mar. 2, 2010. The log returns were calculated using adjusted closing prices and involves 5429/1124 observations in each daily/weekly time series data set.

### 1.2.1 Non-Gaussian Property

In this section, we consider properties such as the standard deviation, skewness and kurtosis of the log returns of the set of securities and over the period specified above. Table 1.1 gives a summary of the empirical mean, standard deviation, skewness and kurtosis of the securities under consideration. The standard deviation of the daily/weekly log returns for these securities is shown in Figure 1.1.

| Securities | Mean | | Standard Deviation | | Skewness | | Kurtosis | |
|---|---|---|---|---|---|---|---|---|
| | Daily | Weekly | Daily | Weekly | Daily | Weekly | Daily | Weekly |
| S&P 500 Index | -2.6818E-04 | -0.0013 | 0.0115 | 0.0234 | 0.0235 | 0.797 | 12.3628 | 10.3792 |
| INTC | -5.9408E-04 | -0.0029 | 0.0268 | 0.0550 | 0.4096 | 0.4448 | 8.1257 | 5.1171 |
| IBM | -3.5023E-04 | -0.0017 | 0.0187 | 0.0397 | -0.0143 | 0.1861 | 9.8719 | 5.6604 |
| DELL | -9.0465E-04 | -0.0045 | 0.0361 | 0.0715 | 0.2607 | 0.2783 | 7.8757 | 6.0804 |

**Table 1.1.** Mean, standard deviation, skewness and kurtosis of the log returns of major securities.

### Skewness

A measure of the degree to which a distribution is asymmetric is known as its skewness. To calculate this, the third central moment is divided by the third power of the standard deviation given by:

$$\text{Skewness} = \frac{\mathbb{E}[(X - \mu_X)^3]}{\sigma_X^3} ,$$

where $\mu_X$ is the mean. It is well known that the normal distribution has zero skewness and hence is said to be a symmetric distribution. A distribution can either be negatively skewed or positively skewed if not symmetric. From Table 1.1, we observe positive skewness except for the daily log returns of IBM. We can therefore say that these empirical data are likely not from a normal distribution.

### Kurtosis/Tail Behaviour

The kurtosis of a distribution is a statistical measure which describes the distribution of observed data around the mean. It measures the degree of peakedness of the distribution and is calculated by the formula:

$$\text{Kurtosis} = \frac{\mathbb{E}[(X - \mu_X)^4]}{\sigma_X^4} .$$

When a distribution has a high kurtosis, this implies that it has fat tails and is more sharply peaked than the normal distribution, while when it has a low kurtosis, the distribution is concentrated around the mean and has slim tails.

A distribution is said to have excess kurtosis when its kurtosis is higher than that of the normal distribution and this quantity is calculated by:

$$\text{Excess Kurtosis} = \frac{\mathbb{E}[(X - \mu_X)^4]}{\sigma_X^4} - 3 , \tag{1.1}$$

where 3 is the kurtosis of the normal distribution. Table 1.2 displays the excess kurtosis of the daily/weekly log returns of the major securities we are considering. It is obvious from this table that we have excess kurtosis ranging from 2.12 to 9.36 (2 decimal places) for all the indices. This is a major reason for considering asset price models with jumps. With this excess kurtosis in mind, it gives an indication that the tails of the normal distribution

| Index | Daily Data | Weekly Data |
|---|---|---|
| S&P 500 Index | 9.3628 | 7.3792 |
| INTC | 5.1257 | 2.1171 |
| IBM | 6.8719 | 2.6604 |
| DELL | 4.8757 | 3.0804 |

**Table 1.2.** Excess kurtosis of major securities

will go to zero faster than that suggested by the empirical data. This result can be traced back to Fama [35].

We can therefore conclude that from the empirical results presented in this section, the distributions of the log returns of these major securities tend to be non-Gaussian, leptokurtic and heavy tailed. This serves as one major reason why we are not going to be pricing in the Black-Scholes model. These properties are not enough in identifying the distribution of these returns, we shall therefore fit these returns to different asset price models later in this work, after we have presented these models. To be able to choose a model for this purpose, the model should have at least four parameters [27]: a location parameter, a scale (volatility) parameter, an asymmetry parameter allowing the left and right tails of the distribution to behave differently and a parameter describing the decay of the tails. Examples of models that satisfy the above conditions are: generalized hyperbolic model, the normal inverse Gaussian model, and exponentially truncated stable processes. Lastly, all our models will satisfy this requirement as even the variance gamma model which is considered as a three parameter model has a location parameter given as zero [32].

## 1.3 Review of the Literature

The pricing of barrier options has attracted attention from several authors. Merton [67] provided the first analytical formula for the valuation of down-and-out call options. Reiner and Rubinstein [75] presented further analytical formulas for the single knock-in and knock-out barrier options. These papers provide formulas to price barrier options in continuous time. In practice, the underlying asset is observed at discrete times. In Broadie, Glasserman and Kou [17], a continuity correction for approximate pricing of discrete barrier options was introduced. Here, the analytic formulas for the prices of the continuous barrier options are

used with a shift on the barrier to correct for discrete monitoring. This method shifts the barrier away from the underlying by a factor of $\exp(\beta\sigma\sqrt{\Delta t})$, where $\beta \approx 0.5826$, $\sigma$ is the asset's volatility, and $\Delta t$ denotes the monitoring frequency.

Carr [21] presented two extensions in the valuation of barrier options. The first entails adding an initial protection period during which the option cannot be knocked out while the second involves a situation where the option can only be knocked out if a second asset touches an upper barrier. Closed form solutions for the valuation of these options were also provided. Further work by Mitov, Rachev, Kim and Fabozzi [69] examines the pricing of barrier options when the price of the underlying asset is modeled by a branching process in random environment (BRPE). This process is reported to allow for possible jumps in stock prices and also takes into account the possibility of bankruptcy. They derived a formula for the price of an up-and-out call option and compared the results with that of the lognormal model.

Cheng [26] presents an overview of techniques used in the pricing of barrier options, some of which have been discussed above. Apart from these, others include pricing via a lattice tree such as binomial or trinomial, and adaptive mesh models which entail solving the partial differential equation (PDE) using a generalized finite difference method. He further showed that the adaptive mesh model gives more accurate results in the pricing of barrier options than its lattice counterparts. In this case, a mesh is constructed with the nodes placed along the barriers to give more accurate simulated paths. The barrier option value can then be computed via backwards induction on the tree, and this can be implemented within a Monte Carlo framework.

Most of the methods discussed above have been carried out in the Black-Scholes framework. Having discussed the pitfalls of the Black-Scholes model, we wish to explore other possible frameworks in which barrier options can be priced. In order to deal with the non-Gaussian character of the log-returns of empirical data, several models have been proposed over the last few decades which are based on other distributions. Amongst these models are the stochastic-interest-rate option models in [67] and [3], the jump-diffusion/pure jump models in [68] and [12], the pure jump processes in [31], the stochastic-volatility models of [44], [48], and [86], and the stochastic-volatility jump-diffusion models as presented in [13], [14] and [87]. We will not fail to mention pure jump Lévy processes which are the focus of

several papers (as will be discussed below) and our area of interest too.

Lévy models have become popular over the last few years due to their ability to capture market fluctuations better than the classical Black-Scholes model. They have been shown to give a much better fit to historic data, and also calibrate model prices of vanilla options to their market counterparts much better than in the BS-framework (see [84], [81], [24] and [83]). Cont and Tankov [29] and Schoutens [81] give a detailed study on this subject. These models have been recognized to capture both rare large moves and frequent small moves in the stock price process [24]. Amongst these models, we shall consider the Variance-Gamma (VG) process as put forward by Madan and Seneta [63] and the Normal Inverse Gaussian (NIG) process proposed by Barndorff-Nielsen [6]. In this work, apart from the above mentioned processes, we will be exploring the CGMY model developed by Carr, Geman, Madan and Yor [23], which is a generalization of the VG model. In later chapters, a summary of Lévy processes and these models will be presented.

In pricing of barrier options under the Lévy framework, Cont and Tankov [29] present three different approaches. These approaches include the Wiener-Hopf factorization, the Monte Carlo and the partial integro-differential equations (PIDE) methods. A major drawback of the first approach is that in most cases, the Wiener-Hopf factors are not known in closed form and computing option prices requires integration in several dimensions. The Monte Carlo method has been discovered to perform well for the pricing of barrier options. The third approach entails solving corresponding PIDE with natural boundary condition (that is a price of either zero or the rebate on the barrier). A major drawback of this method is that as the dimension of the problem grows, it becomes more difficult to implement because computational complexity for fixed precision grows exponentially with dimension. Schoutens [82] gives an overview of pricing barrier options using the Wiener-Hopf factorization and PIDE methods, and arrives at similar conclusions to those in [29]. The Monte Carlo method was used for the valuation of barrier options in [81], [76], [84] and [83]. In [81], [84] and [83], the pricing of barrier options was carried out in a Lévy stochastic volatility (SV) framework. Schoutens [81], concludes that the prices from the Lévy SV models are close to each other and more reliable than those of the Black-Scholes model. Ribeiro and Webber [76] considered barrier options with continuous reset conditions for the variance gamma and normal inverse Gaussian models. They show how to correct for simulation bias when using Monte Carlo methods to value options with

continuous reset conditions. This correction can only be applied to Lévy processes whose subordinator representation is known, and where the subordinator bridge distribution can be sampled.

Considering the above literature on the pricing of barrier options, a major question we have to ask ourselves is this: 'Are there any risks associated with these models for pricing barrier options'? Hirsa, Courtadon and Madan [45] showed that despite the close fit of vanilla options to different models, the prices of up-and-out call options differ noticeably when different stochastic processes are used to calibrate the vanilla options surface. They compared the prices obtained for two continuous models (CEV and local volatility model) and two purely discontinuous models (VG and VGSA) and discovered that the latter gave a substantially higher price for the option under consideration. Their result illustrates the fact that the prices of path dependent options will depend on the model used to represent the underlying price process over time.

Schoutens, Simons and Tistaert [83] focused on models incorporating stochastic volatility and discovered that they all lead to almost identical European vanilla option prices. These models include the Heston stochastic volatility model, the Barndorff-Nielsen-Shephard model and Lévy models with stochastic time. The similarity of the vanilla option prices led them to try these models on a range of exotic options and it was discovered that the prices varied significantly due to the different structure in path-behaviour of the models. This result is in line with that reported in [45]. For the Lévy models with stochastic time, the prices were seen to be quite close to each other. A similar result was obtained by Schoutens and Symens [84]. In their paper, they priced exotic options by Monte Carlo simulations using Lévy models with stochastic volatility and concluded that these models were more reliable for pricing exotic options. It is necessary to point out that the models were calibrated to a single maturity in [45] while in [83] and [84], the models were calibrated across several maturities.

With the above results in mind, we shall investigate the risks associated with the variance gamma, normal inverse Gaussian and CGMY models when used to price barrier options. To achieve this, we will firstly calibrate these models to a set of vanilla options and then price barrier options via Monte-Carlo simulation using the parameters obtained from the calibration. Our work will focus on the approach presented in [24], [81] and [83].

## 1.4 Outline of the Dissertation

In this chapter, we presented a basic introduction to barrier options. We further considered the non-Gaussian character of log returns for INTC, DELL, IBM and S&P 500 Index, and also presented a review of the relevant literature of the models we hope to work with. The remainder of this dissertation is organized as follows.

In Chapter 2, we present the mathematical aspects of Lévy processes with a view to assisting the reader in understanding the fundamentals of the Lévy option pricing models that will be used in this work. Here, basic definitions and properties of Lévy processes will be presented and the major results on which these processes are built will also be discussed. Chapter 3 gives a thorough exposition of our chosen models, which are driven by Lévy dynamics. We shall then present a justification of our choice of models using the properties of empirical data. We shall also fit a number of asset returns to different distributions in other to estimate their densities.

In Chapter 5, we shall analyze the model risk associated with the variance gamma, normal inverse Gaussian and CGMY models in terms of calibration. Questions like "what is the importance of the number of parameters to accuracy for each model?" will be addressed. The robustness of calibration is another important issue we will consider. Calibration to two data sets will be carried out in this chapter and we hope to see how well the models perform in both cases.

In our next chapter, we will price barrier options using the model parameters obtained from the calibrations in Chapter 5. This we will do using Monte Carlo simulation as discussed in [84] and [81]. Calibration risks and their effects on the prices of barrier options will also be considered. Finally, we shall conclude with a formal discussion of the results obtained.

# Chapter 2

# Lévy Processes

Levy processes were first studied by Paul Lévy in the 1930s [4]. He studied sums of independent variables and characterized their limit distributions. The quest for models which can describe the observed reality of financial markets in a more accurate framework than models based on Brownian motion has led to the use of Lévy processes in finance. These processes are found to describe the observed reality of the financial market data in a more accurate way, both in the real world and in the risk-neutral world. Apart from finance, Lévy processes play an important role in several fields of science, such as physics, economics, engineering, and actuarial science [4].

The main aim of this chapter is to provide a quick summary on the fundamentals of Lévy processes that will be useful in understanding the pricing models driven by Lévy dynamics. To serve this purpose, we have avoided rigorous proofs and only sketch a number of proofs, especially when they offer some insight to the reader. For additional details on Lévy processes, we refer the reader to [80], [29], [5] and [81].

We begin with the definition of a Lévy process and give examples. We then discuss some important properties and present some important results for Lévy processes. These results include the Lévy-Khintchin formula, which links processes to distributions, and the Lévy-Itô decomposition which is vital for the simulation of Lévy processes. We conclude this chapter by discussing subordinators; another important tool for the simulation of certain Lévy processes.

## 2.1 Definition of Lévy Processes

Let $(\Omega, \mathcal{F}, \mathbb{F}, \mathbb{P})$ be a filtered probability space, and the filtration $\mathbb{F} = (\mathcal{F}_t)_{t\geq 0}$ satisfies the usual conditions.

**Definition 2.1.1.** *Suppose that $(\Omega, \mathcal{F}, \mathbb{F}, \mathbb{P})$ is a probability space. A càdlàg[1] stochastic process $(X_t)_{t\geq 0}$ with values in $\mathbb{R}^d$ such that $X_0 = 0$ is called a Lévy process if it possesses the following properties [29]:*

1. ***Independent increments:*** *for every increasing sequence of times $t_0, \ldots, t_n$, the random variables $X_{t_0}, X_{t_1} - X_{t_0}, \ldots, X_{t_n} - X_{t_{n-1}}$ are independent and $X_t - X_s$ is independent of $\mathcal{F}_s$.*
2. ***Stationary increments:*** *the law of $X_{t+h} - X_t$ does not depend on $t$.*
3. ***Stochastic Continuity:*** $\forall\, \epsilon > 0$, $\lim_{h\to 0} \mathbb{P}(|X_{t+h} - X_t| \geq \epsilon) = 0$.

It is worth noting that the last condition does not imply that the sample paths are continuous, but that for given time $t$, the probability of seeing a jump at $t$ is zero. In other words, we cannot predict when jumps occur as they occur at random times.

Brownian motion is an example of a Lévy process. The only continuous Lévy processes are Brownian motion (with drift). Sato [80] gives detailed analysis of Brownian motion as an example of Lévy processes. Other examples of a Lévy process are the Poisson and compound Poisson processes. We go ahead to discuss the Poisson and compound Poisson processes, which form the building blocks for all other kinds of processes we will come across later. Let $\lambda$ denote the intensity measure of a jump event, in other words the probability of occurrence of the jump event over a unit time interval.

**Definition 2.1.2.** *A random variable $X$ is said to be Poisson($\lambda$) if it has values in $\mathbb{N}$, and the probability distribution is given by*

$$\mathbb{P}(X = n) = e^{-\lambda}\frac{\lambda^n}{n!}\,.$$

The mean and variance of the Poisson distribution are both equal to $\lambda$, while the skewness and kurtosis are $\frac{1}{\sqrt{\lambda}}$ and $\lambda^{-1}$ respectively as can easily be verified. The Poisson process is the simplest Lévy process.

[1] Sample paths of $X$ have left limits and are right-continuous almost surely.

**Definition 2.1.3.** *A càdlàg, adapted stochastic process $N = (N_t)_{0\leq t\leq T}$ is called a Poisson process if it satisfies the following properties [72]:*

1. $N_0 = 0$,
2. $N_t - N_s$ *is independent of* $\mathcal{F}_s$ *for any* $0 \leq s < t < T$,
3. $N_t - N_s$ *is Poisson distributed with parameter* $\lambda(t-s)$ *for any* $0 \leq s < t < T$.

For any Lévy process $X$ and any Borel set $B$, the process $N_t^B$ which counts the number of jumps with size in $B$ at time $t$ turns out to be a Poisson process. This implies that Poisson processes are used to count jumps of a Lévy process.

**Definition 2.1.4.** *A compound Poisson process with rate $\lambda > 0$ and jump size distribution $f$ is a continuous time stochastic process $\{X_t : t \geq 0\}$ given by*

$$X_t = \sum_{i=1}^{N_t} Y_i \,, \tag{2.1}$$

*where jump sizes $Y_i$ are i.i.d. with distribution $f$ and $\{N_t : t \geq 0\}$ is a Poisson process with intensity rate $\lambda$, independent from $\{Y_i : i \geq 1\}$.*

Compound Poisson processes are Lévy processes and are also the only Lévy process with piecewise constant sample paths. See Cont and Tankov [29] for a detailed proof of this. A major reason for studying compound Poisson processes is the fact that any càdlàg function may be approximated by a piecewise constant function. It turns out that all Lévy processes can be approximated by compound Poisson processes.

Let us consider sampling the Lévy process $X_t$ at a set of evenly spaced discrete times. For any $n \in \mathbb{N}$, we can write

$$X_t = \sum_{i=1}^{n} Y_i \,, \qquad \text{where } Y_i = X_{\frac{t_i}{n}} - X_{\frac{t_{i-1}}{n}} \,.$$

Because $X$ has independent stationary increments, the $Y_i$ are i.i.d. random variables. A distribution which exhibits this property is said to be infinitely divisible.

**Definition 2.1.5.** *A probability distribution $F$ on $\mathbb{R}^d$ is said to be infinitely divisible if for any integer $n \geq 2$, there exist $n$ i.i.d. random variables $Y_1, \ldots, Y_n$ such that $Y_1 + \cdots + Y_n$ has distribution $F$.*

Given that $X$ is a Lévy process, for any $t > 0$ the distribution of $X_t$ is infinitely divisible. Conversely, given an infinitely divisible distribution $F$ a Lévy process $X$ can be constructed from it so that $X_1$ has distribution $F$, see [29] for details.

Given a random variable $X$, its characteristic function always exists, and it is the Fourier transform of the density where the random variable has a density. We can therefore define the characteristic function of a random variable $X$ by

$$\varphi_X(u) = \mathbb{E}[\exp(iu.X_t)] = \int_{-\infty}^{\infty} \exp(iux)\, dF(x)\,,$$

where $F(x)$ is the distribution function of $X$.

Let $X, Y$ be two independent random variables, then we have that

$$\varphi_{X+Y}(u) = \varphi_X(u)\,\varphi_Y(u)\,.$$

Also, we can characterize an infinitely divisible random variable using its characteristic function as shown below.

The law of a random variable $X$ is infinitely divisible, if for all $n \in \mathbb{N}$, there exists a random variable $X^{(1/n)}$, such that [5]:

$$\varphi_X(u) = (\varphi_{X^{1/n}}(u))^n\,.$$

**Example 2.1.6.** ***(Normal Distribution)***. *Using the above characterization, it is easy to deduce that the Normal distribution is infinitely divisible. Let $X \sim Normal(\mu, \sigma^2)$, then we have*

$$\begin{aligned}
\varphi_X(u) &= \exp\left\{iu\,\mu - \frac{1}{2}u^2\sigma^2\right\}\,, \\
&= \exp\left\{n(iu\,\frac{\mu}{n} - \frac{1}{2}u^2\frac{\sigma^2}{n})\right\}\,, \\
&= \left(\exp\left\{iu\,\frac{\mu}{n} - \frac{1}{2}u^2\frac{\sigma^2}{n}\right\}\right)^n\,, \\
&= (\varphi_{X^{1/n}}(u))^n\,,
\end{aligned}$$

*where $X^{1/n} \sim Normal(\frac{\mu}{n}, \frac{\sigma^2}{n})$.*

Other examples of distributions that posses the infinite divisibility property are: gamma, Poisson, inverse Gaussian, lognormal amongst others. For further details on these, Sato

in [80] gives a detailed discussion. Again, every probability distribution is completely determined by its characteristic function, which is the Fourier transform of the density of the distribution where applicable. This is very important in our work as we shall be computing the prices of options via the fast Fourier transform method introduced by Carr and Madan [25], which uses the characteristic function of the process. Also, the characteristic function of an infinitely divisible distribution has a very special form, given by the Lévy-Khintchin formula, this will be discussed in the next section. The characteristic function of a Lévy process is defined by the proposition below.

**Proposition 2.1.7.** ***(Characteristic function of a Lévy process)*** *Let $(X_t)_{t\geq 0}$ be a Lévy process on $\mathbb{R}^d$. Then there exist a continuous function $\psi : \mathbb{R}^d \mapsto \mathbb{R}$ known as the characteristic exponent of $X$, such that*

$$\mathbb{E}[e^{iu.X_t}] = e^{t\psi(u)} , \qquad u \in \mathbb{R}^d . \tag{2.2}$$

*Proof.* [29] Define the characteristic function of $X_t$ by,

$$\varphi_{X_t(u)} \equiv \mathbb{E}[e^{iu.X_t}] , \qquad u \in \mathbb{R}^d .$$

For $t > 0$, we can write $X_{t+s}$ as $X_s + (X_{t+s} - X_s)$ and since we know that $X_{t+s} - X_s$ is independent of $X_s$, implying that the map $t \mapsto \varphi_{X_t}(u)$ is multiplicative:

$$\begin{aligned} \varphi_{X_{t+s}}(u) &= \varphi_{X_s}(u)\, \varphi_{X_{t+s}-X_s}(u) , \\ &= \varphi_{X_s}(u)\, \varphi_{X_t}(u) . \end{aligned}$$

The stochastic continuity of $t \mapsto X_t$ implies that $X_t \to X_s$ in distribution as $t \to s$. Hence $\varphi_{X_s}(u) \to \varphi_{X_t}(u)$ when $s \to t$ so $t \mapsto \phi_{X_t}(u)$ is a continuous function in $t$. When we combine this with the multiplicative property, we have that $t \mapsto \varphi_{X_t}(u)$ is an exponential function. □

The characteristic function of a compound Poisson process is given by the following proposition:

**Proposition 2.1.8.** *Let $(X_t)_{t\geq 0}$ be a compound Poisson process on $\mathbb{R}^d$. Its characteristic function has the following representation:*

$$\mathbb{E}[\exp\{iu.X_t\}] = \exp\left\{t\lambda \int_{\mathbb{R}^d} (e^{iu.x} - 1) f\,(dx)\right\} , \quad (\forall\, u \in \mathbb{R}^d) \tag{2.3}$$

*where $\lambda$ denotes the jump intensity and $f$ the jump size distribution.*

*Proof.* Let us denote the characteristic function of $f$ by $\hat{f}$ and condition the expectation on $N_t$, we have that

$$\begin{aligned}
\mathbb{E}[\exp\{iu\,X_t\}] &= \sum_n \mathbb{E}\left[e^{iu\,X_t}|N_t=n\right]\mathbb{P}[N_t=n]\,, \\
&= \sum_n \mathbb{E}\left[e^{iu\,\sum_{k=1}^n Y_k}|N_t=n\right]\mathbb{P}[N_t=n]\,, \\
&= \sum_n \mathbb{E}\left[e^{iu\,\sum_{k=1}^n Y_k}\right]\mathbb{P}[N_t=n]\,, \\
&= \sum_n \mathbb{E}\left[e^{iu\,Y}\right]^n\mathbb{P}[N_t=n]\,, \\
&= \sum_{n=0}^{\infty}\frac{e^{-\lambda t}(\lambda t)^n(\hat{f}(u))^n}{n!}\,, \\
&= \exp\{\lambda t\,(\hat{f}(u)-1)\}\,, \\
&= \exp\left\{t\lambda\int_{\mathbb{R}^d}(e^{iu.x}-1)f\,(dx)\right\}\,.
\end{aligned}$$

□

## 2.2 Analysis of Jump Measures and Major Results

The sample path of a Lévy process is usually not continuous (i.e. it involves jumps), with the exception of the arithmetic Brownian motion which is the only Lévy process with continuous sample paths. To be able to understand this jump structure, a knowledge of the Lévy measure of the Lévy processes is vital. To achieve this, we first consider random measure and with this, study other measures that will aid the reader in understanding Lévy processes. This will be used in the Lévy-Itô decomposition theorem. This result entails the decomposition of Lévy processes into independent components as will be seen later in this section.

**Definition 2.2.1.** ***(Random measure)***. *Given a probability space $(\Omega,\mathcal{F},\mathbb{P})$ and a measurable space $(E,\mathcal{B})$, we can define a random measure on $(E,\mathcal{B})$ by the map $M:\mathcal{B}\times\Omega\mapsto\mathbb{R}$ iff*

- *For each $B\in\mathcal{B}$, the map $\omega\mapsto M(B,\omega)$ is a random variable on $(\Omega,\mathcal{F},\mathbb{P})$.*
- *The map $B\mapsto M(B,\omega)$ is a measure on $(E,\mathcal{B})$, for almost every $\omega\in\Omega$.*

- *There exist a partition* $B_1, B_2, B_3 \cdots \in \mathcal{B}$ *of* $E$*, such that* $M(B_k) < \infty$ *almost surely for all* $k$*.*

A random measure is a positive measure as illustrated by the third property above with independent increments iff $M(B_1), \ldots, M(B_n)$ are independent random variables. With this notion in mind, we can construct a point process, and then a Poisson random measure. A *point process* is a random measure $M$ on $(E, \mathcal{B})$ if and only if $M$ is $\bar{\mathbb{Z}}_+-$valued (where $\infty$ is included). More so, a *Poisson random measure* with *intensity measure* $\mu$ (where $\mu$ is a $\sigma$-finite measure on $(E, \mathcal{B})$), is a point process $M$ with independent increments such that for every $B \in \mathcal{B}$, $M(B)$ is a Poisson random variable with mean $\mu(B)$, such that

$$\mathbb{P}[M(B) = k] = e^{-\mu(B)} \frac{\mu(B)^k}{k!} \qquad \text{for all } k \in \bar{\mathbb{Z}}_+ \,. \tag{2.4}$$

Another important measure we wish to consider is the jump measure. Given that $H = (0, \infty) \times \mathbb{R}^d \setminus \{0\}$, we have that every Lévy process $X$ has a Poisson random measure $J_X$ on $(H, \mathcal{B}(H))$ (the jump measure) associated with it. This jump measure can be defined as follows:

**Definition 2.2.2.** ***(Jump measure).*** *Let* $(X_t)_{t \geq 0}$ *be a Lévy process on* $\Omega, \mathcal{F}_t, \mathbb{P}$*. For every* $\omega \in \Omega$ *and* $A \in \mathcal{B}(H)$*, the jump measure* $J_X$ *of the process* $X_t$ *is defined by*

$$J_X(\omega, A) = \#\{t : \ (t, \Delta X_t) \in A\} \,. \tag{2.5}$$

$J_X$ is just a counting measure and contains all information about the jumps of the process $X_t$; it tells us when the jumps occur and their sizes too. This implies that $(J_X(t, B))_t$ is a Poisson process for each $B$ and we will want to know what its intensity will be.

**Definition 2.2.3.** ***(Lévy measure).*** *Let* $(X_t)_{t \geq 0}$ *be a Lévy process on* $\mathbb{R}^d$*. The Lévy measure of* $X$ *is the measure* $\nu$ *on* $\mathbb{R}^d$ *defined by:*

$$\nu(B) = \mathbb{E}[\#\{t \in [0, 1] : \ \Delta X_t \neq 0, \ \Delta X_t \in B\}], \qquad B \in \mathcal{B}(\mathbb{R}^d) \,, \tag{2.6}$$

*where* $\nu(B)$ *is the expected number of jumps whose size belongs to* $B$*, per unit time.*

Hence, $(J_X(t, B))_t$ has intensity $\nu(B)$ for any $B$ bounded away from 0. The Lévy measure $\nu$ is a positive measure on $\mathbb{R}^d$ satisfying the following conditions:

$$\nu(\{0\}) = 0 \qquad \text{and} \qquad \int_{\mathbb{R}^d} (1 \wedge |x|^2) \, \nu(dx) < \infty \,. \tag{2.7}$$

This measure describes the expected number of jumps of a certain height in a given time interval. It has no mass at the origin, but singularities (infinitely many jumps) can occur around the origin.

In one dimension, the characteristic function of a compound Poisson process can be given by

$$\mathbb{E}[\exp\{iu\,X_t\}] = \exp\left\{\int_{-\infty}^{\infty}(e^{iux}-1)\,\nu(dx)\right\}\,, \qquad \forall\, u\in\mathbb{R}\,, \tag{2.8}$$

where $\nu = f\lambda$ is the Lévy measure of the process $(X_t)_{t\geq 0}$.

With a knowledge of the above measures, every compound Poisson process can be represented in the following way:

$$X_t = \sum_{s\in[0,t]} \Delta\, X_s = \int_{[0,t]\times\mathbb{R}^d} x\, J_X(ds\,\times\,dx)\,, \tag{2.9}$$

where $J_X$ is a Poisson random measure with intensity measure given as $\nu(dx)dt$. $X$ has only been rewritten as the sum of its jumps. Given a Brownian motion with drift $\gamma t + W_t$, which is independent from $X$, the sum $\tilde{X}_t = X_t + \gamma t + W_t$ defines another Lévy process that can be decomposed as follows:

$$\hat{X}_t = \gamma t + W_t + \sum_{s\in[0,t]} \Delta X_s = \gamma t + W_t + \int_{[0,t]\times\mathbb{R}^d} x\, J_X(ds\,\times\,dx)\,, \tag{2.10}$$

where $J_X$ is a Poisson random measure on $[0,\infty[\,\times\mathbb{R}^d$ with intensity $\nu(dx)dt$. Looking at this, we are confronted with a major question. Can all Lévy processes be represented in this form? This brings us to the discussion of a crucial result in the theory of Lévy processes, the Lévy-Itô decomposition.

**Theorem 2.2.4.** ***(The Lévy Itô Decomposition).*** *Let $(X_t)_{t\geq 0}$ be a Lévy process on $\mathbb{R}^d$ and $\nu$ its Lévy measure. Then*

- *$\nu$ is a positive measure on $\mathbb{R}^d\setminus\{0\}$ and satisfies:*

$$\int_{|x|\leq 1}|x|^2\nu(dx) \;<\; \infty \qquad\qquad \int_{|x|\geq 1}\nu(dx) \;<\; \infty\,.$$

- *The jump measure of $X_t$ given by $J_X$, is a Poisson random measure on $[0,\infty]\times\mathbb{R}^d$ with intensity measure $\nu(dx)dt$.*

- *There exist a constant vector $\gamma$ and a d-dimensional Brownian motion $(B_t)_{t\geq 0}$ with covariance matrix $A$, such that*

$$X_t = \gamma t + B_t + X_t^l + \lim_{\epsilon \downarrow 0} \tilde{X}_t^\epsilon \ , \tag{2.11}$$

*where*

$$\begin{aligned} X_t^l &= \int_{|x|\geq 1, s\in[0,t]} x\, J_X(ds \times dx) \ , \\ \tilde{X}_t^\epsilon &= \int_{\epsilon\leq|x|<1,\, s\in[0,t]} x\{J_X(ds \times dx) - \nu(dx)ds\} \ , \\ &\equiv \int_{\epsilon\leq|x|<1,\, s\in[0,t]} x\, J_X(ds \times dx) \end{aligned}$$

.

*The terms in Equation* (2.11) *are independent and the convergence of $\tilde{X}_t^\epsilon$ is almost sure and also uniform in $t$ on $[0,T]$. Also, $B$ and $\tilde{X}$ are martingales.*

The above theorem entails that there exist a triplet $(\gamma, A, \nu)$, known as the Lévy or characteristic triplet of the process $X_t$ and these uniquely determine the distribution of the process. Lévy [61] found the theorem by using a direct analysis of the paths of Lévy processes and this was completed by Itô [54]. Cont and Tankov [29] present an outline of the proof, while a detailed proof can be found in [80].

The first two terms $(\gamma t + B_t)$ of Equation (2.11) is a continuous Gaussian Lévy process, where $B_t$ is a Brownian motion with covariance matrix $A$ and $\gamma$ its drift. The last two terms are the discontinuous components of the Lévy process and are responsible for the jumps of $X_t$. The condition $\int_{|x|\geq 1} \nu(dx) < \infty$ implies that there exist a finite number of jumps in $X$ whose absolute value is greater than 1. Hence we have that $X_t^l$ is an almost surely finite sum and a compound Poisson process too. $\tilde{X}_t^\epsilon$ is an infinite superposition of independent compensated jump term. It is worth noting that the Brownian motion and compensated jump components, $B_t$ and $\tilde{X}_t^\epsilon$ respectively are the only components of Equation (2.11) that are martingales. The Lévy-Itô decomposition implies that every Lévy process can be approximated by the sum of a Brownian motion with drift and a compound Poisson process. This is very important especially in the simulation of Lévy processes.

Next, we shall consider another fundamental result which entails expressing the characteristic function of a Lévy process in terms of its Lévy triplet $(\gamma, A, \nu)$. This is very important

to us as it gives a general representation for the characteristic function of any infinitely divisible distribution and a special representation for the characteristic exponent of Lévy processes.

**Theorem 2.2.5.** ***(Lévy-Khinchin Representation).*** *Let $(X_t)_{t\geq 0}$ be a Lévy process on $R^d$. Then the characteristic function is given by the representation:*

$$\mathbb{E}[e^{iu.X_t}] = e^{t\,\psi(u)}\,, \quad u \in \mathbb{R}^d\,, \tag{2.12}$$

*with*

$$\psi(u) = -\frac{1}{2}u.Au + i\gamma.u + \int_{\mathbb{R}^d}\left(e^{iu.x} - 1 - iu.x\,1_{|x|\leq 1}\right)\nu(dx)\,, \tag{2.13}$$

*where $\gamma \in \mathbb{R}^d$, $A$ is a $d \times d$ matrix with positive real valued entries, $\nu$ is the Lévy measure and $\psi(u)$ is the Lévy or characteristic exponent.*

For a proof, see Theorem 8.1 in Sato [80].

For a real-valued Lévy process, the Lévy-Khinchin formula is given by:

$$\mathbb{E}[e^{iuX_t}] = e^{t\psi(u)}, \quad u \in \mathbb{R}$$

with

$$\psi(u) = -\frac{1}{2}Au^2 + i\gamma\,u + \int_{-\infty}^{\infty}(e^{iux} - 1 - iux\,1_{|x|\leq 1})\nu(dx)\,.$$

We can also obtain a similar representation for the Lévy-Khinchin formula by truncating the jumps that are larger than an arbitrary number $\epsilon$ using:

$$\psi(u) = -\frac{1}{2}Au^2 + i\gamma^{\epsilon}\,u + \int_{\mathbb{R}^d}(e^{iux} - 1 - iux\,1_{|x|\leq \epsilon})\nu(dx)\,,$$

where

$$\gamma^{\epsilon} = \gamma + \int_{\mathbb{R}^d} x(1_{|x|\leq\epsilon} - 1_{|x|\leq 1})\nu(dx)\,.$$

Also, the truncation of large jumps will not be necessary if the Lévy measure satisfies the condition that $\int_{|x|\geq 1}|x|\nu(dx) < \infty$. Hence we can now make use of the expression

$$\psi(u) = -\frac{1}{2}u.Au + i\gamma_c\,u + \int_{\mathbb{R}^d}(e^{iux} - 1 - iux)\nu(dx)\,,$$

where $\mathbb{E}[X_t] = \gamma_c\,t$ and $\gamma_c$ is referred to as the center of the process $X_t$. $\gamma$ is related to $\gamma_c$ by the expression $\gamma_c = \gamma + \int_{|x|\geq 1} x\nu(dx)$. Given that a distribution $F$ is infinitely divisible, we can express its characteristic function using the Lévy-Khinchin formula by the following:

$$\phi_F(u) = e^{\psi(u)}, \quad u \in \mathbb{R}^d\,, \tag{2.14}$$

where $\psi(u)$ is defined as in Equation (2.13) and the Lévy measure $\nu$ of the distribution satisfies that

$$\int_{|x|\leq 1} |x|^2 \nu(dx) < \infty \qquad \text{and} \qquad \int_{|x|\geq 1} \nu(dx) < \infty \,.$$

If we have that almost all the trajectories of a Lévy process are piecewise constant, then its characteristic triplet can be written as $(\gamma, 0, \nu)$, where $A = 0$, and $\gamma = \int_{|x|\leq 1} x\nu(dx)$. It is necessary to note that $\gamma$ is not necessarily the drift of a Lévy process which is the case here as the compound Poisson process has no continuous part. The major result presented in this section allows us to work with the Lévy triplet instead of the characteristic function of Lévy processes which are most times quite complicated.

Another important notation we shall consider is the variation of a function as this plays a vital role in classifying Lévy processes. The total variation of a function $g : [a, b] \to \mathbb{R}^d$ is defined by

$$TV(g) = \sup \sum_{i=1}^{n} |g(t_i) - g(t_{i-1})| \,,$$

where the supremum is taken over all finite partitions of the interval $[a, b]$. A Lévy process is said to be of finite variation iff its characteristic triplet $(\gamma, A, \nu)$ satisfies $A = 0$ and $\int_{|x|\leq 1} x\nu(dx) < \infty$. Finite variation Lévy processes are said to be more robust than those with continuous sample paths [62]. Considering this, the Lévy-Itô decomposition and Lévy-Khinchin representation can be simplified as [29]:

**Corollary 2.2.6.** *Given that $(X_t)_{t\geq 0}$ is a Lévy process of finite variation with Lévy triplet $(\gamma, 0, \nu)$, $X$ can be expressed as the sum of its jumps between 0 and $t$ and a linear drift term:*

$$X_t = bt + \int_{[0,t]\times\mathbb{R}^d} x J_X(ds \times dx) = \sum_{s\in[0,t]}^{\Delta X_s \neq 0} \Delta X_s \,, \tag{2.15}$$

*while the characteristic function is given by*

$$\mathbb{E}[e^{iu.X_t}] = \exp\left\{ t\left( ibu + \int_{\mathbb{R}^d} (e^{iu.x} - 1)\nu(dx) \right) \right\} \,, \tag{2.16}$$

*where $b = \gamma - \int_{|x|\leq 1} x\nu(dx)$.*

## 2.3 Subordinators

Subordinators are processes with non-negative increments and are crucial to our work as all our models are simulated via subordination of other Lévy processes, as will be seen in the next chapter. These processes form a sub-class of Lévy processes that are easy to deal with mathematically. Subordination involves a random time-change by an independent subordinator. A subordinator can be defined by

**Definition 2.3.1.** ***(Subordinator)*** *Let $(S_t)_{t\geq 0}$ be a Lévy process on $\mathbb{R}$. It is called a subordinator if it satisfies one of the following equivalent properties [29]:*

- *$S_{t\geq 0}$ a.s. for some $t > 0$.*
- *$S_{t\geq 0}$ a.s. for all $t > 0$.*
- *Sample paths of $S_t$ are almost surely non-decreasing: $t \geq s \Rightarrow X_t \geq X_s$.*
- *The characteristic triplet $(\gamma, A, \nu)$ of $S_t$ satisfies that $A = 0$, $\nu((-\infty, 0]) = 0$, $\int_{(0,1)} x\nu(dx) < \infty$ and $\gamma \geq 0$. This implies that $S_t$ has no diffusion component, has only positive jumps of finite variation and positive drift too.*

Subordinators can be used as time changes for other Lévy processes. This we shall discuss in the next section. Before we go into that, we shall consider another interesting concept which is the subordination of a Lévy process. From definition 2.3.1, the trajectories of $S_t$ are almost surely increasing as $S_t$ is a positive random variable for all $t$. We can then represent the moment generating function of $S_t$ in terms of the Laplace exponent, $l(u)$, in place of the characteristic exponent, $\psi(u)$ by [29]:

$$\mathbb{E}[e^{u\,S_t}] = e^{t\,l(u)} \quad \forall u \leq 0 \text{ , where } l(u) = \hat{\gamma}u + \int_0^\infty (e^{ux} - 1)\rho(dx) \text{ .} \tag{2.17}$$

The characteristic triplet is given by $(\hat{\gamma}, 0, \rho)$. The use of the process $S$ as a time-change for other Lévy processes is illustrated by the following theorem:

**Theorem 2.3.2.** ***(Subordination of a Lévy Process)*** *Fix $(\Omega, \mathcal{F}, \mathbb{P})$ to be a probability space. Let $(X_t)_{t\geq 0}$ be a Lévy process on $\mathbb{R}^d$ with characteristic exponent $\psi(u)$ and triplet $(\gamma, A, \nu)$. Let $(S_t)_{t\geq 0}$ be a subordinator with Laplace exponent $l(u)$ and triplet $(\hat{\gamma}, 0, \rho)$. Then the process $(Y_t)_{t\geq 0}$ defined by:*

$$Y(t, \omega) = X(S(t, \omega), \omega) \quad \text{for each } \omega \in \Omega \text{ ,} \tag{2.18}$$

*is also a Lévy process with characteristic function given by:*

$$\mathbb{E}[e^{iuY_t}] = e^{t\,l(\psi(u))}\ . \tag{2.19}$$

*This implies that the characteristic exponent of $Y$ is obtained by composition of the Laplace exponent of $S$ with the characteristic exponent of $X$. Let $p_t^X$ be the probability distribution of $X_t$ then the characteristic triplet $(\gamma^Y, A^Y, \nu^Y)$ of $Y$ is given by:*

$$\gamma^Y = \hat{\gamma}\gamma + \int_0^\infty \rho(ds) \int_{|x|\leq 1} x\, p_s^X(ds)\ , \tag{2.20}$$

$$A^Y = \hat{\gamma}A\ ,$$

$$\nu^Y(B) = \hat{\gamma}\nu(B) + \int_0^\infty p_s^X(B)\,\rho(ds)\,, \quad \forall B \in \mathcal{B}(\mathbb{R}^d)\ . \tag{2.21}$$

*The Lévy process $(Y_t)_{t\geq 0}$ is said to be subordinate to the process $(X_t)_{t\geq 0}$.*

Cont and Tankov [29], present an outline of discussion on this theorem, but the reader is referred to [80] for a detailed proof.

## 2.4 Construction of Lévy Processes

In constructing a Lévy process, a discussion of three popular methods will be given in this section. These methods include Brownian subordination, specifying the probability density and specifying the Lévy measure.

### 2.4.1 Brownian Subordination

To obtain a Lévy process using this approach, we subordinate a Brownian motion by an independent increasing Lévy process (a subordinator). In Finance, this independent increasing process is referred to as 'Business Time' [72]. In this case, we can immediately obtain the characteristic function of the resulting process, but it is also worth emphasizing that explicit formula for the Lévy measure may not always be available. We can characterize Lévy measures of processes that can be interpreted as subordinated Brownian motion with drift using the following theorem:

**Theorem 2.4.1.** *Let $\nu$ be a Lévy measure on $\mathbb{R}$ and $\mu \in \mathbb{R}$. Then there exists a Lévy process $(X_t)_{t\geq 0}$ with Lévy measure $\nu$ such that $X_t = W(Z_t) + \mu Z_t$ for some subordinator*

*$(Z_t)_{t\geq 0}$ and some Brownian motion $(W_t)_{t\geq 0}$ independent from $Z$ if and only if the conditions below are satisfied:*

1. *$\nu$ is absolutely continuous with density $\nu(x)$.*
2. *$\nu(x)e^{-\mu x} = \nu(-x)e^{\mu x}$ for all $x$.*
3. *$\nu(\sqrt{u})e^{-\mu\sqrt{u}}$ is a completely monotonic function[2] on $(o, \infty)$.*

*Proof.* See Cont and Tankov [29]. □

With this theorem in mind, one can describe the jump structure of a process which can be represented as time-changed Brownian motion with drift. Also, this time-changed Brownian motion representation can be deduced for an exponentially tilted Lévy measure from the representation for its symmetric modification.

The simulation of processes using this method is quite easy if we actually know how to simulate the subordinator. Examples of Brownian subordinated models include the variance gamma process, where the Brownian motion is time-changed by the gamma process and the normal inverse Gaussian process, where Brownian motion is time-changed by the inverse Gaussian process.

### 2.4.2 Specifying the Probability Density

For this method, we specify an infinitely divisible density as the density of increments at a given time scale, $\Delta$. Estimation of the parameters of the distribution is quite easy if the data are actually sampled with the same period and also, the simulation of the increments of the process is easy as long as it is carried out on the same time scale. This approach is used for the construction of the generalized hyperbolic (GH) processes. The Lévy measure is also not known in this method and hence, the law of increments is unknown at other time scales. Lastly, we cannot infer the nature of the process from its density (i.e. whether it contains a Gaussian component or whether it is a process with finite or infinite variation/activity).

[2] A function $f : [a, b] \to \mathbb{R}$ is said to be completely monotonic if all its derivatives exist and $(-1)^k \frac{d^k f(u)}{du^k} > 0$ for all $k \geq 1$.

### 2.4.3 Specifying the Lévy Measure

This method involves the direct specification of the Lévy measure. A major advantage of this method is that one has a clear picture of the path-wise properties of the process as a result of the specification of the jump structure of the process. The distribution of the process at any time can be obtained from the Lévy-Khinchin formula though in some cases, this may not be so explicit. Estimation of the parameters of the process can be done by approximating the transition density. The use of this method exposes one to a rich variety of models, but simulation is quite an involved process here. The tempered stable processes are examples of models that can be simulated using this method.

# Chapter 3

# Models Driven by Lévy Dynamics

In this chapter, we discuss in detail some of the models for asset pricing driven by Lévy dynamics. Our choice of models is based on some advantages of these models over others which include that they have been widely studied or used. Their theory is often simple and aids the simulation of these processes with ease as compared to others whose theories are more complicated. We pay attention to their characteristic function, Lévy triplets and some other important properties. Their density functions will not be given much attention in this work as we hope to price vanilla options using the characteristic function of these processes via the fast Fourier transform method introduced by Carr and Madan [25]. We shall also compute moments, variance, skewness and kurtosis where possible. The models we have chosen for discussion include: the variance gamma model, the normal inverse Gaussian model and the CGMY model. Other models driven by Lévy dynamics include the generalized hyperbolic model [34] and the Meixner model [85].

A discussion on the procedures for the simulation of these processes will also be carried out in this chapter. We shall conclude by fitting historic returns data of INTC, DELL, IBM and S&P 500 index to these model. This density fit will be carried out via the FFT method using the characteristic functions of the models. The fitting is aimed at showing why these models are prefered for modeling returns dynamics. We begin with an overview of the models.

## 3.1 The Variance Gamma Model

The variance gamma process was introduced by Madan and Seneta [63]. In their paper, they presented a symmetric version of the process. An extension to allow for a risk neutral asymmetric form in the model was presented by Carr, Cheng and Madan [22], and they also presented a closed form formula for European options under this model. The pricing of American options under this model was carried out by Hirsa and Madan [46]. Fiorani [36] presents numerical solutions for European and America barrier options under this model using the finite difference scheme. This model is a purely discontinuous process which was introduced as an extension of the geometric Brownian motion in order to help overcome the weaknesses of the Black-Scholes model.

The variance gamma (VG) model is a three parameter $(\sigma, \nu, \theta)$ model for the dynamics of the logarithm of the stock price. This model is also an evaluation of Brownian motion with drift $\theta$ and volatility $\sigma$ at a gamma time, this implies replacing the time in the Brownian motion with a gamma process [38]. It allows one to control the skewness via the parameter $\theta$, and the kurtosis of the distribution of stock price returns through the $\nu$ parameter. Let the process $b(t; \theta, \sigma)$ given by

$$b(t; \theta, \sigma) = \theta t + \sigma W(t)\,, \tag{3.1}$$

be a Brownian motion with drift $\theta$ and volatility $\sigma$, where $W(t)$ is a standard Brownian motion and another process $\gamma(t; \mu, \nu)$ be a gamma process of independent gamma increments over non-overlapping intervals of time $(t, t+h)$, with mean rate $\mu$ and variance rate $\nu$. We can define the VG process $X(t; \sigma, \nu, \theta)$ in terms of the Brownian motion with drift $b(t; \theta, \sigma)$ and the gamma process with unit mean rate $\gamma(t; 1, \nu)$ by

$$X(t; \sigma, \nu, \theta) = b(\gamma(t; 1, \nu); \theta, \sigma)\,. \tag{3.2}$$

The density function for the variance gamma process at time $t$ can be expressed as a normal density function conditional on the realization of the gamma time change, $g = \gamma(t+h; \mu, \nu) - \gamma(t; \mu, \nu)$. Integrating over the gamma distributed increments $g$, and employing its density given by

$$f_h(g) = \left(\frac{\mu}{\nu}\right)^{\frac{\mu^2 h}{\nu}} \frac{g^{\frac{\mu^2 h}{\nu}-1} \exp(-\frac{\mu}{\nu} g)}{\Gamma(\frac{\mu^2 h}{\nu})},\ g > 0, \qquad \text{where } \Gamma(x) \text{ is the gamma function}\,, \tag{3.3}$$

the unconditional density of the variance gamma process $X(t)$ is obtained as [22]:

$$f_{X(t)}(X) = \int_0^\infty \frac{1}{\sigma\sqrt{2\pi g}} \exp\left(-\frac{(X-\theta g)^2}{2\sigma^2 g}\right) \frac{g^{\frac{t}{\nu}-1}\exp(-\frac{g}{\nu})}{\nu^{\frac{t}{\nu}}\Gamma(\frac{t}{\nu})} dg\,. \tag{3.4}$$

This process has a characteristic function given by [81]:

$$\phi_{VG}(u;\sigma,\nu,\theta) = \left(1 - iu\theta\nu + \frac{1}{2}\sigma^2\nu u^2\right)^{-\frac{1}{\nu}}\,. \tag{3.5}$$

Considering that this distribution is infinitely divisible, we have that

$$\begin{aligned}\mathbb{E}\left[e^{iuX_{VG}(t)}\right] &= \phi_{VG}(u;\sigma\sqrt{t},\nu/t,t\theta)\\ &= (\phi_{VG}(u;\sigma,\nu,\theta))^t\\ &= \left(1 - iu\theta\nu + \frac{1}{2}\sigma^2\nu u^2\right)^{-\frac{t}{\nu}}\,.\end{aligned} \tag{3.6}$$

Carr, Chang and Madan [22] showed that the variance gamma process can be expressed as the difference of two independent gamma processes. With this characterization, the Lévy density can be determined as shown below [23]:

$$\nu_{VG}(dx) = \begin{cases} \dfrac{C\exp\{Gx\}}{|x|}dx\,, & x<0,\\ \dfrac{C\exp\{-Mx\}}{x}dx\,, & x>0\,,\end{cases}$$

where

$$\begin{aligned} C &= \frac{1}{\nu}\,,\\ G &= \left(\sqrt{\frac{\theta^2\nu^2}{4}+\frac{\sigma^2\nu}{2}}-\frac{\theta\nu}{2}\right)^{-1}\,,\\ M &= \left(\sqrt{\frac{\theta^2\nu^2}{4}+\frac{\sigma^2\nu}{2}}+\frac{\theta\nu}{2}\right)^{-1}\,.\end{aligned}$$

The first four central moments of the return distribution over an interval of length $t$ can be found in [22]. Below is a table which shows the mean, variance, skewness and kurtosis for when $\theta = 0$ and otherwise.

| | $VG(\sigma,\nu,\theta)$ | $VG(\sigma,\nu,0)$ |
|---|---|---|
| Mean | $\theta$ | 0 |
| Variance | $\sigma^2+\nu\theta^2$ | $\sigma^2$ |
| Skewness | $\theta\nu(3\sigma^2+2\nu\theta^2)/(\sigma^2+\nu\theta^2)^{\frac{3}{2}}$ | 0 |
| Kurtosis | $3(1+2\nu-\nu\sigma^4(\sigma^2+\nu\theta^2)^{-2})$ | $3(1+\nu)$ |

From the above table it can be seen that when $\theta = 0$, the kurtosis is $3(1+\nu)$, this implies that $\nu$ is the percentage excess kurtosis over that of a Standard Normal.

The variance gamma process has infinitely many jumps in any finite interval and also has paths of finite variation as

$$\int_{-1}^{1} |x| \nu_{VG}(dx) < \infty .$$

The VG process has no Brownian component and its Lévy triplet is given by $[\gamma, 0, \nu_{VG}(dx)]$, where

$$\gamma = \frac{-C(G(\exp\{-M\} - 1) - M(\exp\{-G\} - 1))}{MG} .$$

With the parameterization in terms of $C, G, M$, the characteristic function of the VG process can be written as

$$\phi_{VG}(u; C, G, M) = \left( \frac{GM}{GM + (M - G)iu + u^2} \right)^C . \tag{3.7}$$

It is worth noting that the parameter $C = 1/\nu$ controls the overall activity rate of the process as shown by Figure 3.1, while the parameters $G$ and $M$ govern the rate at which arrival rates decline with the size of the move. The greater the value of $C$ (that is, when $\nu$ is very small), the more the trajectory looks like a typical stock price process. The parameter $\theta$ measures the directional premium since it majorly affects the skewness of the process [24]. When $\theta = 0$ then $G = M$ and this gives rise to a symmetric distribution. For $\theta < 0$, we have a resulting case of negative skewness as $G < M$. The opposite holds when $\theta > 0$. Likewise, the kurtosis of the distribution is controlled by the parameter $\nu = \frac{1}{C}$. Another important fact to note is that the representation of this model makes its simulation easy since the distribution of increments is known. This process can be simulated as the difference of two independent gamma processes or by subordinating the standard Brownian motion or a Brownian motion with drift by an independent positive Lévy process (gamma process).

## 3.2 The Normal Inverse Gaussian Model

The normal inverse Gaussian (NIG) process was introduced by Barndorff-Nielsen [6] in 1995. In his paper, he only proposed it as a possible model for financial data. The process

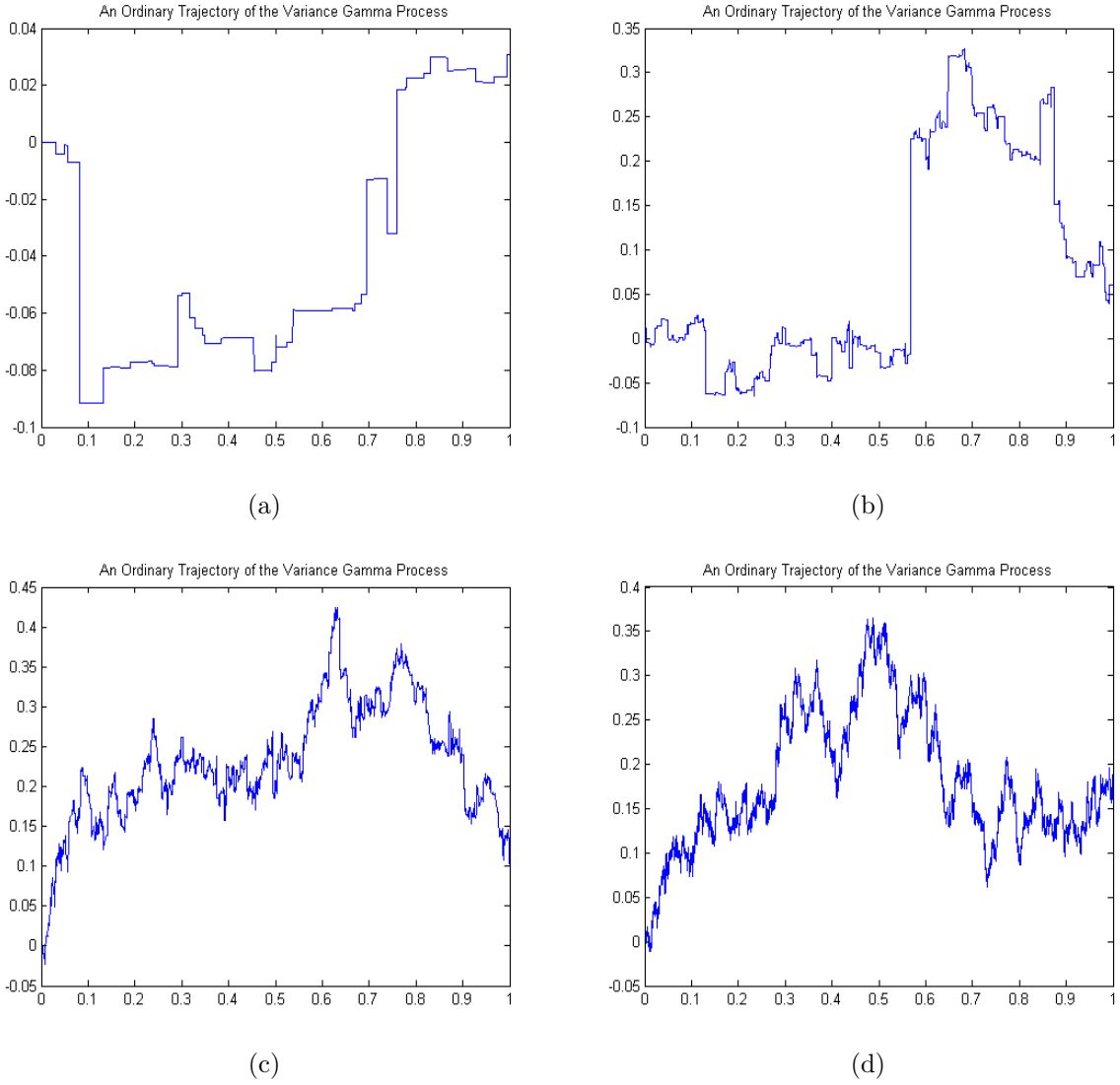


(a) (b)

(c) (d)

**Figure 3.1.** Typical trajectories of the variance gamma process. All trajectories were simulated with $\sigma = 0.3$ and $\theta = 0.05$. The varying parameter $\nu$ is 0.22, 0.022, 0.002, and 0.00022 for (a), (b), (c) and (d) respectively. These parameters were chosen at random.

derives its name from its representation as the distribution of Brownian motion with drift time changed by a subordinator (the inverse Gaussian Lévy process). Rydberg [79] showed that it is capable of accurately modeling the returns on a number of assets on German, Danish, and U.S. exchanges. This model has been investigated by a number of authors ([7], [8], [84], [24], [34], [91], and [1]), and applied to option valuation under several frameworks.

There are several common parametrizations of the NIG process. Some of them use four

parameters. However, we use a three-parameter representation given in [79] and [81]. This model is an infinitely divisible process with stationary increments and has its characteristic function defined by

$$\phi_{NIG}(u;\alpha,\beta,t\delta) = \exp\{-t\delta(\sqrt{\alpha^2-(\beta+iu)^2}-\sqrt{\alpha^2-\beta^2})\}\ , \tag{3.8}$$

where $\alpha > 0$, $-\alpha < \beta < \alpha$ and $\delta > 0$. The Lévy measure for the NIG process has the simplified form

$$\nu_{NIG}(dx) = e^{\beta x}\frac{\delta\alpha}{\pi|x|}K_1(\alpha|x|)dx\ ,$$

where $K_\lambda(x)$ is the modified Bessel function of the third kind with index $\lambda$. Also, the density of the NIG distribution is given by

$$f_{NIG}(x;\alpha,\beta,\delta) = \frac{\delta\alpha}{\pi}\exp\{\delta\sqrt{\alpha^2-\beta^2}+\beta x\}\frac{K_1(\alpha\sqrt{\delta^2+x^2})}{\sqrt{\delta^2+x^2}}\ . \tag{3.9}$$

The NIG distribution is a special case of the Generalized Hyperbolic (GH) distribution for $\lambda = -\frac{1}{2}$. This is the only subclass of the GH that is closed under convolution (see [72]) i.e if $X \sim NIG(\alpha,\beta,\delta_1)$ and $Y \sim NIG(\alpha,\beta,\delta_2)$ with $X$ independent of $Y$, then

$$X + Y \sim NIG(\alpha,\beta,\delta_1+\delta_2)\ .$$

The NIG process has no Brownian component and its Lévy triplet is given by $[\gamma, 0, \nu_{NIG}(dx)]$, where

$$\gamma = \frac{2\delta\alpha}{\pi}\int_0^1 \sinh(\beta x)K_1(\alpha x)dx\ .$$

The NIG process is an infinite variation process with stable-like variation of small jumps. The NIG distribution is symmetric if $\beta = 0$. Below is the sample path of the NIG model and a table that shows some characteristics of the NIG distribution [81]:

| | $NIG(\alpha,\beta,\delta)$ | $NIG(\alpha,0,\delta)$ |
|---|---|---|
| Mean | $\delta\beta/\sqrt{\alpha^2-\beta^2}$ | 0 |
| Variance | $\alpha^2\delta(\alpha^2-\beta^2)^{-\frac{3}{2}}$ | $\delta/\alpha$ |
| Skewness | $3\beta\alpha^{-1}\delta^{-1}(\alpha^2-\beta^2)^{-\frac{1}{4}}$ | 0 |
| Kurtosis | $3\left(1+\frac{\alpha^2+4\beta^2}{\delta\alpha^2\sqrt{\alpha^2-\beta^2}}\right)$ | $3(1+\delta^{-1}\alpha^{-1})$ |

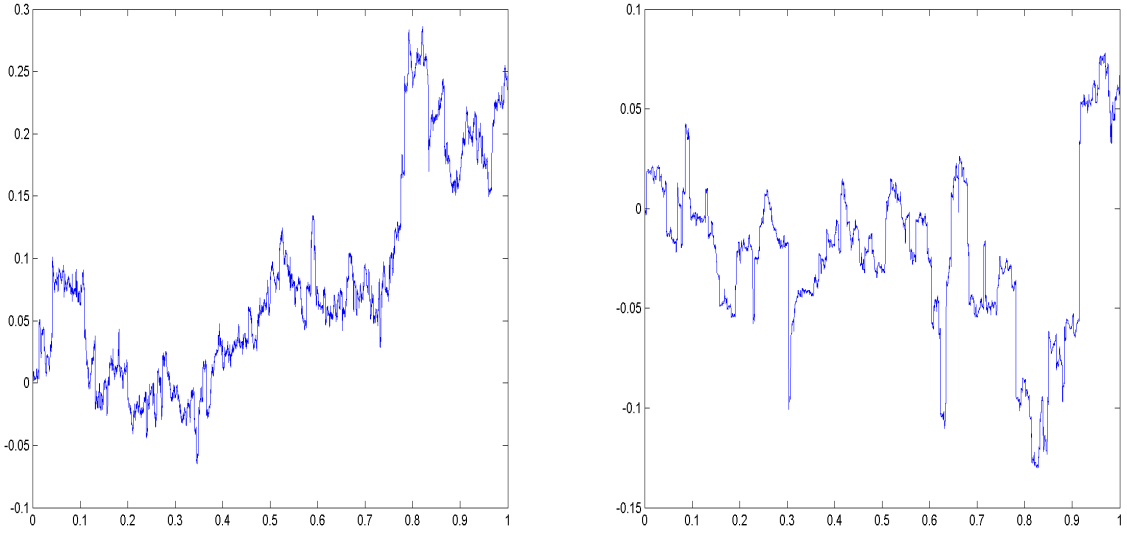

(a) NIG sample path with $\kappa = 0.05$.

(b) NIG sample path with $\kappa = 0.9$.

**Figure 3.2.** Simulated trajectories of the NIG process with $\sigma = 0.3$, $\theta = 0.1$ and $\kappa = 0.05,\ 0.9$ respectively. These trajectories were simulated using Algorithm 3.4.3.

## 3.3 The CGMY Model

The CGMY process unlike the two processes described above is a four-parameter distribution. This process was introduced by Carr, Geman, Madan and Yor [23] as a generalization of the VG process. This model was analysed for the pricing of American options in [65] and [2]. A further valuation of European and American options under the CGMY model was carried out in [53]. This model has been used in the literature in other frameworks ([24], [84], [83], [81] and [29]). It was referred to as the generalised tempered stable process in [29]. At different ranges, the parameter $Y$ defines the properties of the process. The Lévy density of the CGMY process is given by

$$\nu_{CGMY}(x) = \begin{cases} \dfrac{C\exp\{-G|x|\}}{(|x|)^{1+Y}}dx\,, & x < 0, \\ \dfrac{C\exp\{-M|x|\}}{|x|^{1+Y}}dx\,, & x > 0\,, \end{cases}$$

where $C > 0$, $G, M \geq 0$ and $Y < 2$. When $Y$ is greater than or equal to two, the model does not yield a valid Lévy measure. Setting $Y = 0$ yields the VG process. For $Y < 0$ we have a process of finite activity and variation, while for $0 \leq Y < 1$ the process is of infinite

activity but finite variation. For $1 \leq Y < 2$, the process has infinite activity and infinite variation as is the case with the NIG process.

The characteristic function of the CGMY distribution is given by

$$\phi_{CGMY}(u; C, G, M, Y) = \exp\{C\Gamma(-Y)((M - iu)^Y - M^Y + (G + iu) - G^Y)\} . \quad (3.10)$$

The CGMY distribution is an infinitely divisible process with independent increments, hence we can define the characteristic function of a CGMY Lévy process $X_t^{CGMY}$ by

$$\begin{aligned} \mathbb{E}\left[e^{iuX_t^{CGMY}}\right] &= \phi_{CGMY}(u, t; C, G, M, Y) , \\ &= (\phi_{CGMY}(u; C, G, M, Y))^t , \\ &= \exp\{tC\Gamma(-Y)[(M - iu)^Y - M^Y + (G + iu) - G^Y]\} . \end{aligned} \quad (3.11)$$

*Proof.* From the Lévy-Khinchin theorem, we have

$$\phi_{CGMY}(u, t) = \exp\left(t \int_{-\infty}^{\infty} (e^{iux} - 1)\nu_{CGMY}(x)dx\right) . \quad (3.12)$$

If we write the integral in Equation (3.12) as the sum of two integrals of the form

$$\int_0^{\infty} (e^{iux} - 1)\, C\frac{\exp(-\beta x)}{x^{1+Y}}\, dx , \quad (3.13)$$

where $\beta = G, M$, respectively, with $iu$ replaced by $-iu$ for $\beta = G$, we have that

$$\begin{aligned} &\int_0^{\infty} \frac{C}{x^{1+Y}} \left(\exp[-(\beta - iu)x] - \exp(-\beta x)\right) dx \\ &= C\left(\int_0^{\infty} (\beta - iu)^Y w^{-Y-1} \exp(-w)\, dw - \int_0^{\infty} \beta^Y w^{-Y-1} \exp(-w)\, dw\right) , \\ &= C\Gamma(-Y)[(\beta - iu)^Y - \beta^Y] . \end{aligned} \quad (3.14)$$

Substituting $\beta$ by $M$ and $G$ in Equation (3.14), and evaluationg the case $\beta = G$ at $-iu$, we obtain the characteristic function given by Equation (3.11). □

The CGMY process does not contain a Brownian component, it is a pure jump process. The Lévy triplets of the CGMY process is given as $[\gamma, 0, \nu_{CGMY}(dx)]$, where

$$\gamma = C\left(\int_0^1 \exp\{-Mx\}x^{-Y}dx - \int_{-1}^0 \exp\{Gx\}|x|^{-Y}dx\right) .$$

Details on the mean, variance, skewness and kurtosis of the CGMY process are presented below (see [81] and [23]).

| | $CGMY(C,G,M,Y)$ |
|---|---|
| Mean | $C(M^Y - 1 - G^Y - 1)\Gamma(1-Y)$ |
| Variance | $C(M^{Y-2} - 1 - G^{Y-2} - 1)\Gamma(2-Y)$ |
| Skewness | $\frac{C(M^{Y-3} - 1 - G^{Y-3} - 1)\Gamma(3-Y)}{[C(M^{Y-2} - 1 - G^{Y-2} - 1)\Gamma(2-Y)]^{3/2}}$ |
| Kurtosis | $3 + \frac{C(M^{Y-4} - 1 - G^{Y-4} - 1)\Gamma(4-Y)}{[C(M^{Y-2} - 1 - G^{Y-2} - 1)\Gamma(2-Y)]^2}$ |

## 3.4 Simulation of Lévy Processes

In this section, we briefly describe simulation algorithms for the Lévy models discussed above. It is important to state at this point that we will be using lines to plot discontinuous paths of these processes for clarity of the graphs. We follow Cont and Tankov [29] closely except where stated otherwise (see also [81], [72], [78] and [15]).

### 3.4.1 Simulation of the Variance Gamma Process

In simulating a sample path of the variance gamma process, one can either do this as the difference of two different gamma processes (see [81]) or as a time-changed Brownian motion [29]. The algorithm for the latter is outlined below.

**Algorithm 3.4.1.** ***Simulation of*** $X_t \sim VG(t;\sigma,\theta,\kappa)$ ***process***

*To simulate a variance gamma (VG) process with parameters* $\sigma,\theta,\kappa$*; we can simulate a discretized trajectory for fixed times* $t_1,\ldots,t_n$ *as follows:*

- *Simulate* $n$ *independent gamma variables* $\Gamma_i$ *with parameter* $\frac{\Delta t_i}{\kappa}$*;*
- *Set* $\Gamma_i = \kappa\Gamma_i$ *for all* $i$*;*
- *Simulate* $n$ *i.i.d.* $N(0,1)$ *variables* $D_i$*;*
- *Set* $\Delta Y_i = \sigma D_i\sqrt{\Gamma_i} + \theta\Gamma_i$.

*The discretized trajectory is*

$$Y_{t_i} = \sum_{k=1}^{i} \Delta Y_k \ .$$

Note that $\sigma$ and $\theta$ are the volatility and drift respectively of the Brownian motion, and $\kappa$ is the variance of the subordinator. Figure 3.3 shows a simulated trajectory of the variance gamma process.

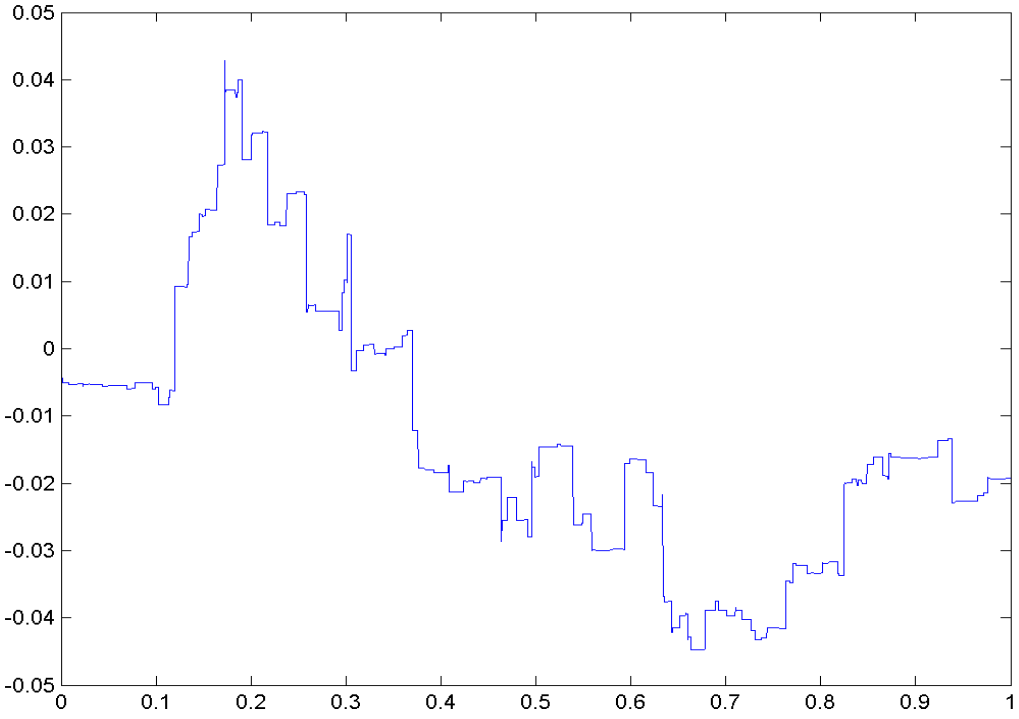


**Figure 3.3.** Simulated trajectory of the variance gamma process

### 3.4.2 Simulation of the Normal Inverse Gaussian Process

The normal inverse Gaussian process just like the variance gamma process can also be simulated as a time-changed Brownian motion. Before we go into the main algorithm for simulating the NIG process, we present an algorithm for simulating the inverse Gaussian random variable.

**Algorithm 3.4.2.** ***Simulating inverse Gaussian variables***

- *Generate a normal random variable $N$;*

- *Set* $Y = N^2$*;*
- *Set* $X_1 = \mu + \frac{\mu^2 Y}{2\lambda} - \frac{\mu}{2\lambda}\sqrt{4\mu\lambda Y + \mu^2 Y^2}$*;*
- *Generate a uniform[0,1] random variable* $U$*;*
- *IF* $U \leq \frac{\mu}{X_1+\mu}$ *RETURN* $X_1$ *ELSE RETURN* $\frac{\mu^2}{X_1}$*.*

**Algorithm 3.4.3.** ***Simulation of*** $X_t \sim NIG(t;\sigma,\theta,\kappa)$ ***process***

*To simulate a normal inverse Gaussian (NIG) process with parameters* $\sigma,\theta,\kappa$*; we can simulate a discretized trajectory for fixed times* $t_1,\ldots,t_n$ *as follows:*

- *Simulate* $n$ *independent inverse Gaussian variables* $I_i$ *with parameters* $\lambda_i = \frac{(t_i - t_{i-1})^2}{\kappa}$ *and* $\mu_i = t_i - t_{i-1}$*,* $t_0 = 0$*;*
- *Simulate* $n$ *i.i.d.* $N(0,1)$ *variables* $D_i$*;*
- *Set* $\Delta Y_i = \sigma D_i\sqrt{I_i} + \theta I_i$ *for all* $i$*.*

*The discretized trajectory is*

$$Y_{t_i} = \sum_{k=1}^{i} \Delta Y_k \ .$$

Figure 3.4 shows a simulated trajectory of the NIG process.

### 3.4.3 Simulation of the CGMY process

The CGMY process, also referred to as the tempered stable process, is one which does not have an elegant simulation algorithm like the processes discussed previously. Rosinki [78] proposed its simulation using a rejection method, Poirot and Tankov [73] showed that under an appropriate equivalent probability measure, a tempered stable process becomes a stable process whose increments can be simulated exactly. This in turn provides a fast Monte Carlo algorithm used in computing the expectation of any functional of a tempered stable process. Finally, Madan and Yor [64] described the CGMY process as a time changed Brownian motion. We follow closely the algorithm outlined in [64].

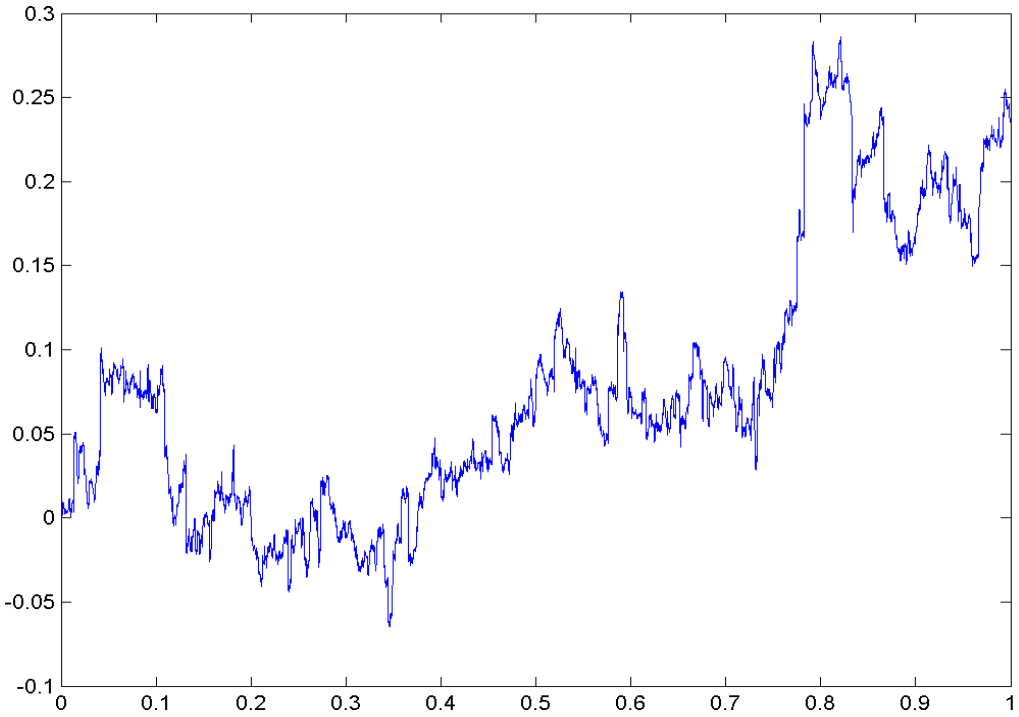


**Figure 3.4.** Simulated trajectory of the NIG process

**Algorithm 3.4.4.** ***Simulation of*** $X_t \sim$***CGMY(t;C,G,M,Y) process***

- *Define* $t = C$ *to be the time step, and let*

$$\begin{aligned} A &= \frac{G-M}{2} \\ B &= \frac{G+M}{2}\,. \end{aligned}$$

- *Next simulate at* $t$ *the one-sided stable subordinator. Let* $\epsilon = 0.0001$ *and truncate jumps below* $\epsilon$ *replacing them by their expected value at a rate of*

$$\begin{aligned} d &= \int_0^{\epsilon} y \frac{1}{y^{1+\frac{Y}{2}}} dy \\ &= \frac{\epsilon^{1-\frac{Y}{2}}}{1-\frac{Y}{2}}\,. \end{aligned}$$

- *Calculate the arrival rate $\lambda$ for jumps bigger than $\epsilon$ by*

$$\begin{aligned}\lambda &= \int_{\epsilon}^{\infty} \frac{1}{y^{1+\frac{Y}{2}}} dy \\ &= \frac{2}{Y} \frac{1}{\epsilon^{Y/2}} .\end{aligned}$$

- *The interval jump times are exponential and are simulated by*

$$t_i = -\frac{1}{\lambda} \log(1 - u_{2i}) ,$$

*where $u_{2i}$ is an independent uniform sequence.*

- *Generate the actual jump times*

$$\Gamma_j = \sum_{i=1}^{j} t_i .$$

- *Generate the jump size $y_j$ given by*

$$y_j = \frac{\epsilon}{(1 - u_{1j})^{\frac{2}{Y}}} ,$$

*where $u_{1j}$ is an independent uniform sequence.*

- *The process $S(t)$ for the stable subordinator is given by*

$$S(t) = dt + \sum_{j=1}^{\infty} y_j 1_{\Gamma_j < t} .$$

- *Simulate the CGMY subordinator $H(t)$ by*

$$H(t) = dt + \sum_{j=1}^{\infty} y_j 1_{\Gamma_j < t} 1_{h(y) > u_{3j}} ,$$

*where $u_{3j}$ is an independent uniform sequence. The calculation of $h(y)$ is presented below.*

- *The CGMY process is given by*

$$X_t = AH(t) + \sqrt{H(t)} W ,$$

*where $W$ is a standard normal random variable.*

***Calculation of the Truncation Function h(y)***

1. $h(y) = e^{-\frac{B^2 y}{2}} \dfrac{\Gamma(\frac{Y+1}{2})}{\Gamma(Y)\,\Gamma(\frac{1}{2})}\, 2^Y \left(\dfrac{B^2 y}{2}\right)^{\frac{Y}{2}} I(Y, B^2 y, \frac{B^2 y}{2})$ .

2. $I(Y, 2\lambda, \lambda) = \dfrac{H_Y(\sqrt{2\lambda})\Gamma(Y)}{(2\lambda)^{\frac{Y}{2}}}$ , *where* $H_\alpha(.)$ *is the Hermite function.*

3. *The Hermite function is explicitly known in terms of the Confluent Hypergeometric function* ${}_1F_1$, *where*

$$\begin{aligned} H_\alpha(z) &= 2^{\alpha/2}\left[\frac{1}{\Gamma(\frac{1-\alpha}{2})\Gamma(\frac{1}{2})}\,{}_1F_1(\frac{-\alpha}{2}, \frac{1}{2}, \frac{z^2}{2})\right] \\ &- 2^{\alpha/2}\left[\frac{z}{\sqrt{2}\Gamma(\frac{-\alpha}{2})\Gamma(\frac{3}{2})}\,{}_1F_1(\frac{1-\alpha}{2}, \frac{3}{2}, \frac{z^2}{2})\right] . \end{aligned}$$

Figure 3.5 shows a simulated path of the CGMY process with a varying of the $Y$ parameter. Similar algorithms can also be found in [29] and [73].

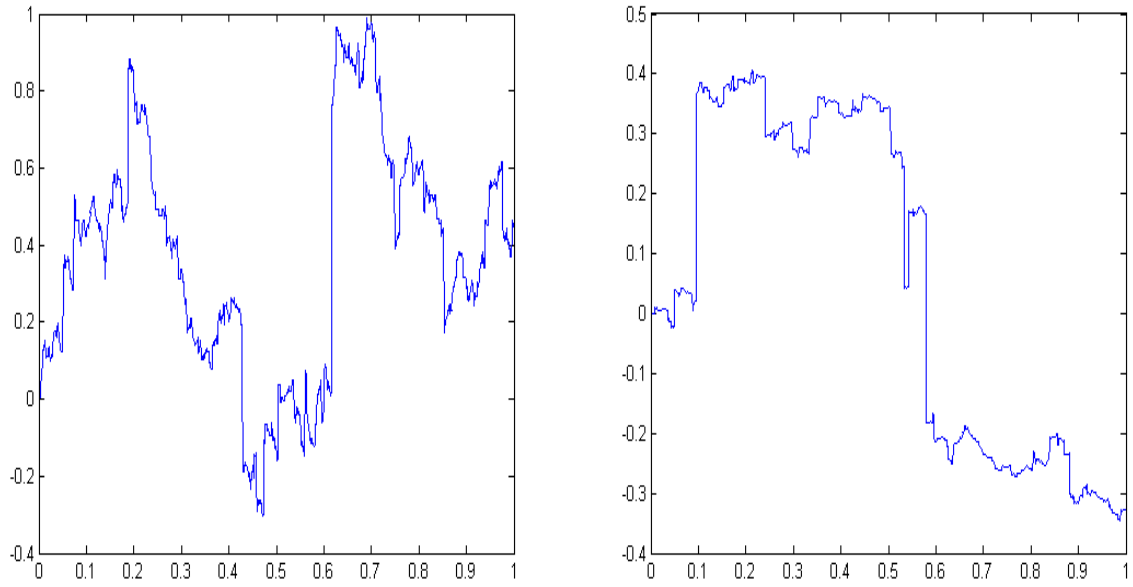


(a) CGMY trajectory with $Y = 1.45$.

(b) CGMY trajectory with $Y = 0.90$.

**Figure 3.5.** Simulated trajectory of the CGMY process with $C = 0.50$, $G = 0.90$, $M = 7.15$ and the $Y$ parameter varied.

The statistical properties of financial time series as suggested by empirical research are not well described by the famous Black-Scholes model. This has led to a search for more suitable models that will describe these properties better. In Chapter 1, we considered the non-Gaussian property of log returns and discovered that they exhibit excess kurtosis and skewness that do not reflect that they are from a normal distribution. In the next section, we proceed to estimate the density of these financial time series. This will further justify our claim and choice of Lévy models as a preferred option.

## 3.5 Density Estimation of Historic Data

The data set used in this section contains daily/weekly log returns of the DELL, IBM, INTC and S&P 500 Index over the period Aug. 17 1988 to Mar. 2 2010. This section entails the fitting of the returns of the major securities under discussion to specific distributions. We shall for each stock/index fit the daily/weekly returns to the normal distribution, an empirical density (kernel density) and our three choice models (VG, NIG, and CGMY). We again fit the weekly returns as a check on whether the daily returns over-fit the given distributions. Below is a discussion on how we estimated the empirical density and the densities of the variance gamma, normal inverse Gaussian and CGMY distributions.

### 3.5.1 Empirical Density

In other to estimate the empirical density, we make use of a non-parametric method of estimating the probability density function of a random variable known as *kernel density* estimator. Estimators of this kind have no given fixed structure, but depend upon all the data points to reach an estimate. Given the random sample $x_1, \ldots, x_n$ with unknown density $f(x)$, the kernel density estimator $\hat{f}_h(x)$ is defined as [56]

$$\hat{f}_h(x) = \frac{1}{nh} \sum_{i=1}^{n} K\left(\frac{x - x_i}{h}\right) , \tag{3.15}$$

where $K$ is the kernel function and $h$ is the bandwidth. The bandwidth is a very important parameter that has a strong influence on the resulting estimate. When $h$ is too small, it leads to an under smoothed kernel density estimate while when it is too large, the density

is over smoothed. This leaves us with a very crucial problem of how best to choose an optimal $h$. There are several ways of choosing this parameter, Turlach [90] gives a review of possible ways of choosing the bandwidth (see also [88]). To estimate this density, we shall be working in MATLAB using the *ksdensity* function which provides an automatic data-driven bandwidth. This function also makes use of the Gaussian kernel which is the most frequently used of all kernel types. Other kernels that exist include Uniform, Triangle, Quartic, Epanechnikov, Triweight and Cosinus kernel functions.

### 3.5.2 Model Density

In estimating the model densities, one needs to know the density function of the distribution and the values of its parameters. For our chosen models, the density function is not known in all cases and may also have a very complex form when known. The parameters are also unknown. To be able to estimate the model densities, we will follow a numerical procedure where the characteristic function of these processes are used. The procedure is as outlined below:

- We use the FFT technique to invert the characteristic functions of the given processes in order to obtain their density functions. This technique introduced by Carr and Madan [25], will be discussed in detail in the next chapter.
- Next, we use the method of Maximum Likelihood estimation (MLE) (details on this will be discussed in the next chapter) to estimate the values of the parameters of our models, for the different returns data of the major securities under consideration. It is important to note that in order to be able to obtain good optimized values for the parameters, one can choose to start with possible values that can be calculated from the data. These will always be a good starting point for the optimization problem as special caution needs to be applied at this stage of the simulation [29].
- After obtaining values of the parameters for the different models, we plug these back into the characteristic function and via the FFT method obtain a data set with which we plot the density function for each of the models.

Below are the probability density plots generated for the variance gamma, normal inverse Gaussian and CGMY models. For each case, we have their corresponding normal density and empirical density. In Figures 3.6 - 3.9, we have the corresponding plots for the weekly log returns of the different securities for the variance gamma model. Similar results were obtained for the normal inverse Gaussian model and the CGMY model. Wu [94] showed that increasing the sample data to five days in a row as against one day gives parameters that are more stabilized and with very low range of errors in its estimation.

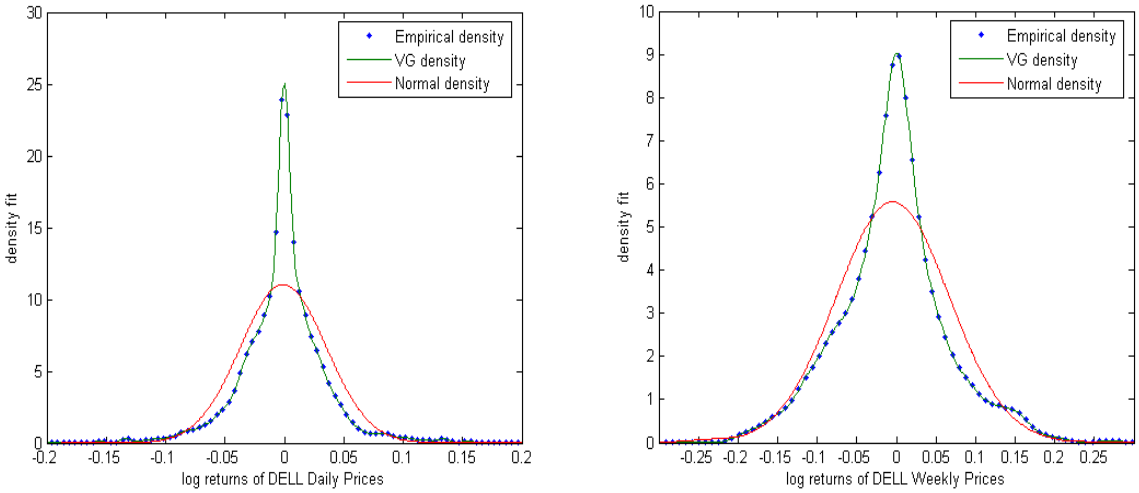


(a) DELL daily data (b) DELL weekly data

**Figure 3.6.** VG density plots for DELL data

From these plots, we see sharp peaked distributions and also a good fit between the empirical and model densities. To be able to justify how well this distributions fit, we need to perform a statistical test on them. This is the focus of the next section.

### 3.5.3 Kolmogorov-Smirnov Test

The Kolmogorov-Smirnov test is a non-parametric test for comparing two distributions. This test is based on the empirical distribution function $F_n$ of a set of sample data. Given $Y_1, \ldots, Y_n$ i.i.d. sample data with some unknown distribution $F$, we want to test the hypothesis that $F$ is equal to a particular distribution $F_0$. We can represent this as follows:

$$H_0 : F = F_0, \qquad H_1 : F \neq F_0 \, .$$

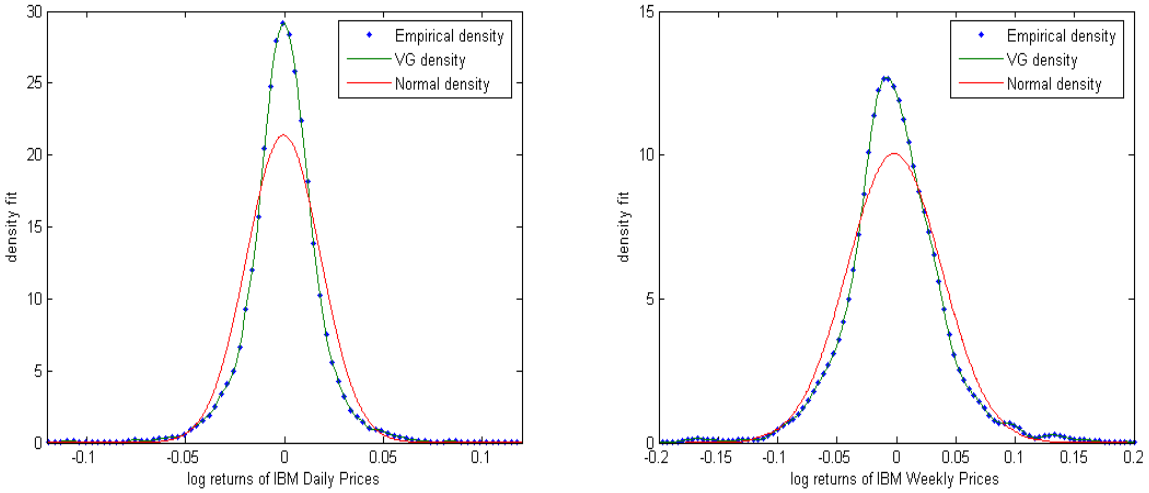


(a) IBM daily data (b) IBM weekly data

**Figure 3.7.** VG density plots for IBM data

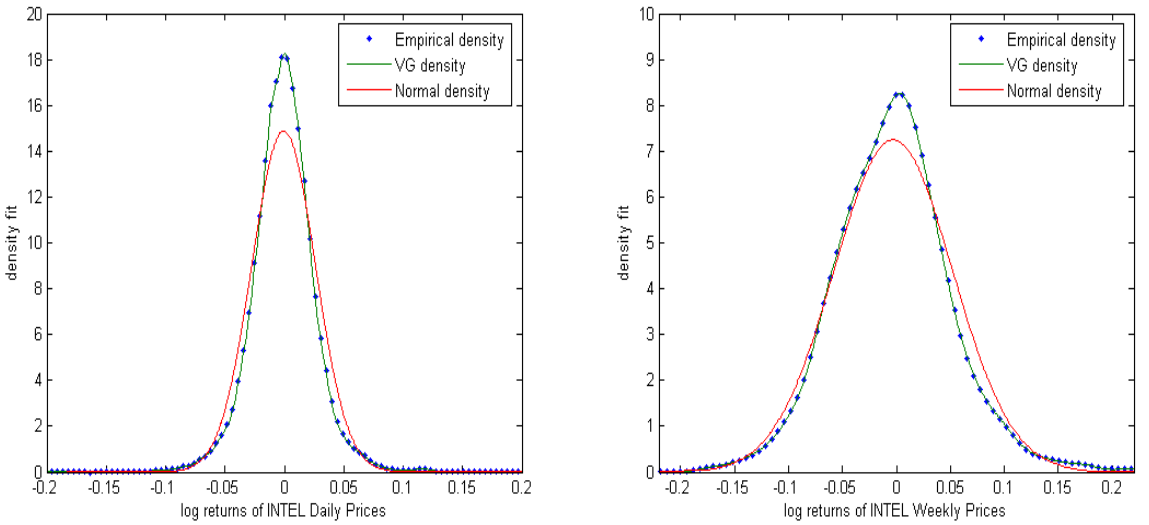


(a) INTC daily data (b) INTC weekly data

**Figure 3.8.** VG density plots for INTC data

To achieve this, we need to obtain a value based on the empirical distribution function known as the *Kolmogorov-Smirnov (K-S) Statistic*. The K-S statistic is the largest deviation of the empirical distribution function from a hypothesized theoretical distribution

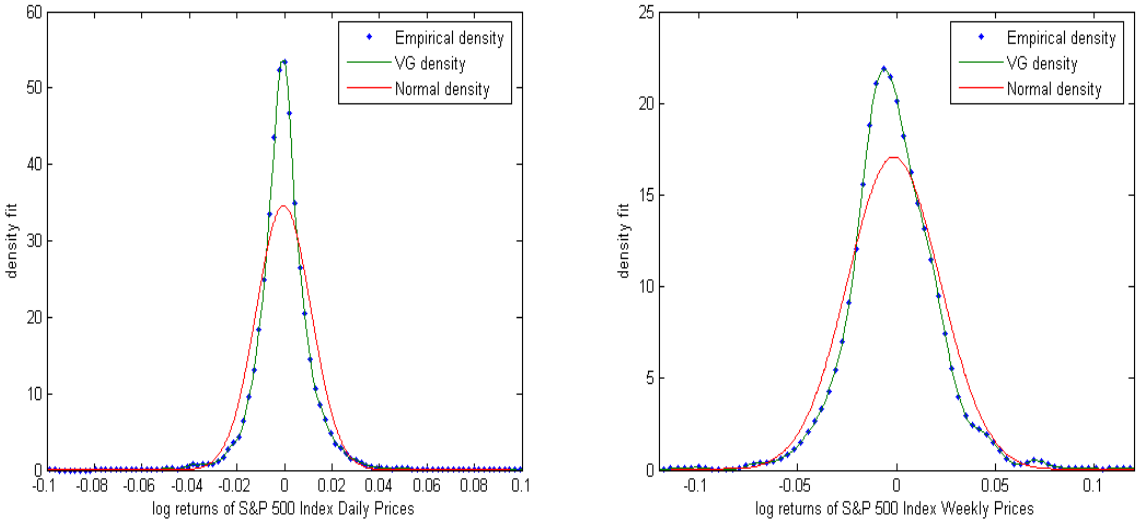


(a) S&P daily data (b) S&P weekly data

**Figure 3.9.** VG density plots for S&P 500 index data

function. Let the empirical distribution $F_n$ for $n$ i.i.d. observations $Y_i$ be defined as

$$F_n(y) = \frac{1}{n} \sum_{i=1}^{n} I_{Y_i \leq y} \ ,$$

where $I_{Y_i \leq y}$ is the indicator function that is equal to 1 if $Y_i \leq y$ and 0 otherwise.

For a given cumulative distribution function $F(y)$, the K-S statistic is given by

$$D_n = \sup_y |F_n(y) - F(y)| \ , \tag{3.16}$$

where $\sup S$ is the supremum of set $S$.

An important feature of this test is that the distribution of the K-S statistic does not in itself depend on the underlying cumulative distribution function that is being tested. Also, due to the fact that it is a non-parametric test, it performs well under a large range of distributional assumptions (i.e. it is robust). It is more powerful than the $\chi^2$ test.

We shall start by testing our data sets for all the major indices to know if they are from a normal distribution. Table 3.1 gives an overview of the result. It is clear that none of our data sets comes from a normal distribution, as our P-values are all less than 0.05 and the test statistic (KSSTAT) is greater than the critical value (CV) for all cases. The

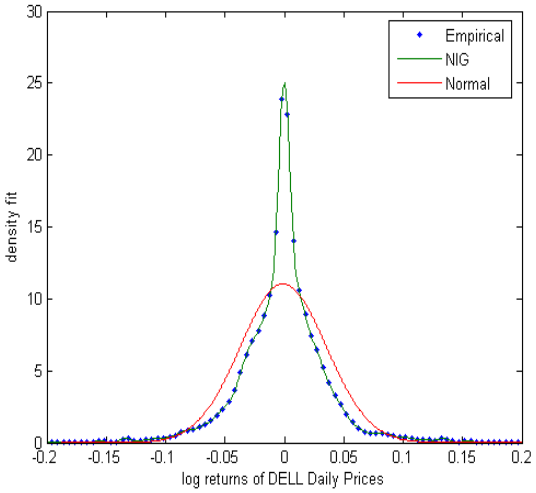


(a) DELL daily data

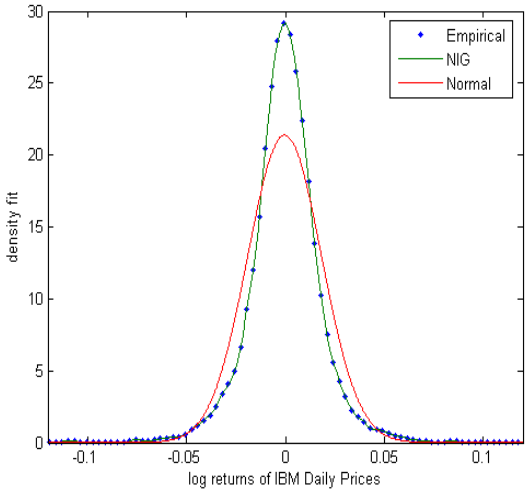


(b) IBM daily data

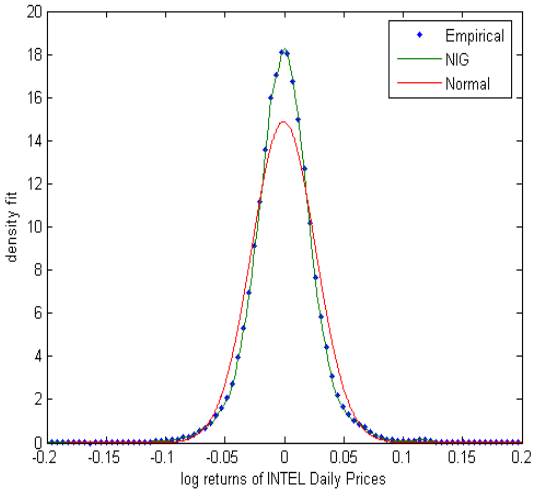


(c) INTC daily data

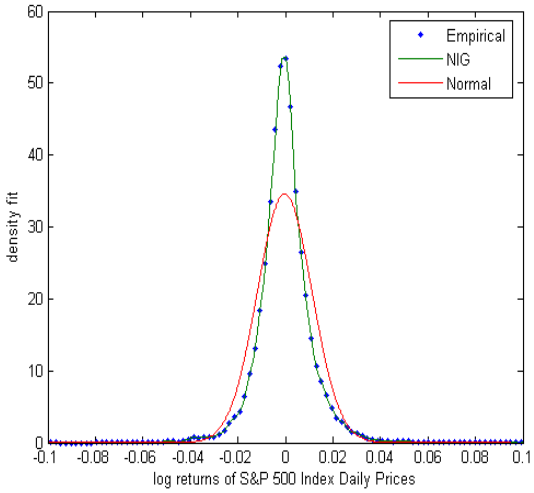


(d) S&P 500 Index daily data

**Figure 3.10.** Density plots for the NIG Model

null hypothesis $H_0$ is rejected for all cases. Next we compare the empirical distribution to the normal and model distributions. From Table 3.2, we can see a higher value for the test statistic for the normal than for the NIG distribution. This goes further to confirm the results we saw in the plots. Similar results were obtained for the VG and CGMY distributions. Therefore we can conclude that the VG, NIG, and CGMY models give better fit to our data than their Gaussian counterpart.

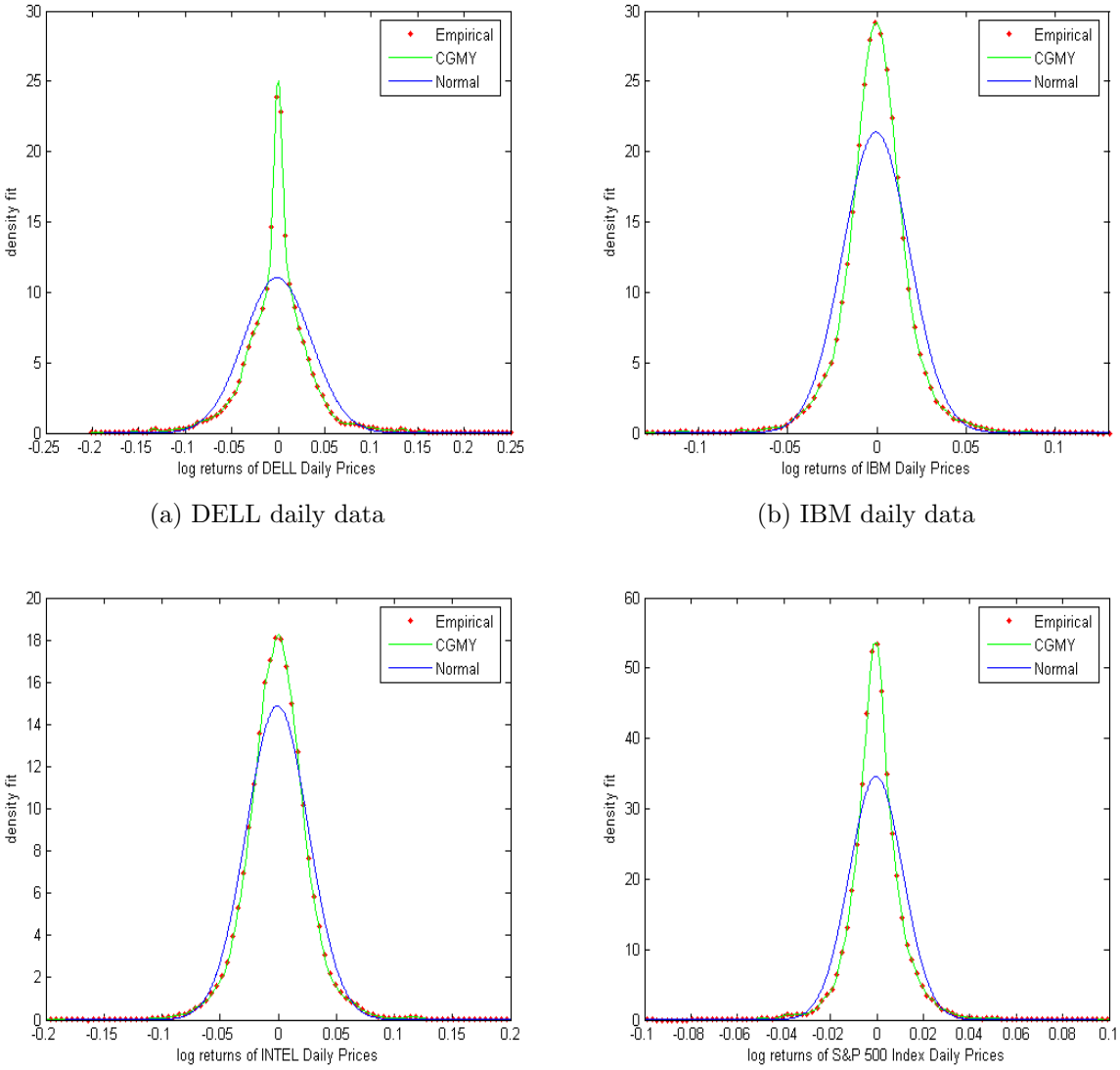


(a) DELL daily data

(b) IBM daily data

(c) INTC daily data

(d) S&P 500 Index daily data

**Figure 3.11.** Density plots for the CGMY Model

| Index | H-value | P-value | KSSTAT | CV | Remark |
|---|---|---|---|---|---|
| IBM | 1 | $2.3439e-022$ | 0.0681 | 0.0184 | Reject $H_0$ |
| IBM Weekly | 1 | $4.4512e-004$ | 0.0610 | 0.0404 | Reject $H_0$ |
| INTC | 1 | $1.0901e-011$ | 0.0488 | 0.0184 | Reject $H_0$ |
| INTC Weekly | 1 | 0.0212 | 0.0448 | 0.0404 | Reject $H_0$ |
| DELL | 1 | $2.5373e-035$ | 0.0859 | 0.0184 | Reject $H_0$ |
| DELL Weekly | 1 | $5.7493e-007$ | 0.0816 | 0.0404 | Reject $H_0$ |
| S&P | 1 | $2.7002e-032$ | 0.0821 | 0.0184 | Reject $H_0$ |
| S&P Weekly | 1 | $6.9830e-004$ | 0.0593 | 0.0404 | Reject $H_0$ |

**Table 3.1.** Kolmogorov-Smirnov test for normality of log returns

| Index | Model | H-value | P-value | KSSTAT | Remark |
|---|---|---|---|---|---|
| DELL | Normal | 1 | $5.8860e-018$ | 0.0860 | Reject $H_0$ |
| | NIG | 0 | 1 | $1.8416e-004$ | Accept $H_0$ |
| IBM | Normal | 1 | $2.2680e-011$ | 0.0680 | Reject $H_0$ |
| | NIG | 0 | 1 | $1.8416e-004$ | Accept $H_0$ |
| INTC | Normal | 1 | $4.5285e-006$ | 0.0488 | Reject $H_0$ |
| | NIG | 0 | 1 | $1.8416e-004$ | Accept $H_0$ |
| S&P | Normal | 1 | $2.0607e-016$ | 0.0822 | Reject $H_0$ |
| | NIG | 0 | 1 | $1.8413e-004$ | Accept $H_0$ |

**Table 3.2.** Kolmogorov-Smirnov test for comparing distributions of daily log returns for the NIG Model

# Chapter 4

# Model Calibration

Calibration to market option prices can also be referred to as an *Inverse Problem*. This is due to the fact that while the pricing problem entails calculating option prices with given model parameters, the calibration problem on the other hand involves obtaining model parameters from observed option prices. It is a well known fact that the prices of barrier options are not quoted on the market like vanilla options. On this note, following the statement made by Emmanuel Derman "If you want to know the value of a security, use the price of another security that is as similar to it as possible. All the rest is modeling" [29], we want to calibrate the prices of vanilla options and with the parameters obtained, go ahead to price barrier options.

The calibration problem is not without challenges, some of which are highlighted below:

- There could exist many pricing models which generate the same prices for the options hereby making the solution of the inverse problem not to be necessarily unique.
- There is need for efficient and stable algorithms in computing a solution for the inverse problem.
- Since we seek risk-neutral models of the exponential-Lévy type, there is no assurance that a solution exists. Hence, we can only look out for the best approximation of the market prices for the given options.
- The calibrated measure could be very sensitive to both input prices and numerical starting point in the minimization algorithm when the calibration constraints

(number of option prices) are not very large.

This chapter is organized as follows: We start by presenting the different methods of calibrating option prices. We then go ahead to give a summary of what pricing in the Lévy framework entails, and hence, the pricing of European options within this framework. A very important concept we will conclude this chapter with is the fast Fourier transform method for the valuation of options as presented by Carr and Madan in [25]. This is crucial as all option prices computed in all calibration procedures in this work, are based on this technique.

## 4.1 Methods of Calibration

In this section, we discuss three different methods of estimating model parameters from a set of data. The methods include: the generalized method of moments (GMM), maximum likelihood estimation (MLE) method and least-squares estimation (LSE). We will give more attention to the last two methods since they are used in this work.

### 4.1.1 Generalized Method of Moments (GMM)

The generalized method of moments calibration technique was introduced by Lars Peter Hansen in 1982 [42]. In his paper, he presents a discussion of the large sample properties of a class of econometric estimators that are defined in terms of orthogonality conditions. This method is a general statistical method for obtaining estimates of parameters of statistical models and does not require an explicit representation of the density function. Its application in the field of finance was presented in [55]. In other to use the GMM technique to estimate parameters, only specified moments derived from an underlying model are needed.

The GMM estimator is efficient when the number of moments conditions equals the number of parameters and also, when we have more moment conditions than parameters. In this method, an estimate of the parameter vector is carried out by minimizing the sum of squares of the differences between the population moments and the sample moments, using the

variance of the moments as a metric [41]. When strong distributional assumptions need to be made about a model, the MLE performs better than the generalized method of moments. For more details on this method, the reader is referred to [42], [55], and [52].

### 4.1.2 Maximum Likelihood Estimation (MLE)

Maximum-likelihood estimation was developed and presented by R. A. Fisher between 1912 and 1922 [58]. MLE is a popular statistical method used for fitting statistical models to data, and providing estimates for the models' parameters. The main idea behind this estimation technique is to determine the parameter values that maximize the probability (likelihood) of the sample data. MLE focuses on knowing the density function of the given distribution and where this is mis-specified, it leads to inconsistent estimation of the parameters. A description of how this method works is presented below.

Let $f(y;\theta)$ denote a density function, where $\theta$ is the set of unknown parameters to be estimated. Given $n$ independent observations $y_1, \ldots, y_n$ of a random variable $Y$ assumed to be the log returns of a financial asset, we can from these observations deduce reasonable estimators for the parameter set $\theta$. The likelihood function is given by

$$L(y_1, \ldots, y_n|\theta) = L = \prod_{i=1}^{n} f(y_i;\theta)\,. \tag{4.1}$$

Since it is sometimes easier to maximize the logarithm of an expression instead of the expression itself, we go ahead to present the logarithmic likelihood function as

$$\log L = \sum_{i=1}^{n} \log\ f(y_i;\theta)\,. \tag{4.2}$$

By maximizing $\log\ L$, the maximum likelihood estimators of $\theta$ are given by the simultaneous solutions of $m$ (number of parameters in the parameter set) equations such that:

$$\frac{\partial(\log\ L)}{\partial\theta_j} = 0\,, \qquad j = 1, 2, \ldots, m\,.$$

The density fit for our chosen models in Chapter 3 was computed using this method. For cases where the density function is not known explicitly, the discrete Fourier transform can be used to approximate the density. We relied strongly on numerical procedures to carry out this method. Further detail on these can also be found in [51] and [81].

### 4.1.3 Least-Squares Estimation (LSE)

The method of least squares estimation is used to model numerical data obtained from a set of observations, by adjusting the parameters of a given model so as to get an optimal fit of the data. The best fit is given by that particular case of the model for which the sum of squared residuals[1] has its least value. LSE can be described as linear or non-linear. It is said to be linear when the model comprises a linear combination of the parameters. Here, a closed form solution is available. For the non-linear case, there exists no closed form solution. Initial values must be chosen for the model's parameters, and then the parameters are refined iteratively (that is, the values are obtained by successive approximation). If we have a set of option prices and wish to perform least-squares estimation in order to obtain the model parameters for a given model, the procedure is represented by the equation below:

$$\text{Least-squares} = \arg\min \sum_{\text{options}} (\text{Model price} - \text{Market price})^2 .$$

This method was first described by Carl Friedrich Gauss around 1794 [71]. It is widely used in finance for the calibration of option prices. This method was used in [24] and [81] for computing the parameters of a number of models. In their papers they minimized the root-mean-squared error between the model and market prices. Cont and Tankov [29] recommend a regularization approach based on relative entropy minimization to help resolve the numerical instability of the calibration problem using this approach. This method was also used in [28], [84] and [83].

We have been able to present the calibration problem and methods for its solution, of which one has been used to fit the density of distributions in the previous chapter. The next task ahead is to calibrate the prices of vanilla options, and then to use these parameters to price our option of interest, the barrier option. To achieve this, we need to clearly summarize the framework in which we will be pricing these options using the models discussed in Chapter 3. This pricing framework is the Lévy market model in which we will be computing both the model option prices during the calibration procedure and the barrier option prices in the subsequent chapters. Here, we shall model the stock price process as the exponential of a Lévy process. Considering the fact that Lévy models are incomplete, we shall discuss a

[1] A residual is the difference between an observed value and the value given by the model.

method of determining the equivalent martingale measure for the pricing of options. This is the focus of the next section.

## 4.2 The Lévy Market Model: The Pricing Framework

Let $X = \{X_t,\ t \geq 0\}$ be a Lévy process. If we model our stock price process as an exponential of a Lévy process, we have that the price process is given by:

$$S_t = S_0 \exp(rt + X_t)\ . \tag{4.3}$$

This model is referred to as an exponential-Lévy model. These models can be constructed from those presented in Chapter 3 by exponentiating them and imposing the martingale condition on their characteristic triplet. In order to obtain the pricing rule for our options, there is need for these models to be arbitrage-free and that leads us to the discussion of the equivalent martingale measure (EMM), which plays a vital role in ensuring that a market model satisfies this condition.

### 4.2.1 Equivalent Martingale Measure (EMM)

An arbitrage opportunity refers to a self-financing strategy which can lead to a positive terminal gain, with no probability of any intermediate loss. This imposes some constraints on the way financial instruments are priced in a given market. In an arbitrage-free market, the prices of any financial asset is represented by its discounted expected payoff under an appropriate probability measure (the risk-neutral measure). This notion is referred to as *risk-neutral pricing*. The following result sheds more light on this.

**Proposition 4.2.1.** *(Fundamental Theorem of Asset Pricing) [29]. The market model defined by* $(\Omega, \mathcal{F}, (\mathcal{F}_t), \mathbb{P})$ *and asset prices* $(S_t)_{t\in[0,T]}$ *is arbitrage-free if and only if there exists a probability measure* $\mathbb{Q} \sim \mathbb{P}$ *such that the discounted asset prices* $(\tilde{S}_t)_{t\in[0,T]}$ *are martingales with respect to* $\mathbb{Q}$*.*

From the above result, we can see that the existence of an equivalent martingale measure leads to the absence of arbitrage opportunities. This raises a very fundamental question on how best to obtain the EMM. [29], [80], and [81] give detailed discussion on how to

specify the EMM for a given model. In this work, we shall concentrate on the use of the mean-correcting martingale measure.

The equivalent martingale measure $\mathbb{Q}$ can be obtained by mean-correcting the exponential of a Lévy process. This is done by introducing an additional 'drift' parameter $m \in \mathbb{R}$ to the Lévy process, which plays a crucial role in the risk-neutral modeling of the risky asset. This is only reflected in the first parameter of the Lévy triplet given by

$$\gamma = \bar{\gamma} + m$$

where $\bar{\gamma}$ is the drift coefficient of the original process. We start by estimating all the parameters of the process and then change the $m$ parameter in an appropriate way so as to ensure that the discounted stock process is a martingale. The $m$ parameter can be obtained by [81]:

$$m_{new} = m_{old} + r - q - \log \phi(-i) \,, \tag{4.4}$$

where $\phi(x)$ is the characteristic function of the log return involving the $m_{old}$ parameter, $r$ is the risk-free interest rate and $q$ the dividend rate. An example is the case of the Black-Scholes model where the mean $\mu - \frac{1}{2}\sigma^2$ (i.e. the $m_{old}$ parameter) is changed into $r - q - \frac{1}{2}\sigma^2$ (i.e. the $m_{new}$ parameter). A list of the $m_{new}$ parameters for our chosen models is presented in Table 4.1 below.

| Model | $m_{new}$ |
|---|---|
| CGMY | $r - q - C\Gamma(-Y)((M-1)^Y - M^Y + (G+1)^Y - G^Y)$ |
| VG | $r - q - C\log(GM/(M-1)(G+1))$ |
| NIG | $r - q + \delta(\sqrt{\alpha^2 - (\beta+1)^2} - \sqrt{\alpha^2 - \beta^2})$ |

**Table 4.1.** The m parameter for the mean-correcting EMM

It is worth noting that there exist many equivalent martingale measures for exponential-Lévy models and this feature is responsible for the better calibration of market prices of options compared to the Black-Scholes model with a unique EMM. We go ahead to show how these $m_{new}$ parameters are used in our given models. Let $\bar{X}$ be our original process, when we translate this process by the value $m \in \mathbb{R}$, it implies an addition of a term $mt$ to $\bar{X}$ given by

$$X_t = \bar{X}_t + mt \,.$$

Therefore, we have that the dynamics of our stock price process under the risk-neutral measure is given by

$$S_t = S_0 \exp(mt + X_t)\,. \tag{4.5}$$

To ensure that the dynamics of our stock price process satisfies the martingale condition, we have

$$\begin{aligned}
\mathbb{E}[S_t] &= S_0 \exp(mt)\mathbb{E}[\exp(X_t)]\,, \\
&= S_0 \exp((r - q - \log\phi(-i))t) \exp(t \log\phi(-i))\,, \\
&= S_0 \exp((r-q)t)\,.
\end{aligned}$$

Also, the risk-neutral characteristic function of the log price process is given by

$$\phi_{\ln(S_t)}(u) = \exp[iu(\ln(S_0 + mt))]\,\phi(u)\,,$$

where $\phi(u)$ is the characteristic function of the VG, NIG or CGMY process in our case. This characteristic function will be used in computing European option prices via the fast Fourier transform method for the calibration of our Lévy models. Having seen how to price in the Lévy market framework, we wish to consider the pricing of European options. A good understanding of this concept is very important for generating our model prices during the calibration procedure.

### 4.2.2 Pricing Formula for European Options

A European call/put option on a given underlying $S$, is defined as a contract which gives its holder the right to buy/sell the underlying at a date $T$ and for a fixed price $K$. Let $H(S_T)$ denote the payoff of the option at its maturity $T$, we have that for a call and put option, the payoff is $H(S_T) = (S_T - K)^+$ and $H(S_T) = (K - S_T)^+$ respectively.

Considering our framework where the stock price process is driven by the exponential of a Lévy process, we have that the price of the call option can be written in terms of the risk-neutral conditional expectation of the payoff as:

$$C_t(T,K) = e^{-r(T-t)}\,\mathbb{E}_{\mathbb{Q}}[(S_T - K)^+|\mathcal{F}_t]\,. \tag{4.6}$$

Let $\tau = (T - t)$, we have that [29],

$$\begin{aligned} C(t, S, T = t + \tau, K) &= e^{-r\tau}\,\mathbb{E}[(S_T - K)^+ | S_t = S]\,, \\ &= e^{-r\tau}\,\mathbb{E}[(S\,e^{r\tau + X_\tau} - K)^+]\,, \\ &= Ke^{-r\tau}\,\mathbb{E}(e^{x + X_\tau} - 1)^+)\,, \end{aligned}$$

where $x$ is the log forward moneyness given by $x = \ln(\frac{S}{K}) + r\tau$ and is zero for options that are at the money. With the above in mind, we can now present three different methods of pricing vanilla[2] options.

The first entails the pricing of vanilla options through the density functions of the Lévy processes. Here, the equivalent martingale measure is best derived from the Esscher transform equivalent martingale measure. Next is the use of the Lévy triplet. In this case, the price of the derivative can be obtained by solving a partial differential integral equation whose boundary conditions are all in terms of the Lévy triplet of the process. Details on this and more can be found in [81], [29] and [72].

The Last method is the one we are working with and entails the pricing of vanilla options through the characteristic function of the Lévy process. This method is widely used especially when the characteristic function of the risk-neutral log stock-price process is known. In order to price an option in this framework, the Fast Fourier Transform pricing technique as will be presented in the next section is very necessary. Here, $\phi_T$ in Equation (4.10) is the characteristic function of the logarithm of the stock price process in the risk-neutral world in terms of $(\upsilon - (\alpha + 1)i)$ at maturity. Our choice of this method was based on the fact that our chosen models all have explicit expressions for their characteristic function. We now set out to discuss the FFT method for option pricing.

## 4.3 FFT Option Pricing Technique

In this section, we describe a numerical approach for the pricing of options using the characteristic function of the underlying instrument's price process. This approach is based on the Fast Fourier Transform (FFT) and was introduced by Carr and Madan [25]. The FFT method offers a speed advantage and has the possibility of calculating prices for

[2] In our case, this term refers to European options.

a whole range of strikes. In addition, the characteristic function of log price is known and has a simple form for many models considered in the literature while the densities of the models are often not known in closed form. The basic idea of this method is to develop an analytic expression for the Fourier transform of the price of the option and then get the price by Fourier inversion.

Let $k$ denote the log of strike $K$, and $C_T(k)$ be the desired value of a call option with maturity $T$ and strike $\exp(k)$. Also, let $S = \{S_t,\ 0 \leq t \leq T\}$ denote the stock price process and $q_T(s)$ be the risk-neutral density of the log price $s_T = \ln(S_T)$. The characteristic function of $s_T$ is defined by:

$$\phi_T(u) = \mathbb{E}[\exp(ius_T)] \ . \tag{4.7}$$

The characteristic function of this density is defined by:

$$\phi_T(u) = \int_{-\infty}^{\infty} e^{ius}\, q_T(s)ds \ . \tag{4.8}$$

The desired value of a $T$ maturity call option $C_T(k)$ is related to the risk-neutral density $q_T(s)$ by:

$$C_T(k) \equiv \int_k^{\infty} e^{-rT}\,(e^s - e^k)q_T(s)ds \ .$$

This call pricing function is not square integrable because $C_T(k)$ tends to $S_0$ as $k$ tends to $-\infty$. Hence, to obtain a square integrable function, the call price will be modified to the following:

$$c_T(k) \equiv \exp(\alpha k)C_T(k) \ , \tag{4.9}$$

where $\alpha > 0$. The choice of $\alpha$ may depend on the model for $S_t$. Let us consider the Fourier transform of $c_T(k)$ defined by:

$$\psi_T(\upsilon) = \int_{-\infty}^{\infty} e^{i\upsilon k}\, c_T(k)dk \ .$$

To begin, we first develop an analytical expression for $\psi_T(\upsilon)$ in terms of $\phi_T$ and then go ahead to obtain call prices numerically using the inverse transform:

$$\begin{aligned} C_T(k) &= \frac{\exp(-\alpha k)}{2\pi} \int_{-\infty}^{\infty} e^{-i\upsilon k}\, \psi_T(\upsilon)d\upsilon \ , \\ &= \frac{\exp(-\alpha k)}{\pi} \int_{0}^{\infty} e^{-i\upsilon k}\, \psi_T(\upsilon)d\upsilon \ . \end{aligned}$$

The second equality holds because $C_T(k)$ is real, which implies that the function $\psi_T(\upsilon)$ is odd in its imaginary parts and even in its real parts. The expression for $\psi_T(\upsilon)$ can be computed directly by interchanging integrals:

$$\begin{aligned}
\psi_T(\upsilon) &= \int_{-\infty}^{\infty} e^{i\upsilon k} \int_{k}^{\infty} e^{\alpha k}\, e^{-rT}(e^s - e^k)\, q_T(s) ds\, dk \,, \\
&= \int_{-\infty}^{\infty} e^{-rT} q_T(s) \int_{-\infty}^{s} \left(e^{s+\alpha k} - e^{(1+\alpha)k}\, e^{i\upsilon k}\, dk\, ds\right) \,, \\
&= \int_{-\infty}^{\infty} e^{-rT} q_T(s) \left[\frac{e^{(\alpha+1+i\upsilon)s}}{\alpha + i\upsilon} - \frac{e^{(\alpha+1+i\upsilon)s}}{\alpha + 1 + i\upsilon}\right] ds \,, \\
&= \frac{e^{-rT}\, \phi_T(\upsilon - (\alpha+1)i)}{\alpha^2 + \alpha - \upsilon^2 + i(2\alpha+1)\upsilon} \,,
\end{aligned} \tag{4.10}$$

where $\phi_T$ is the Fourier transform of $q_T$. It is worth noting that if $\alpha = 0$, then the denominator vanishes when $\upsilon = 0$, giving rise to a singularity in the integrand. The use of the factor $\exp(\alpha k)$ or something similar is required since the FFT evaluates the integrand at $\upsilon = 0$. A sufficient condition for the modified call value $c_T(k)$ to be square-integrable is given by $\psi_T(0)$ being finite. From Equation (4.10), we observe that $\psi_T(0)$ is finite provided $\phi_T(-\alpha + 1)i$ is finite. Put options can be priced using the put-call parity.

The desired option price in terms of $\psi_T(\upsilon)$ using Fourier inversion can be obtained by:

$$C_T(k) = \frac{\exp(-\alpha k)}{\pi} \int_0^{\infty} e^{-i\upsilon k}\, \psi(\upsilon) d\upsilon \,.$$

We can compute this integral numerically using the Trapezoid rule as:

$$C_T(k) \approx \frac{\exp(-\alpha k)}{\pi} \sum_{j=1}^{N} e^{-i\upsilon_j k} \psi(\upsilon_j) \eta \,, \tag{4.11}$$

where $\upsilon_j = \eta(j-1),\ j = 1, \ldots, N$, and $\eta > 0$ is the distance between the points of the integration grid. The effective upper limit for the integration is now:

$$a = N\eta \,.$$

Equation (4.11) suggests we calculate the prices using the FFT, which is an efficient algorithm for computing the sum:

$$w(k) = \sum_{j=1}^{N} e^{-i\frac{2\pi}{N}(j-1)(k-1)}\, x(j) \qquad \text{for } k = 1, \ldots, N \,, \tag{4.12}$$

where $N$ is typically a power of 2. The strikes near the spot price are of interest because such options are traded most frequently. The FFT returns $N$ values of $k$ and we employ a regular space of size $\lambda$ and these gives the following values for $k$:

$$k_u = -b + \lambda(u-1)\,, \qquad \text{for } u = 1, \ldots, N\,. \tag{4.13}$$

This gives us log strike level in the range of $-b$ to $b$ with:

$$b = \frac{N\lambda}{2}\,.$$

Substituting Equation (4.13) into (4.11) yields:

$$C_T(k_u) \approx \frac{\exp(-\alpha k_u)}{\pi} \sum_{j=1}^{N} e^{-i\upsilon_j(-b+\lambda(u-1))}\,\psi_T(\upsilon_j)\eta\,, \qquad \text{for } u = 1, \ldots, N\,. \tag{4.14}$$

Recalling that $\upsilon_j = \eta(j-1)$, we can write:

$$C_T(k_u) \approx \frac{\exp(-\alpha k_u)}{\pi} \sum_{j=1}^{N} e^{-i\lambda\eta(j-1)(u-1)}\, e^{i\,b\upsilon_j}\,\psi_T(\upsilon_j)\eta\,. \tag{4.15}$$

From Equation (4.12), applying the fast Fourier transform we have that:

$$\lambda\eta = \frac{2\pi}{N}\,. \tag{4.16}$$

Caution needs to be applied in the choice of $\eta$ as small values of $\eta$ which give a fine grid for integration, lead to call prices at strike spacings that are relatively large. As a result, we only have a few strikes lying in the desired region near the stock price. To be able to obtain an accurate integration with larger values of $\eta$, we incorporate Simpson's rule weightings into our summation. Using Simpson's rule and the restriction in Equation (4.16), our call price can be written as:

$$C_{k_u} \approx \frac{\exp(-\alpha k_u)}{\pi} \sum_{j=1}^{N} e^{-i\frac{2\pi}{N}(j-1)(u-1)}\, e^{i\,b\upsilon_j}\,\psi(\upsilon_j)\,\frac{\eta}{3}(3 + (-1)^j - \delta_{j-1})\,, \tag{4.17}$$

where $\delta_n$ is the Kronecker delta function whose value is 1 for $n = 0$ and zero otherwise. The summation in Equation (4.17) gives an exact application of the FFT.

In this chapter, we have been able to present the inverse problem and three different methods of addressing it. One of these methods was used in Chapter 3 to fit financial time series to empirical/model densities. We also presented the pricing framework in which we will be computing asset prices. Our next task is to calibrate current option prices to our given models and see how well these models perform. This is the focus of the next chapter.

# Chapter 5

# Calibration to Option Prices

An analysis of the historic data of four major securities has been carried out in Chapters 1 and 3. In this chapter, we wish to conduct another analysis on two of these securities (INTC and S&P 500 Index) for today's option prices ($t = 0$). We start by calibrating these call options prices to the VG, NIG and CGMY models. This will be carried out by minimizing the root-mean-squared error between the model and market prices. An analysis of the parameters obtained from these procedures shall then be carried out. After this, we shall compare the prices computed by these models via the FFT procedure to the market option prices.

Using the parameters obtained from these calibration procedures, we will see whether the models' implied volatility surfaces capture the smile behaviour of the market's implied volatility surface. We shall conclude this chapter by simulating ordinary trajectories and stock price processes of these models, using the parameters obtained from the calibration. These exercises are meant to validate the model parameters since they are going to be used in the pricing of barrier options, as barrier option prices are not listed on the exchanges like their vanilla counterparts. We begin with a discussion of the estimation procedure.

## 5.1 The Estimation Procedure

We obtained data on INTC closing option prices for maturities between one and eighteen months across eleven strikes and having a spot price of 21.39 on July 20th, 2010. The data

set consists of thirty-eight plain vanilla call option prices. We also obtained data on the S&P 500 Index closing option prices for maturity ranging between one and twenty months across twenty-seven strikes and having a spot price of 1124.47 on April 18th, 2002. The data set consists of seventy-five plain vanilla call option prices. The option prices can be found in Tables A.1 and A.2. We set the risk-free interest rate to 1.13% and the dividend yield as 3.00% for INTC, while for the S&P 500 Index, we have 1.9% and 1.2% respectively. We mention also that the call option prices obtained for the S&P 500 Index are delayed quotes from [81].

Our procedure entails, firstly a search for a global set of parameters for each model which fits across the full range of maturities and strikes in the data set. This is suitable for the pricing of path-dependent options (barrier options) across different time frames. The global set of parameters is different from the parameter set that is obtained when calibrating option prices to a single maturity date as in principle, this can only be used to price options at that given maturity.

Next, we perturb our data sets and see how stable the parameters are. This is carried out across all maturities and strikes by slightly changing the prices in our data set. The parameters obtained from this procedure shall be referred to as the 'perturbed' parameter set. The third procedure shall be an investigation of the stability of prices when the last maturity and all corresponding prices on that date are removed from the data sets. The parameters obtained from this procedure shall be referred to as the 'local' parameter set.

The last procedure shall entail calibration to a single maturity across all strikes. This will be for October 2010 and December 2002 for the INTC and S&P 500 index respectively. Though the parameters obtained from this last procedure (single parameter set) will only be used to price options at the same maturity, we wish to see if this gives more reasonable prices for the barrier options as compared to the three other procedures (as will be studied in the next chapter). The parameters obtained from the procedures above will be referred to as

- Global set;
- Perturbed set;
- Local set and

- Single set.

We begin with a discussion of the results from the calibration procedures.

### 5.1.1 Results of Estimation

In this section, we will start by presenting the results of our calibration taken over all strikes and maturities for the three different models we are considering. The model parameters for each case are estimated by minimizing the root-mean-square error (RMSE) between the market's and the model's price. The RMSE indicates the absolute fit of the model to the data, that is, how close the observed data points are to the values predicted by the model. It can be seen as a good measure of how accurately the model predicts the data. Lower values of the root-mean-square error denotes better fit. Mathematically, this global measure of fit is represented as:

$$RMSE = \sqrt{\sum_{\text{options}} \frac{(\text{Model price} - \text{Market price})^2}{\text{number of options}}},$$

where the model prices are computed via the FFT technique. Below is a presentation of the results from the calibration procedure.

The risk-neutral parameter sets are presented in Tables 5.1 and 5.2 with the associated error levels. Figures 5.1 - 5.6 show the calibration results for all models under consideration. It took an average of 90 seconds to run each of these computations on an Intel Pentium Dual CPU T3200 @ 2.00GHz with 3.00GB RAM.

A look at the risk-neutral parameter sets for all the models in both cases show a huge difference especially between the single set and remaining sets. This is evident when we consider the values of the $\alpha$ parameter for the NIG model in Table 5.1. The value for the single set, is approximately 18, 23 and 9 times the values for the global, perturbed and local sets respectively. In the case of the risk-neutral parameter sets for the S&P 500 options, the same scenerio is also evident for the CGMY model. For the NIG model, we discover some similarities between the parameters of the global and perturbed sets and also between the local and single sets. With these differences in mind, we look forward to investigating

| PARAMETER SETS FOR INTC | | | | | | |
|---|---|---|---|---|---|---|
| MODEL | INDICATOR | RISK-NEUTRAL PARAMETERS | | | | RMSE |
| CGMY | Parameters | C | G | M | Y | |
| | Global Set | 0.0998 | 0.5218 | 4.0057 | 1.0703 | 0.0998 |
| | Perturbed Set | 0.0683 | 0.2310 | 2.8675 | 1.1440 | 0.1127 |
| | Local Set | 0.4154 | 3.3371 | 9.7041 | 0.7950 | 0.0824 |
| | Single Set | 0.3766 | 7.2449 | 73.9144 | 1.1570 | 0.0451 |
| NIG | Parameters | $\alpha$ | $\beta$ | $\delta$ | | |
| | Global Set | 3.2503 | -1.8494 | 0.3187 | | 0.1035 |
| | Perturbed Set | 2.5783 | -1.3434 | 0.2773 | | 0.1188 |
| | Local Set | 6.7456 | -3.0925 | 0.5431 | | 0.0824 |
| | Single Set | 59.0065 | -44.7440 | 1.4646 | | 0.0448 |
| VG | Parameters | $\theta$ | $\nu$ | $\sigma$ | | |
| | Global Set | -0.2609 | 0.4888 | 0.3270 | | 0.1146 |
| | Perturbed Set | -0.2029 | 0.5445 | 0.3294 | | 0.1334 |
| | Local Set | -0.3382 | 0.1944 | 0.2954 | | 0.0846 |
| | Single Set | -1.8507 | 0.0250 | 0.0772 | | 0.0562 |

**Table 5.1.** Risk-neutral parameter sets for the INTC options.

the similarity between the barrier option prices computed with these parameters for each model.

From the results presented above, it is evident that the four-parameter model (CGMY model) performed better than the other models (i.e. the three-parameter models) in all cases when we consider the RMSE. This is not surprising as models with more parameters tend to give better results in optimization procedures. We can also observe that the normal inverse Gaussian model seems to perform better than the variance gamma model. Also, the calibration with just one maturity has the least error and that involving all the maturities has the highest error for all cases. This also is not out of place since the former entails few maturities and hence, fewer number of option prices. The next important comparison we need to carry out is that of the prices computed by the different procedures used in the calibration above, on October 2010 and December 2002 maturities for the INTC and S&P 500 data sets. This is dealt with in the next section.

| PARAMETER SETS FOR S&P 500 INDEX | | | | | | |
|---|---|---|---|---|---|---|
| MODEL | INDICATOR | RISK-NEUTRAL PARAMETERS | | | | |
| CGMY | Parameters | C | G | M | Y | RMSE |
| | Global Set | 0.0328 | 0.4179 | 15.7695 | 1.2817 | 2.8659 |
| | Perturbed Set | 0.0255 | 0.2619 | 61.2883 | 1.4161 | 1.4161 |
| | Local Set | 0.0212 | 0.3123 | 53.8647 | 1.4778 | 1.7510 |
| | Single Set | 0.3563 | 4.8590 | 18.0733 | 0.6075 | 0.1996 |
| NIG | Parameters | $\alpha$ | $\beta$ | $\delta$ | | |
| | Global Set | 7.4780 | -4.7430 | 0.1843 | | 3.2150 |
| | Perturbed Set | 7.4223 | -4.7020 | 0.1835 | | 3.2061 |
| | Local Set | 12.6839 | -8.0852 | 0.2494 | | 2.1640 |
| | Single Set | 11.6954 | -7.1637 | 0.2378 | | 0.1663 |
| VG | Parameters | $\theta$ | $\nu$ | $\sigma$ | | |
| | Global Set | -0.1595 | 0.5754 | 0.1753 | | 3.6726 |
| | Perturbed Set | -0.1586 | 0.5796 | 0.1755 | | 3.6643 |
| | Local Set | -0.2323 | 0.2914 | 0.1531 | | 2.5045 |
| | Single Set | -0.1508 | 0.4746 | 0.1690 | | 0.3178 |

**Table 5.2.** Risk-neutral parameter sets for the S&P 500 options.

### 5.1.2 Vanilla Price Comparison

In this section, we present graphs of option prices, computed via the fast Fourier transform (FFT) method for all our given models. Figure 5.7 shows the prices across all strikes for the two cases. Notice that though the parameter sets for the different models may be quite different from one another, their prices are very similar. We can say that using any of these parameter sets could still lead to an approximate price for the vanilla option. A very important fact we wish to point out is that in all models, calibrating to a single maturity gives a better fit if we only need to price at that given time, else it will be best to calibrate across several maturities if we hope to price other exotic options at any time frame. With these results in mind, we move ahead with investigating the implied volatility surface. This is only carried out for the global parameter set.

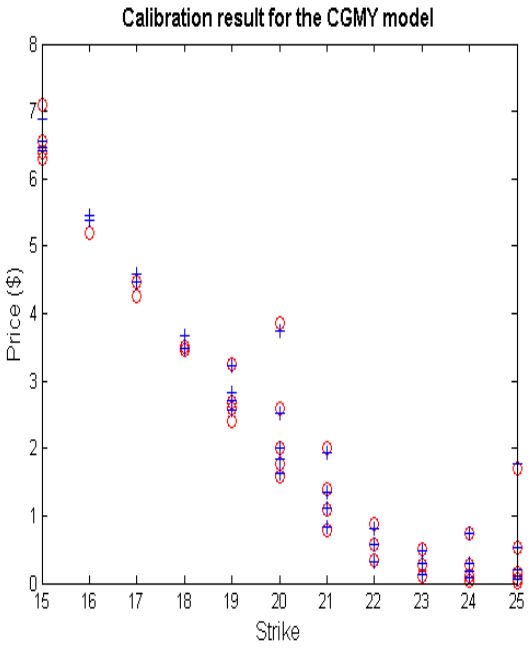


(a) Calibration for global parameter set

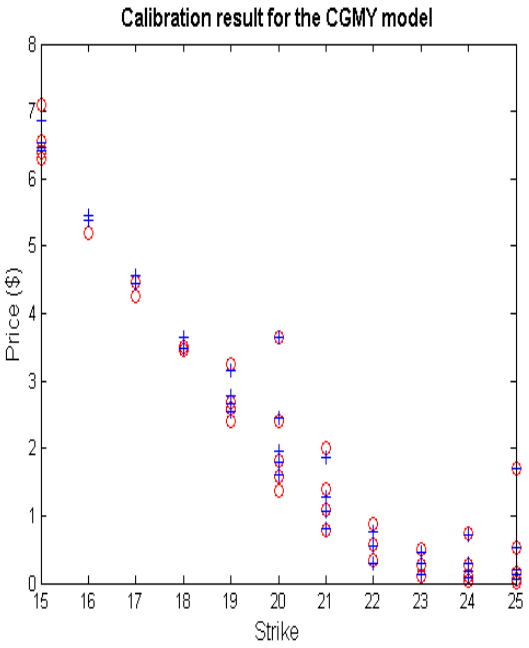


(b) Calibration for perturbed parameter set

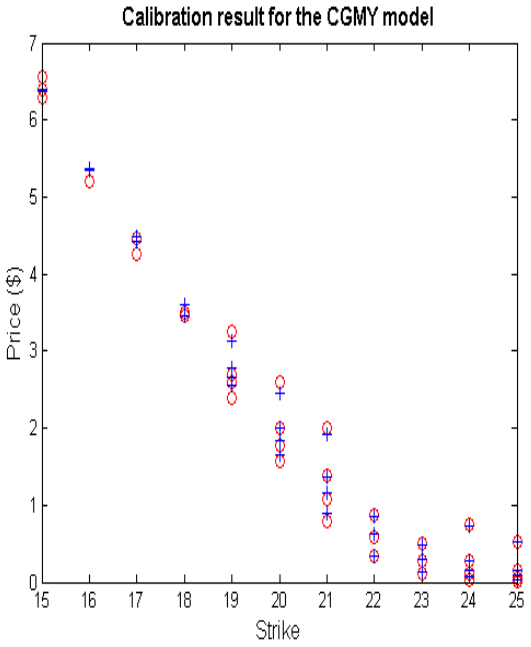


(c) Calibration for local parameter set

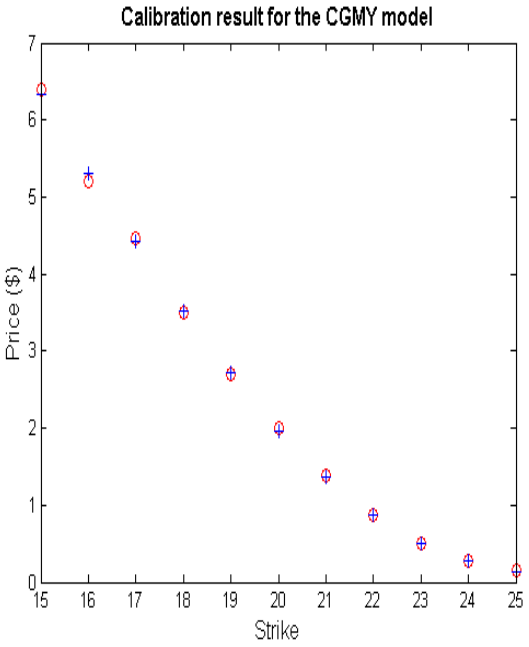


(d) Calibration for single parameter set

**Figure 5.1.** CGMY calibration of INTC options (circles are market prices, pluses are model prices).

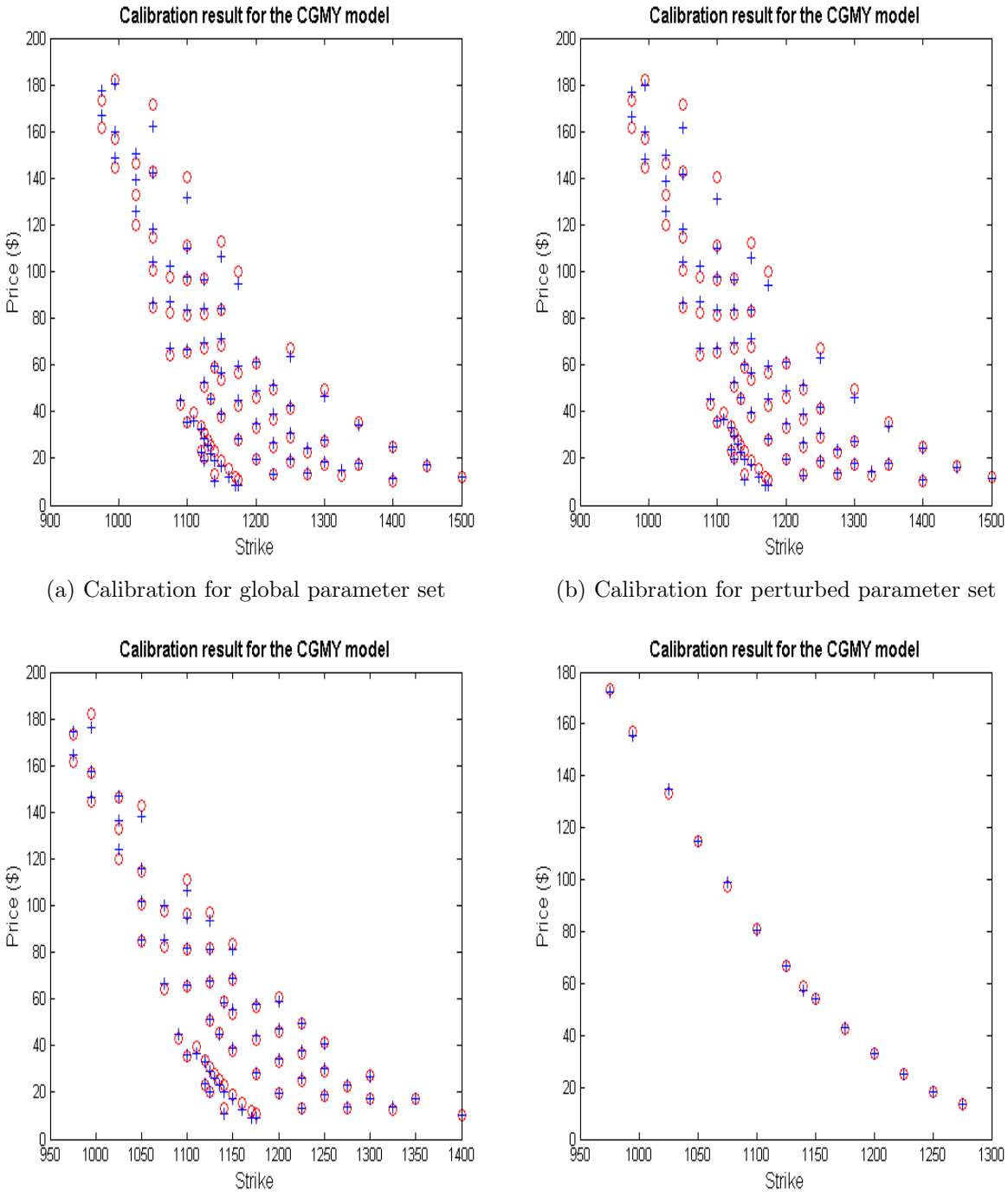


(a) Calibration for global parameter set

(b) Calibration for perturbed parameter set

(c) Calibration for local parameter set

(d) Calibration for single parameter set

**Figure 5.2.** CGMY calibration of S&P 500 options (circles are market prices, pluses are model prices).

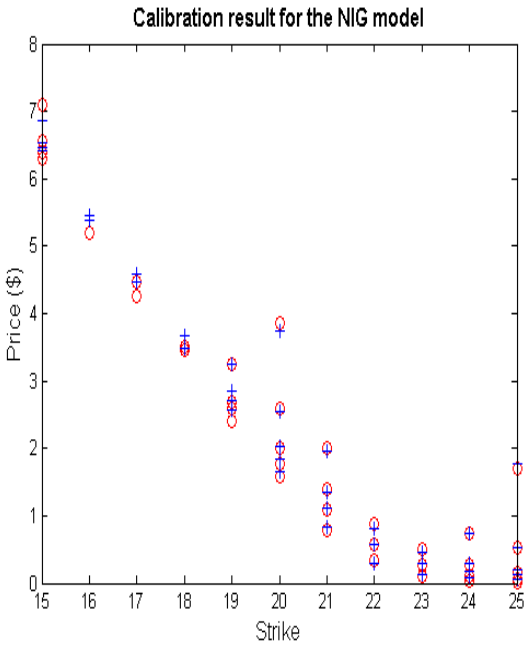


(a) Calibration for global parameter set

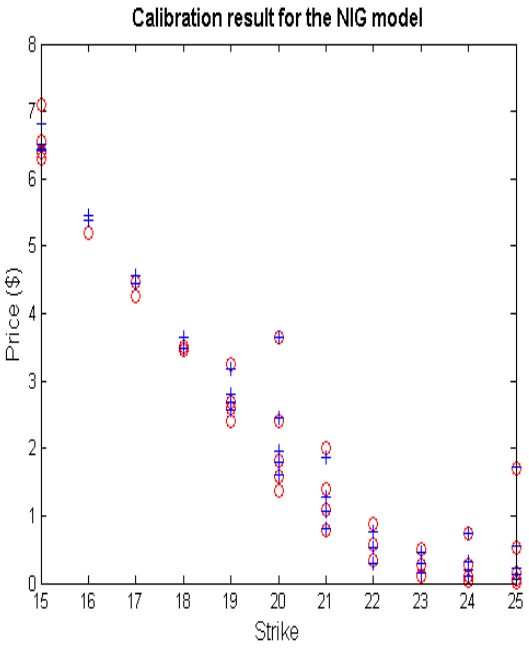


(b) Calibration for perturbed parameter set

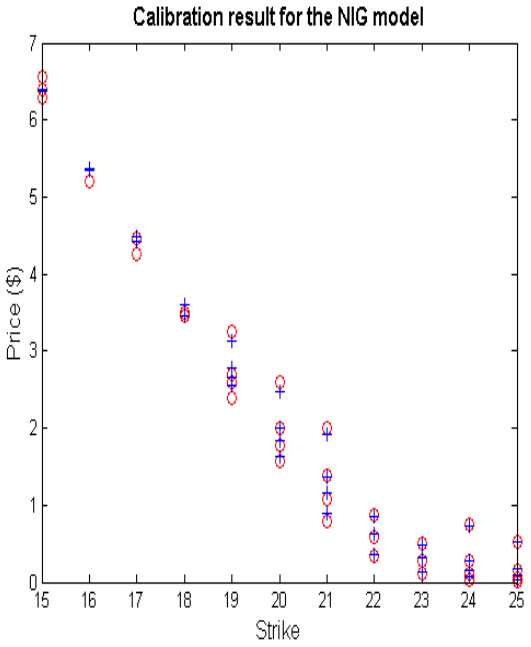


(c) Calibration for local parameter set

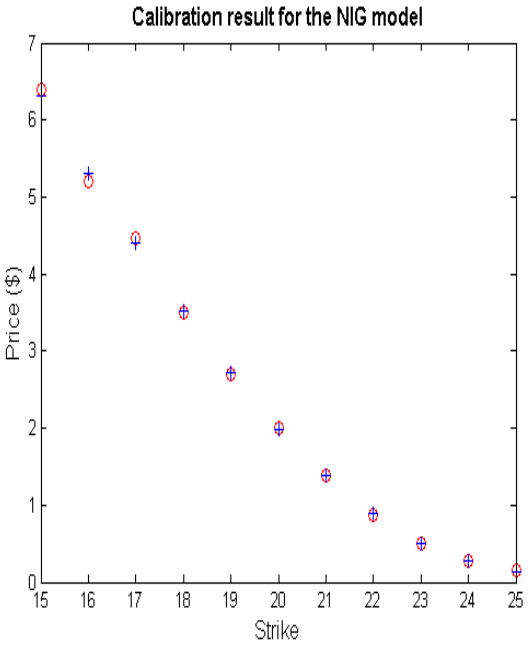


(d) Calibration for single parameter set

**Figure 5.3.** NIG calibration of INTC options (circles are market prices, pluses are model prices).

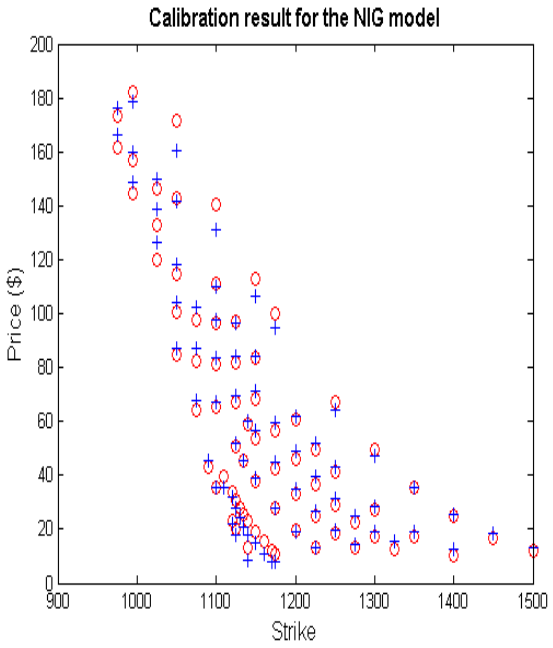


(a) Calibration for global parameter set

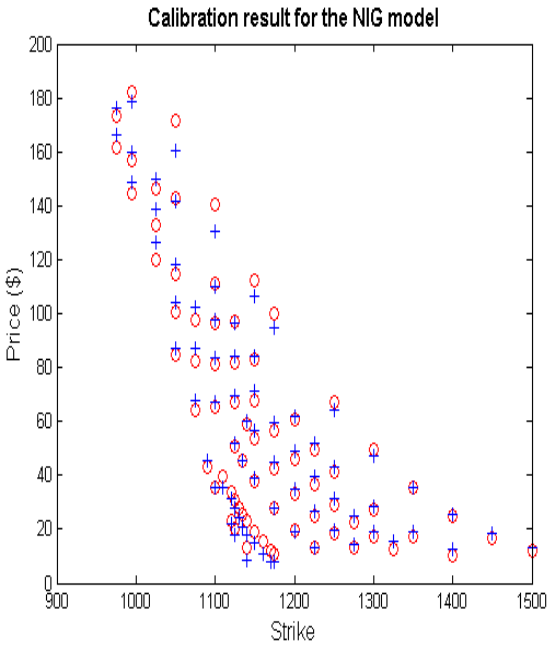


(b) Calibration for perturbed parameter set

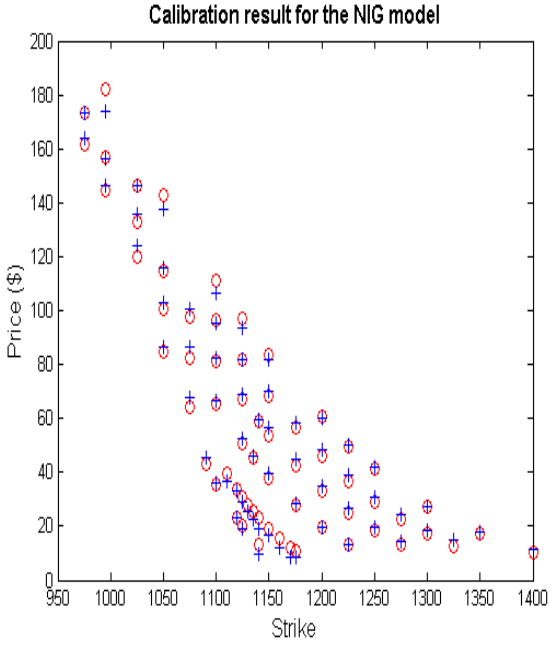


(c) Calibration for local parameter set

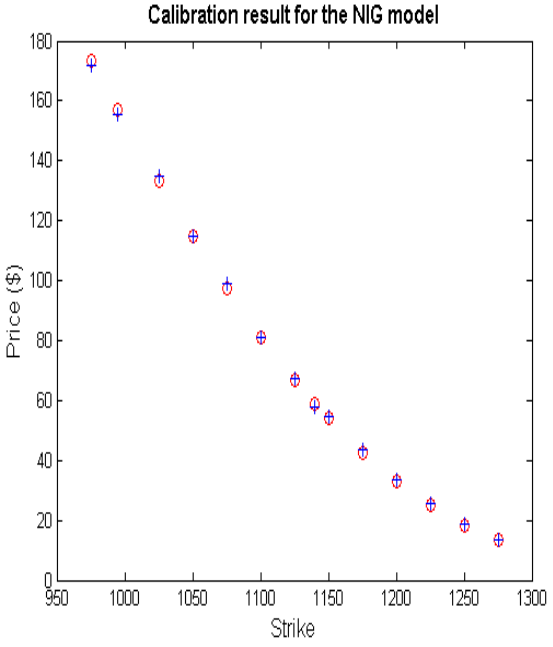


(d) Calibration for single parameter set

**Figure 5.4.** NIG calibration of S&P 500 options (circles are market prices, pluses are model prices).

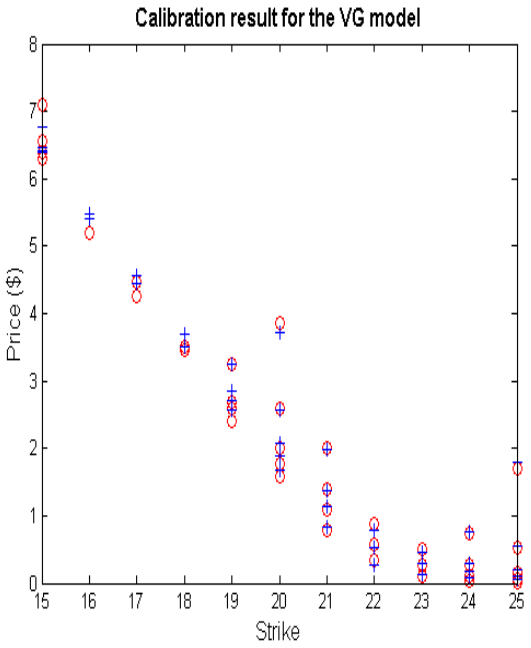


(a) Calibration for global parameter set

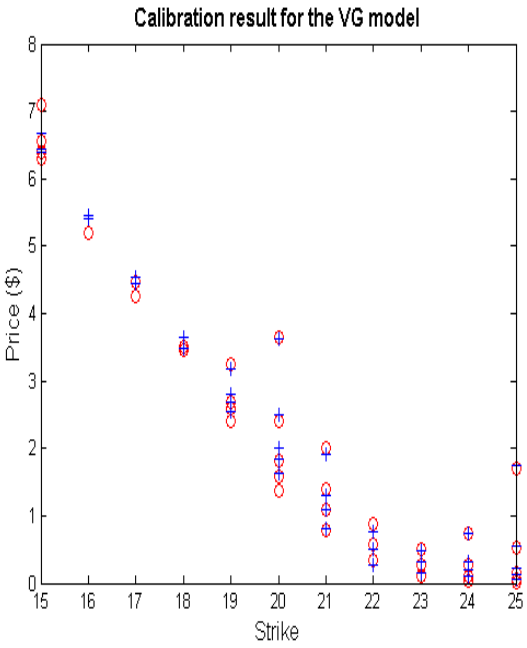


(b) Calibration for perturbed parameter set

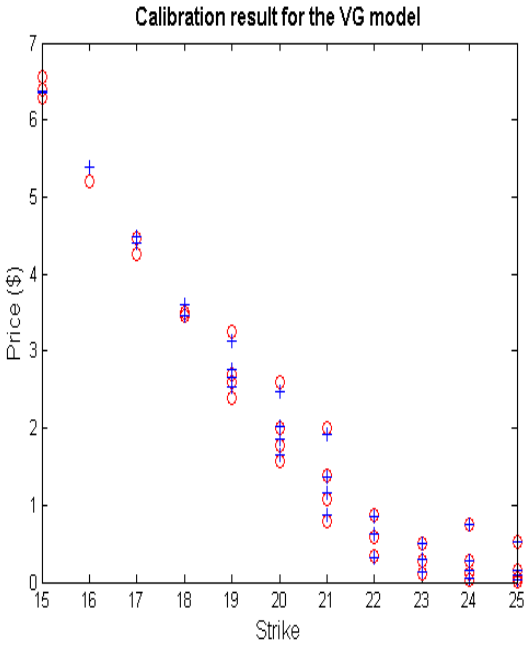


(c) Calibration for local parameter set

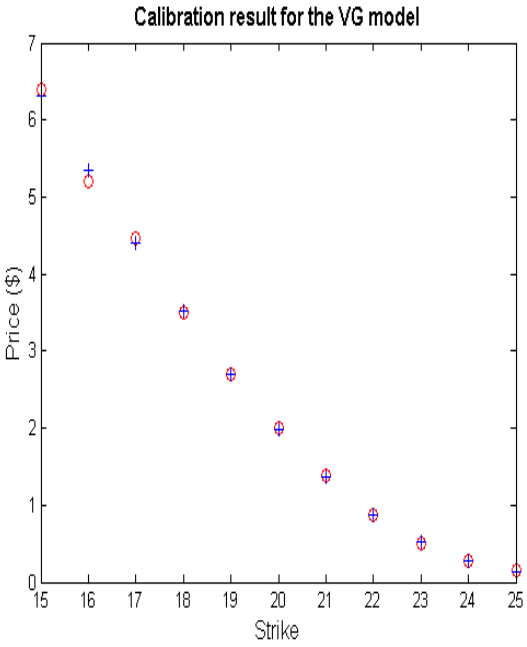


(d) Calibration for single parameter set

**Figure 5.5.** VG calibration of INTC options (circles are market prices, pluses are model prices).

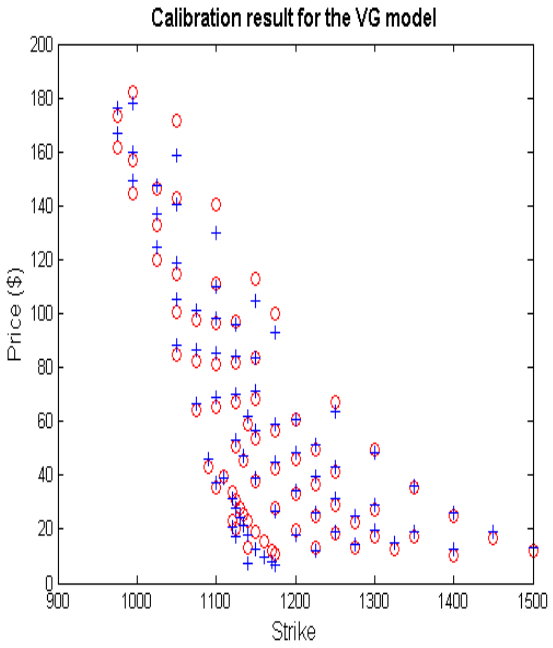


(a) Calibration for global parameter set

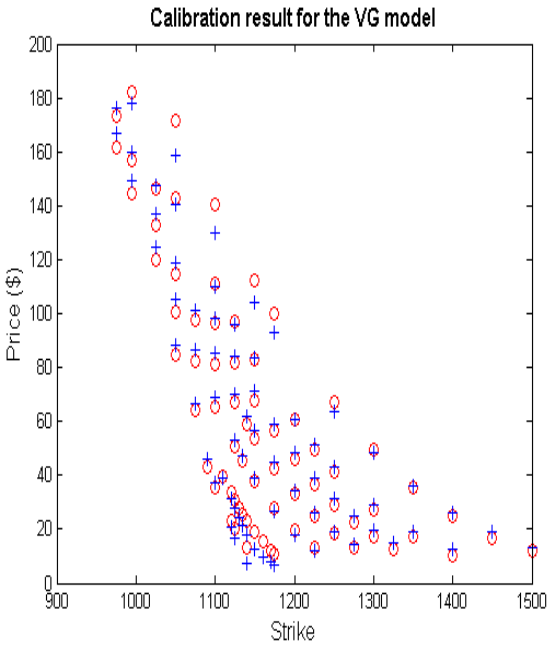


(b) Calibration for perturbed parameter set

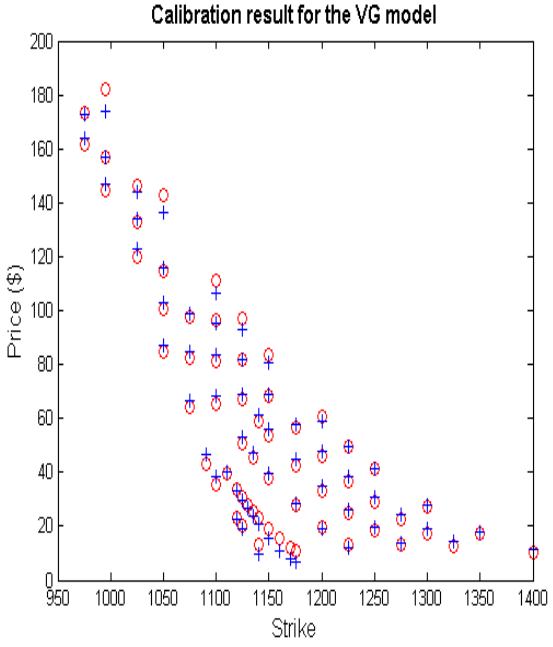


(c) Calibration for local parameter set

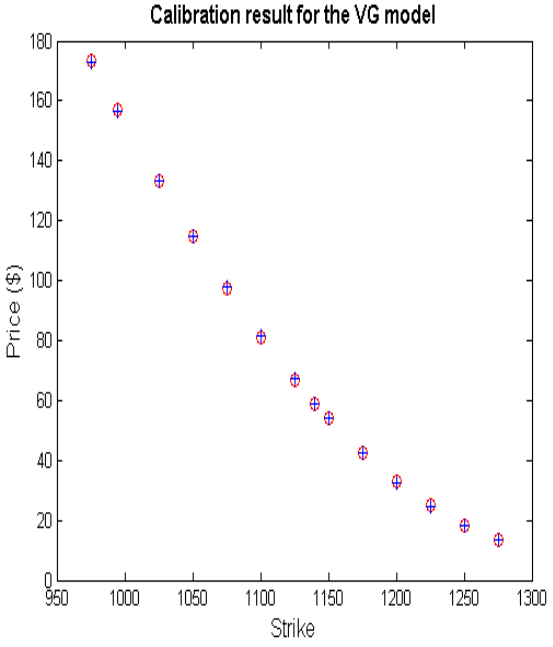


(d) Calibration for single parameter set

**Figure 5.6.** VG calibration of S&P 500 options (circles are market prices, pluses are model prices).

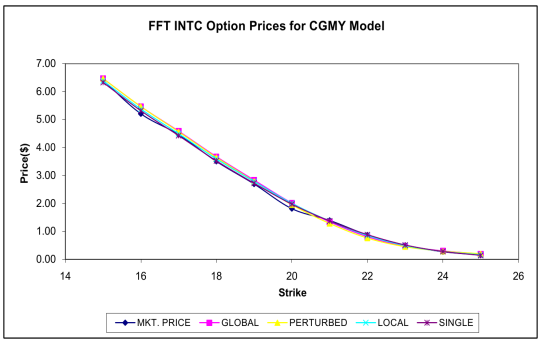


(a) FFT INTC option prices for CGMY model

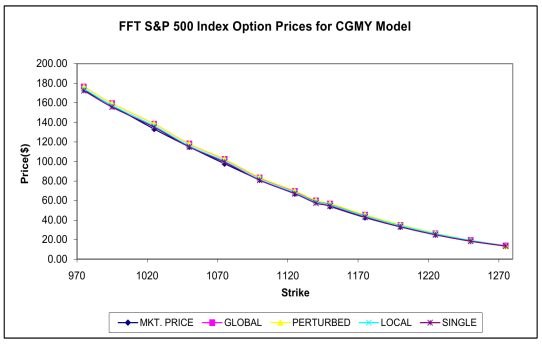


(b) FFT S&P 500 option prices for CGMY model

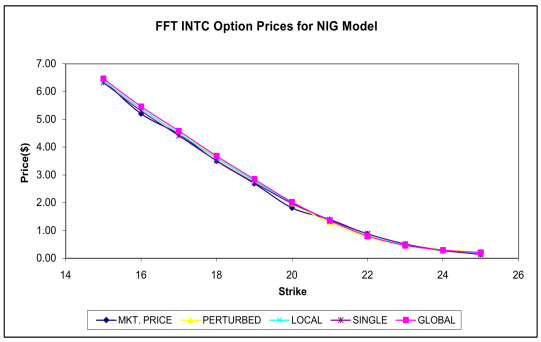


(c) FFT INTC option prices for NIG model

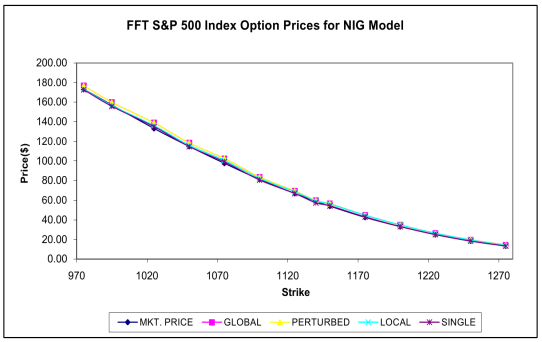


(d) FFT S&P 500 option prices for NIG model

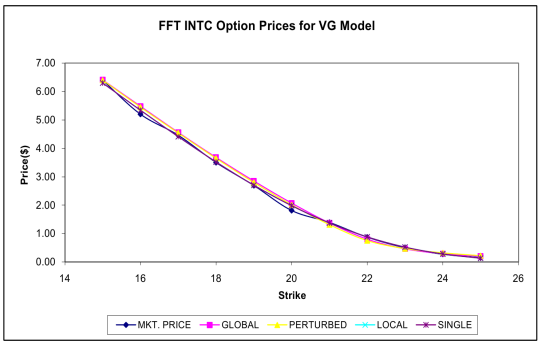


(e) FFT INTC option prices for VG model

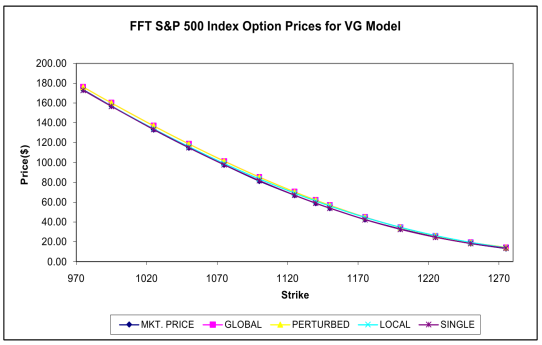


(f) FFT S&P 500 option prices for VG model

**Figure 5.7.** Comparison of market prices of options to those obtained from the models through the different calibration procedures via FFT. This is carried out on the October 2010 and December 2002 maturities, for the INTC and S&P 500 data sets

## 5.2 Implied Volatility Surface

It is well known that the market prices of options are usually represented in terms of the Black-Scholes implied volatilities of the corresponding options. It should still be noted that this does not imply that market participants regard this model as more accurate than others as we have been able to highlight some of its major drawbacks in the previous chapters. This is only regarded as a tool for translating market prices. The *implied volatility surface* at date $t$ is given by the function [29]

$$\sum_t : (T, K) \longrightarrow \sum_t (T, K) \ ,$$

where $T$ is the maturity, $K$ is the strike and $\sum_t (T, K)$ is the implied volatility.

The strong dependence displayed by implied volatilities with respect to the strike price can be said to be 'skewed' when it is decreasing and a 'smile' when it has a U-shape. This dependence decreases and flattens out with maturity. For exponential-Lévy models, the implied volatility surface flattens out too quickly with maturity. Figure 5.8 depicts the implied volatility surface for the INTC options. It can be seen that for the market data, the surface flattens out as the maturity grows but even for the last maturity, it is still a bit skewed. For the exponential-Lévy models, it is obvious that these flatten out more rapidly compared to that of the market data. We can notice the difference around the surface for options with strikes between 15 and 20 with shorter time to maturity. This also is clearly reflected in the poor calibration of these options with a look at the calibration plots. This may be as a result of options not having been traded for a long period of time. For the S&P options data, we notice a better result as shown by Figure 5.9. Hence, we can conclude that the inability of a model to capture to a large extent the market implied volatility surface of a given dataset does not imply that it will not perform well on other datasets. In our case, we represented the implied volatility surface as a function of strike and time to maturity, but it should also be noted that the implied volatility surface can be represented in terms of moneyness $m = K/S_t$ and time to maturity. The implied volatility patterns are typically skewed as out of the money calls have lower implied volatilities than in the money ones. On this note, we can proceed with the simulation of the trajectories of the VG, NIG and CGMY models using the parameters from the calibration.

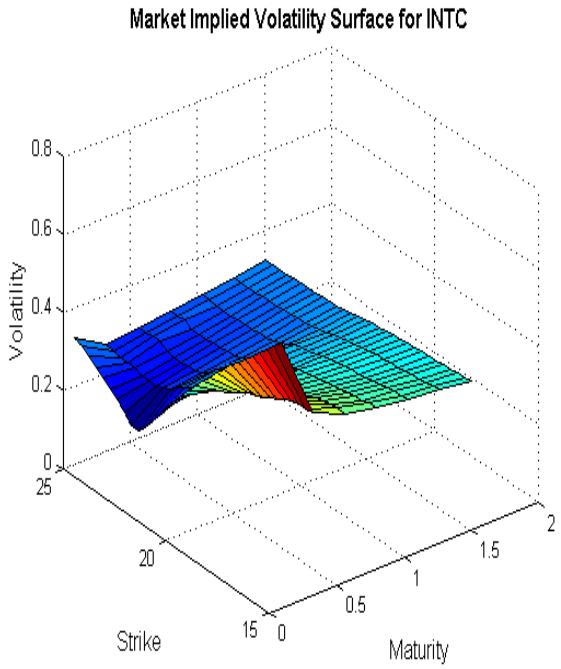


(a) Market implied volatility surface

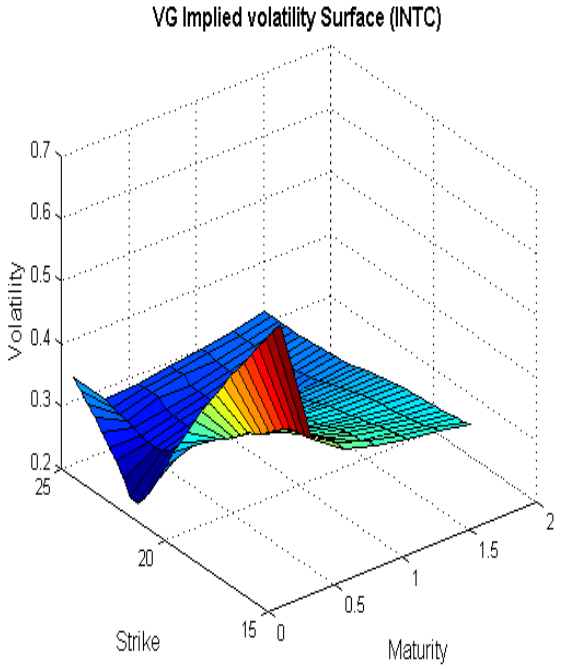


(b) VG implied volatility surface

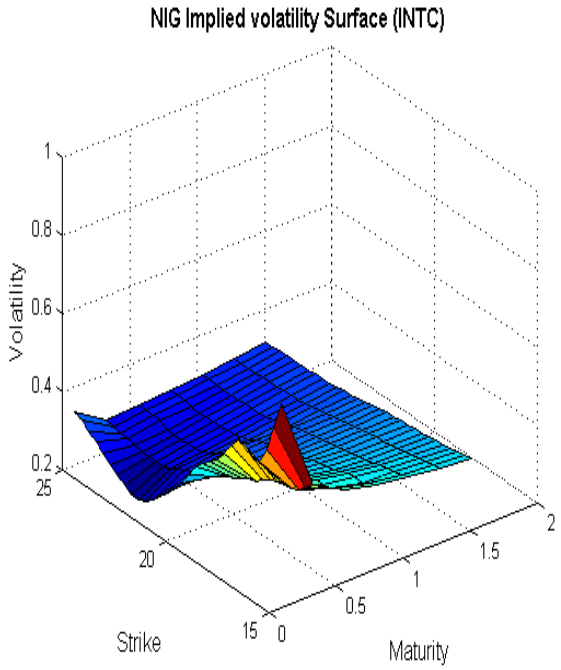


(c) NIG implied volatility surface

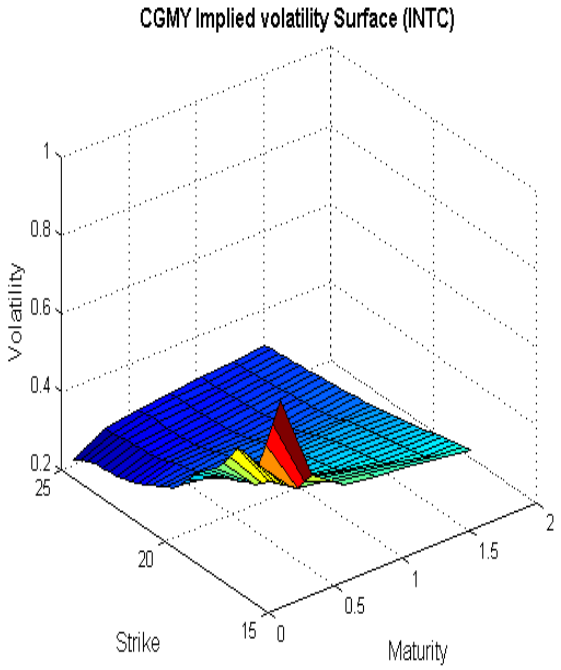


(d) CGMY implied volatility surface

**Figure 5.8.** Implied volatility surface for the INTC call options data.

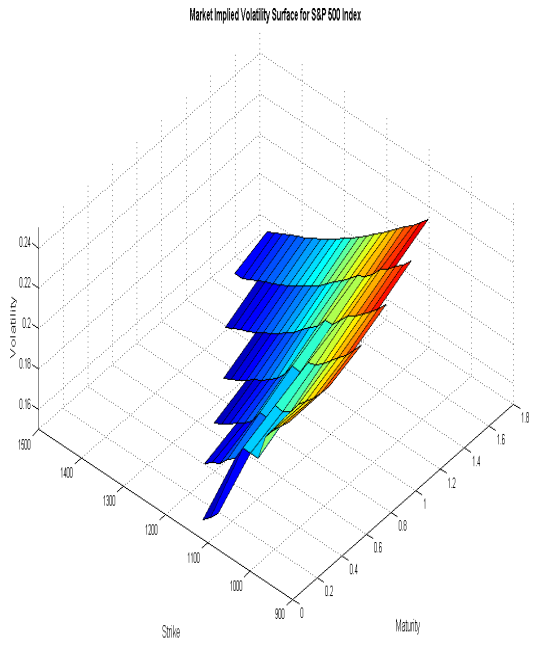


(a) Market implied volatility surface

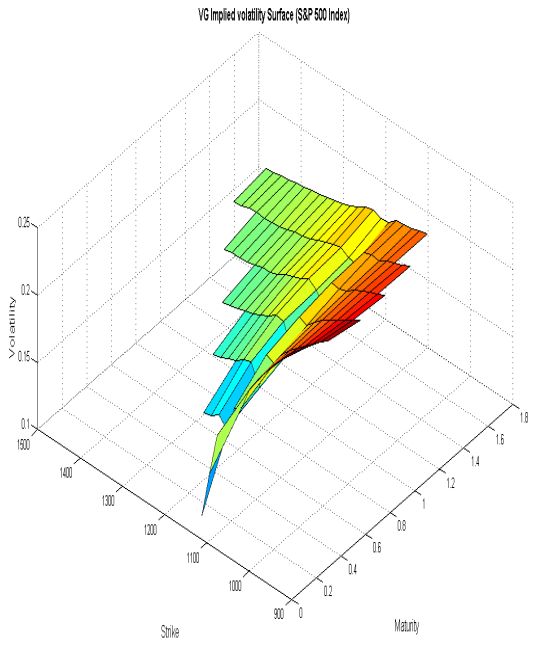


(b) VG implied volatility surface

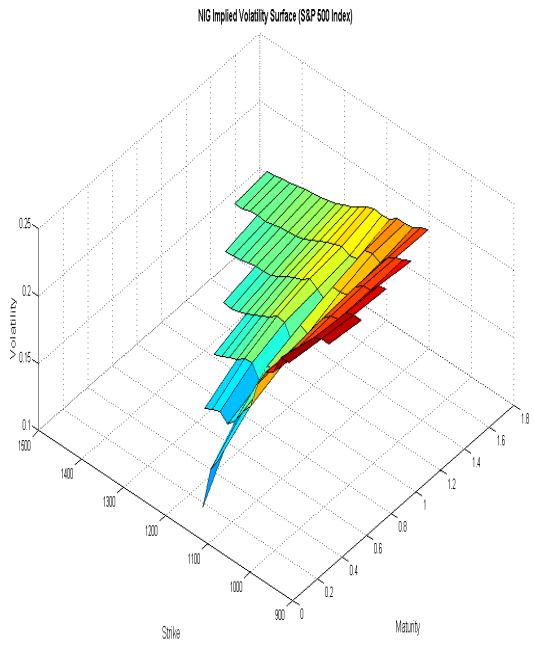


(c) NIG implied volatility surface

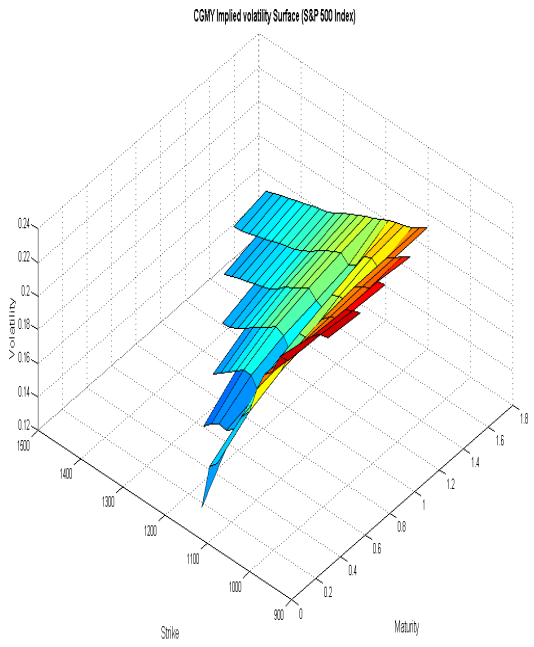


(d) CGMY implied volatility surface

**Figure 5.9.** Implied volatility surface for the S&P 500 call options data.

## 5.3 Simulation of the Stock Price Process

In Chapter 3, we simulated the sample path of the Lévy models under consideration using arbitrary values, but here we shall simulate these processes again using the parameters obtained from our calibration in Section 5.1.1. The aim of this is to check if using these parameters results in similar trajectories of the given processes respectively. Alongside the simulation of the sample path $X_t$, the stock price process given as the exponential of a Lévy process by Equation (4.3) will also be simulated. Also, this is only done for the global parameter set.

Figures 5.10 - 5.12 shows the simulated trajectories and price processes of our chosen models. From these plots, we can clearly see that both data sets yield similar results and the trajectories are not any different from those in Chapter 3. We can also see the effect of the $\nu = 1/C$ parameter on the overall activity of the variance gamma model. This is in agreement with the result presented in Figure 3.1.

Our next task is to price barrier optons. We intend to check the possibility that the above observations may have an effect on the prices that will be obtained. Since the calibration results are similar for the two option data sets considered, a very interesting point we hope to check is the similarity of the option prices that will be obtained using the four different parameter sets. These will be the focus of the next chapter.

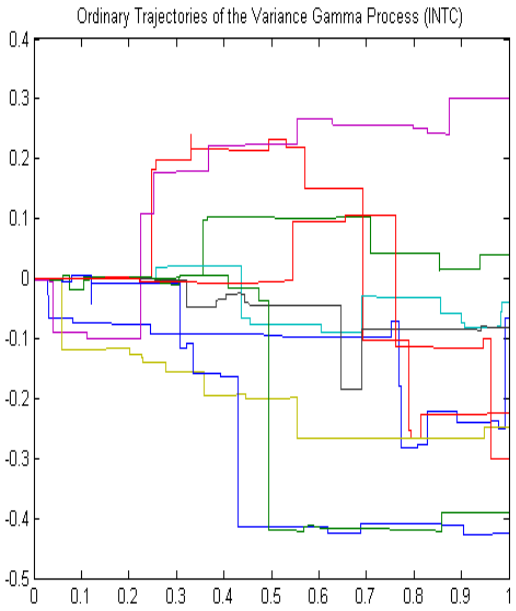


(a) VG trajectories for INTC option prices

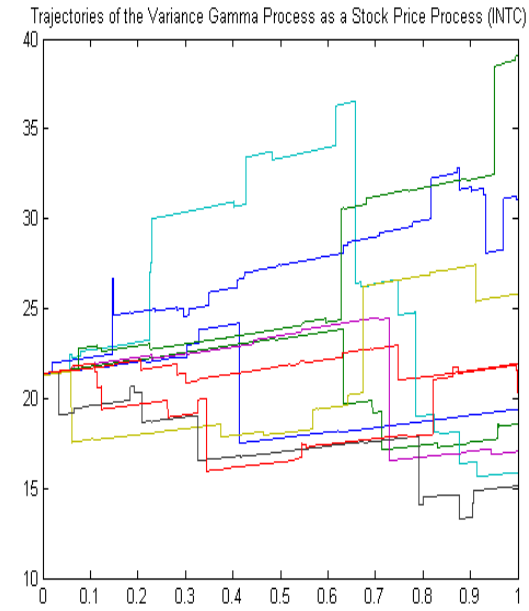


(b) VG stock price process for INTC option prices

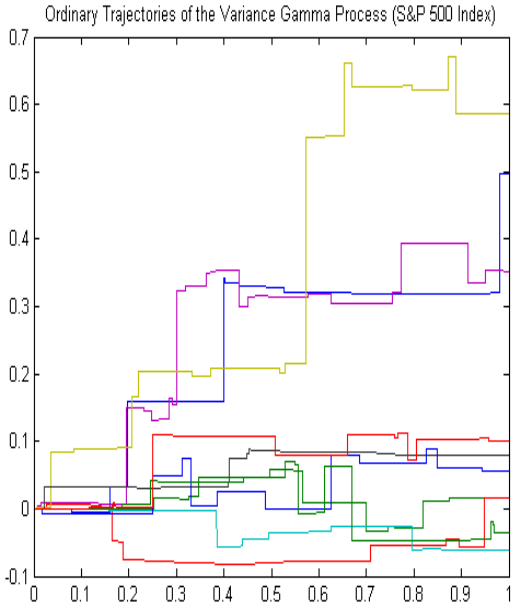


(c) VG trajectories for S&P 500 option

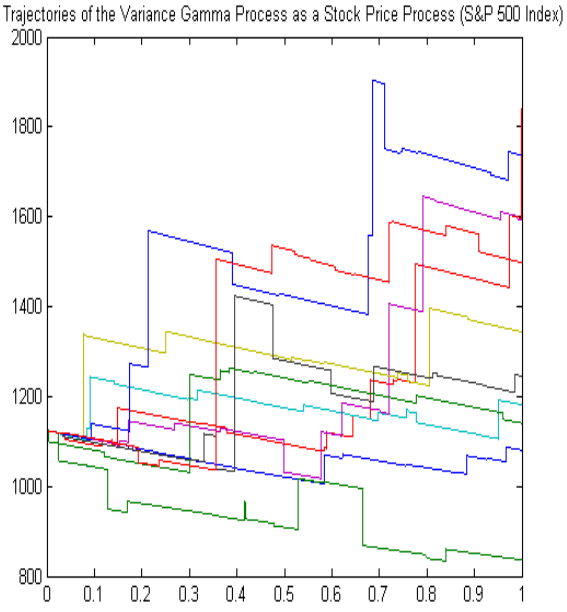


(d) VG stock price process for S&P 500 option

**Figure 5.10.** Simulation of VG trajectories and stock price process using parameters obtained from the global set of parameters.

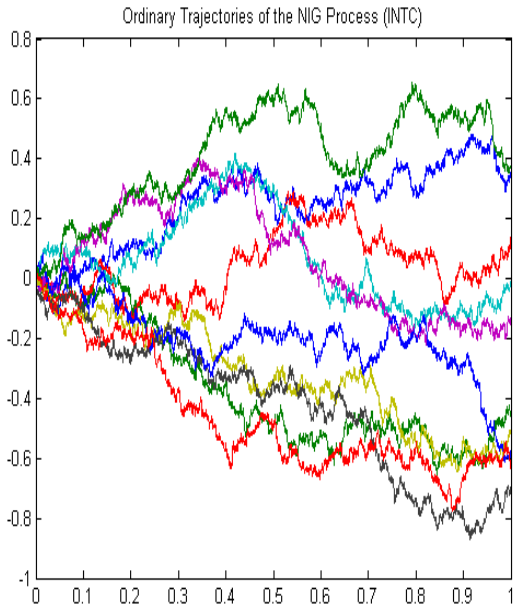


(a) NIG trajectories for INTC option prices

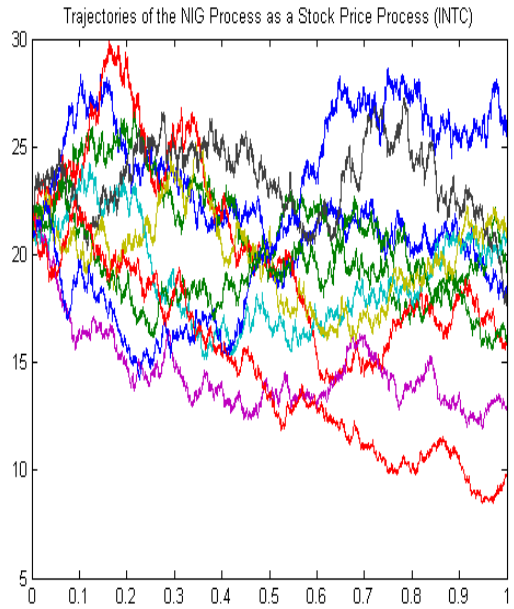


(b) NIG stock price process for INTC option prices

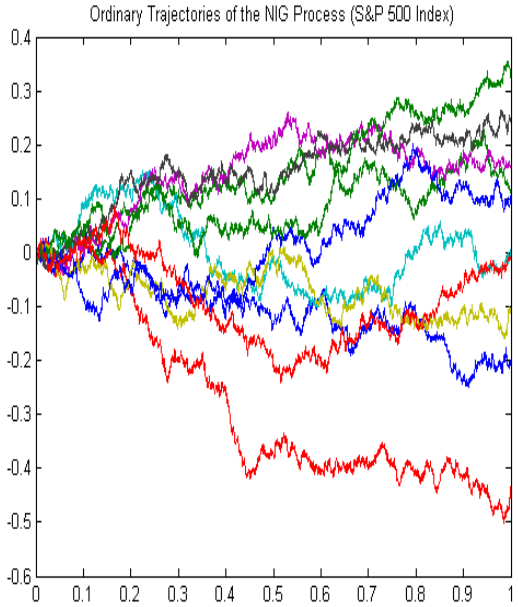


(c) NIG trajectories for S&P 500 option

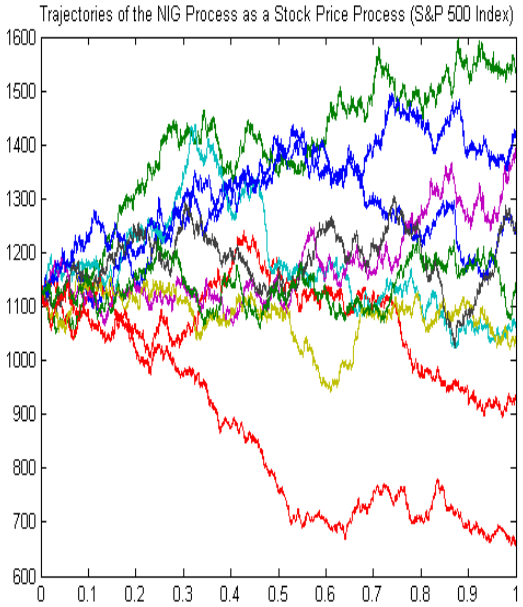


(d) NIG stock price process for S&P 500 option

**Figure 5.11.** Simulation of NIG trajectories and stock price process using parameters obtained from the global set of parameters.

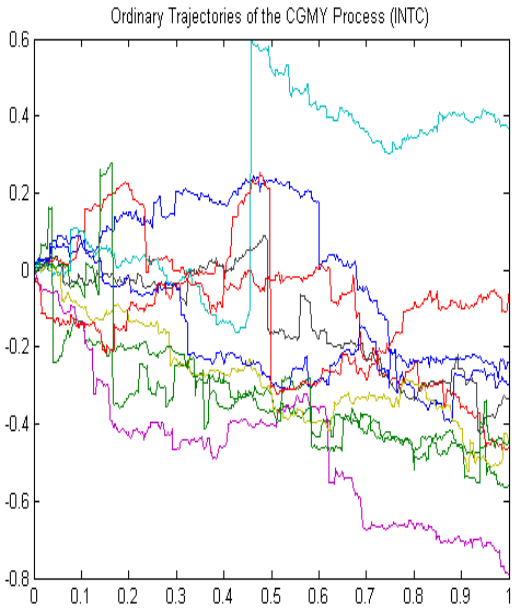


(a) CGMY trajectories for INTC option prices

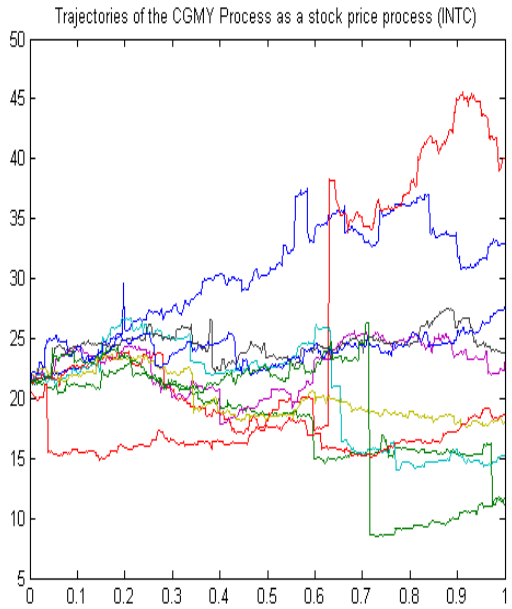


(b) CGMY stock price process for INTC option prices

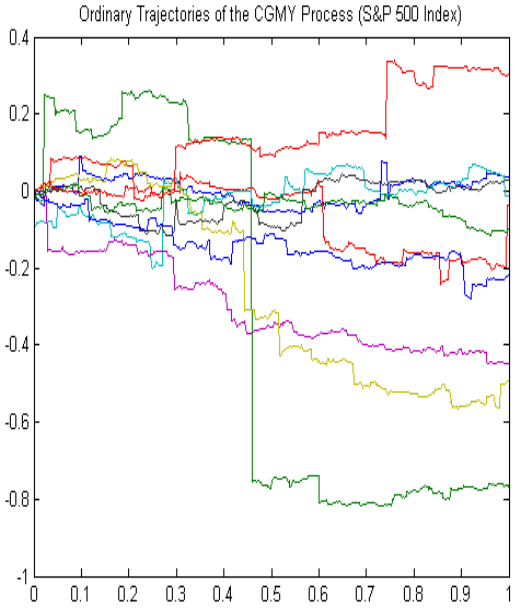


(c) CGMY trajectories for S&P 500 option

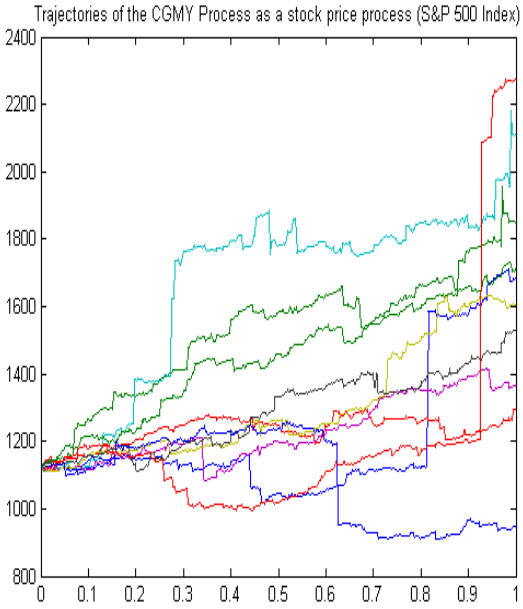


(d) CGMY stock price process for S&P 500 option

**Figure 5.12.** Simulation of CGMY trajectories and stock price process using parameters obtained from the global set of parameters.

# Chapter 6

# The Pricing of Barrier Options

The pricing of barrier options is of great interest and also requires extreme care. So far we have considered options whose payoffs depend only on the value of the underlying asset at maturity. This is not the case with barrier options as their payoff is path-dependent. To price these options, we will make use of the risk-neutral parameters obtained from our calibrations in Chapter 5. In Chapter 1, we discussed barrier options in detail. Based on this, we shall price up-and-in and up-and-out barrier call options in this chapter. This will be done using Monte Carlo simulation. The basic idea of the simulation procedure will be presented in the next section and we shall further describe this algorithm under the Lévy framework.

Our next task will be to present a brief discussion on the pricing of barrier options using the Black-Scholes pricing formula since we will be carrying out a comparison of our prices to those of this benchmark model. A presentation of results obtained will follow and we will conclude this chapter by checking the trend of our prices across different strikes and barrier levels. It is important to mention that barrier options are difficult to hedge even in the Black-Scholes framework [70]. This is due to the fact that even static hedging which is regarded to outperform the dynamic $\Delta$-hedging, uses out-of-the-money options for which Black-Scholes mispricing is large. Hence their performance is greatly affected by the extent to which market data and theoretical model characteristics are taken into account in its implementation. Taleb [89] shows that for a knock-out option, $\Delta$-hedging is even more difficult. This is due to the discontinuity in the deltas as the option crosses the barrier. On this note, we will only be pricing in this chapter and further work needs to be carried

out in order to construct hedges under our pricing framework.

## 6.1 The Concept of Monte Carlo Simulation

The pricing of assets in finance generally comprises of computing the mathematical expectation of payoffs. It is based on this fact, that we chose the Monte Carlo method as a suitable method for pricing these derivatives. The Monte Carlo method is a numerical calculation method used in performing numerical computations that involve functions of random variables. This involves carrying out a sequence of experiments and taking the average value. Most times, if we were to write the relevant expectations in the form of an integral, we would discover that its dimension is large or may even be infinite. This brings to mind the type of setting where Monte Carlo method becomes attractive. To be able to price financial derivatives, we need to simulate paths of the stochastic processes used to describe the evolution of the underlying asset prices, model parameters, interest rates, amongst other factors considered to be relevant to the security in question.

Considering the nature of this method where a large number of sample paths need to be simulated in order to obtain an accurate result, some techniques have been proposed for increasing the efficiency of the Monte Carlo simulations by reducing the variance of the simulation estimates. These techniques include amongst others the control variate technique, the antithetic variable technique, and importance sampling. Schoutens [81] showed that given a large number of sample paths, the standard error of paths without variance reduction technique tend to converge to those of paths simulated with variance reduction methods for exotic options. Considering this, we shall price barrier options with 50,000 sample paths for each model. Further details on this numerical procedure, can be found in [47] and [39].

**Monte Carlo Pricing for Lévy Processes**

An outline of how the Monte Carlo procedure works for Lévy models is presented below:

1. Calibrate the model on the vanilla option prices available in the market (INTC and S&P 500 call option prices in our case) to obtain the risk-neutral parameters of the model. This procedure has been carried out in Chapter 5.

2. With the parameters of Step 1, simulate a significant number $N$ of the stock-price process of the model.

3. Calculate the value of the payoff function $P_i$ for each of the paths simulated, $i = 1, \ldots, N$.

4. Calculate the sample mean of the payoffs to get the estimate of the expected payoff $\hat{P} = \frac{1}{N}\sum_{i=1}^{N} P_i$.

5. Discount the estimated payoff at the risk-free rate to get an estimate of the price of the derivative, $e^{-rT}\hat{P}$.

## 6.2 Pricing in the Black-Scholes Framework

In the Black-Scholes framework, there are closed form formulas for the valuation of barrier options. Since we shall be pricing only 'up' call options in this chapter, we state the formulas for these options and refer the reader to Hull [47], for further details on other types of barrier and exotic options in general. When the barrier level is less than or equal to the strike ($H \leq K$), the value of the up-and-out call option is zero while that of the up-and-in option becomes the price of the vanilla call with the same strike and maturity. For the case where the barrier level is greater than the strike, the price of the up-and-in call option is given by

$$\begin{aligned} UIC \quad = \quad & S_0 N(x_1)\exp(-qT) - K\exp(-rT)N(x_1 - \sigma\sqrt{T}) \\ - \quad & S_0\exp(-qT)(H/S_0)^{2\lambda}(N(-y) - N(-y_1)) \\ + \quad & K\exp(-qT)(H/S_0)^{2\lambda-2}(N(-y+\sigma\sqrt{T}) - N(-y_1+\sigma\sqrt{T}))\,, \end{aligned}$$

where

$$\begin{aligned}
\lambda &= \sigma^{-2}(r - q + \frac{1}{2}), \\
y &= (\sigma\sqrt{T})^{-1}\log(H^2/(S_0K)) + \lambda\sigma\sqrt{T}, \\
x_1 &= (\sigma\sqrt{T})^{-1}\log(S_0/H) + \lambda\sigma\sqrt{T}, \\
y_1 &= (\sigma\sqrt{T})^{-1}\log(H/S_0) + \lambda\sigma\sqrt{T}.
\end{aligned}$$

The price for the up-and-out call option is also given by the in-out parity relation to the price of the vanilla call option:

$$UOC = C_T - UIC.$$

## 6.3 Numerical Results

In this section, we price barrier options both in the Black-Scholes framework and using models driven by Lévy dynamics. Our results will be in two dimensions. Firstly, we compute barrier option prices across several strikes and for the two data sets, when the barrier is equal to the spot price. This is due to the fact that the prices of the up-and-out and up-and-in barrier call options when the barrier is equal to the spot price, are zero and the vanilla call price respectively. The aim of this is to check the efficiency and accuracy of our model prices against those of the market prices since the parameter sets used in the pricing were obtained from the calibration of these same prices. We shall present prices for the maturity dates October 2010 and December 2002 for the INTC and S&P 500 data sets respectively.

Another important dimension will be to consider the prices of the barrier option when the barrier level is varied. This we will do by varying the barrier from 0.5 to 1.5 of the spot price. We only present the prices for a single strike. We start by presenting these results.

The prices for the two data sets are presented in Tables 6.1 and 6.2. For the Lévy models, the prices are very close to each other and give a good indication of what the true prices (market prices) are. This is further illustrated in Figures 6.1 to 6.5. Here, we see that the model prices provide better indication of the vanilla market prices than those of the benchmark model (Black-Scholes). Figures 6.1 to 6.3 show the similarity in prices of the

| UP-AND-IN BARRIER CALL PRICES (INTC) | | | | | | |
|---|---|---|---|---|---|---|
| MODEL | STRIKE | BS | GLOBAL | PERTURBED | LOCAL | SINGLE |
| VG | 18 | 3.2875 | 3.6998 | 3.6459 | 3.5946 | 3.5284 |
| | 19 | 2.3069 | 2.8397 | 2.8141 | 2.7645 | 2.7324 |
| | 20 | 1.4021 | 2.0658 | 2.0164 | 2.0228 | 1.9963 |
| | 21 | 0.6930 | 1.3790 | 1.3161 | 1.3820 | 1.3693 |
| | 22 | 0.2647 | 0.8022 | 0.7501 | 0.8534 | 0.8919 |
| | 23 | 0.0760 | 0.4606 | 0.4769 | 0.4947 | 0.5304 |
| | 24 | 0.0163 | 0.2976 | 0.3081 | 0.2860 | 0.2860 |
| NIG | 18 | 3.2875 | 3.6875 | 3.6476 | 3.5802 | 3.5265 |
| | 19 | 2.3069 | 2.8116 | 2.7613 | 2.7533 | 2.7148 |
| | 20 | 1.4021 | 2.0134 | 1.9646 | 1.9827 | 1.9776 |
| | 21 | 0.6930 | 1.3155 | 1.2493 | 1.3492 | 1.3679 |
| | 22 | 0.2647 | 0.7867 | 0.7341 | 0.8410 | 0.8778 |
| | 23 | 0.0760 | 0.4613 | 0.4698 | 0.4928 | 0.5260 |
| | 24 | 0.0163 | 0.2982 | 0.3207 | 0.2897 | 0.2865 |
| CGMY | 18 | 3.2875 | 3.6057 | 3.6712 | 3.5919 | 3.5175 |
| | 19 | 2.3069 | 2.8212 | 2.7895 | 2.7694 | 2.7171 |
| | 20 | 1.4021 | 1.9855 | 1.9469 | 2.0657 | 2.0933 |
| | 21 | 0.6930 | 1.3366 | 1.2749 | 1.3533 | 1.4244 |
| | 22 | 0.2647 | 0.8024 | 0.7322 | 0.8473 | 0.8519 |
| | 23 | 0.0760 | 0.4864 | 0.4885 | 0.4852 | 0.4889 |
| | 24 | 0.0163 | 0.3010 | 0.2863 | 0.2843 | 0.2825 |

**Table 6.1.** Up-and-in call option prices using the parameters obtained from calibrating the INTC data.

four different parameter sets for each model, despite the differences in the risk-neutral parameter sets as shown in Tables 5.1 and 5.2. For the CGMY model, we notice some noise especially in the prices for the S&P 500 call options. These are attributed to the bias that are introduced due to the truncation of small jumps during the simulation of this model as this is not easy to quantify (see [73]). We can on this ground conclude that the models driven by Lévy dynamics are more suitable for the pricing of exotic options. We ran a total of $50,000$ simulations for each of the models under consideration. It took

| UP-AND-IN BARRIER CALL PRICES (S&P 500 INDEX) | | | | | | |
|---|---|---|---|---|---|---|
| MODEL | STRIKE | BS | GLOBAL | PERTURBED | LOCAL | SINGLE |
| VG | 975 | 156.6920 | 175.9259 | 176.8584 | 173.5763 | 173.2030 |
| | 1050 | 94.7932 | 118.9188 | 119.0857 | 116.1454 | 114.7987 |
| | 1100 | 62.0673 | 85.3894 | 84.7771 | 84.3945 | 81.7081 |
| | 1125 | 48.7909 | 69.9189 | 71.0141 | 69.5248 | 67.3481 |
| | 1140 | 41.8303 | 62.7261 | 62.1025 | 60.8671 | 59.1068 |
| | 1175 | 28.4009 | 43.9825 | 44.6425 | 44.8547 | 42.7372 |
| | 1225 | 15.2600 | 26.1770 | 26.2060 | 26.1021 | 24.6725 |
| NIG | 975 | 156.6920 | 177.2462 | 176.9670 | 174.3145 | 173.5580 |
| | 1050 | 94.7932 | 118.6859 | 118.2608 | 115.5308 | 114.7373 |
| | 1100 | 62.0673 | 84.9579 | 84.7180 | 82.6439 | 82.0916 |
| | 1125 | 48.7909 | 69.3500 | 69.1432 | 69.1547 | 67.1689 |
| | 1140 | 41.8303 | 61.1622 | 60.5686 | 60.7828 | 58.6875 |
| | 1175 | 28.4009 | 43.6082 | 44.0773 | 44.2551 | 42.4960 |
| | 1225 | 15.2600 | 26.1563 | 26.2349 | 26.0610 | 24.5861 |
| CGMY | 975 | 156.6920 | 178.5010 | 178.0389 | 178.1140 | 176.5564 |
| | 1050 | 94.7932 | 119.1091 | 119.0603 | 118.6258 | 115.1016 |
| | 1100 | 62.0673 | 87.6402 | 86.6402 | 85.9959 | 83.6572 |
| | 1125 | 48.7909 | 66.8594 | 67.6013 | 66.9180 | 66.3625 |
| | 1140 | 41.8303 | 60.4052 | 57.8994 | 59.9525 | 58.0087 |
| | 1175 | 28.4009 | 47.8362 | 46.5537 | 45.5209 | 42.5389 |
| | 1225 | 15.2600 | 27.0524 | 28.5182 | 28.1276 | 26.5896 |

**Table 6.2.** Up-and-in call option prices using the parameters obtained from calibrating the S&P 500 index data.

about 28 seconds to run each simulation for the VG and NIG models, while for the CGMY model, it took a total of 38.45 minutes. This brings to light the complexity involved in the simulation of the CGMY process.

Another model risk noticed from this exercise is the effect of computational method for the simulation of random variables for these models. The VG stands out as the model with the easiest method of computation for random variables since there exist inbuilt functions

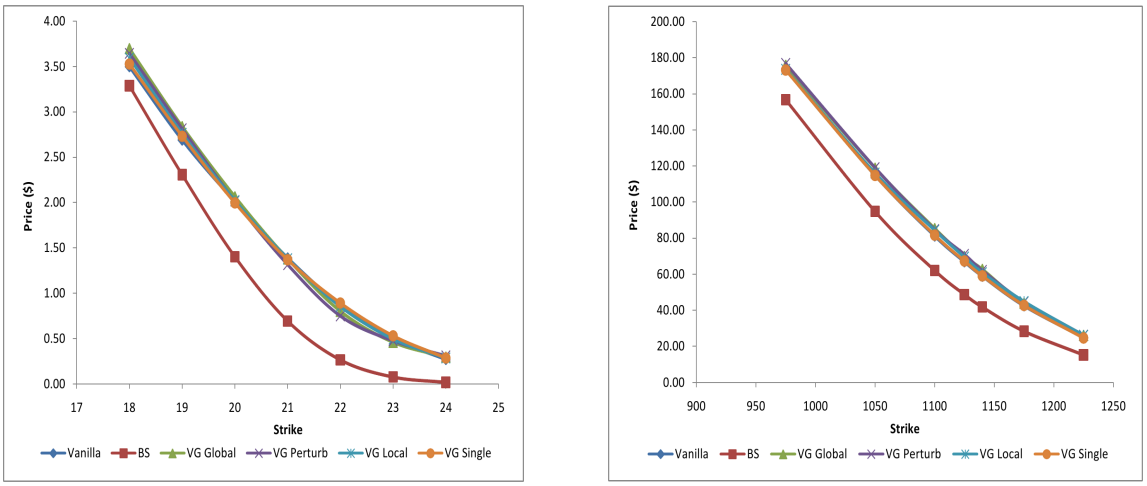


(a) INTC option prices

(b) S&P 500 option prices

**Figure 6.1.** Up-and-in call option prices for the VG model computed using the four parameter sets. This is compared to those of the Black-Scholes model and the vanilla market prices.

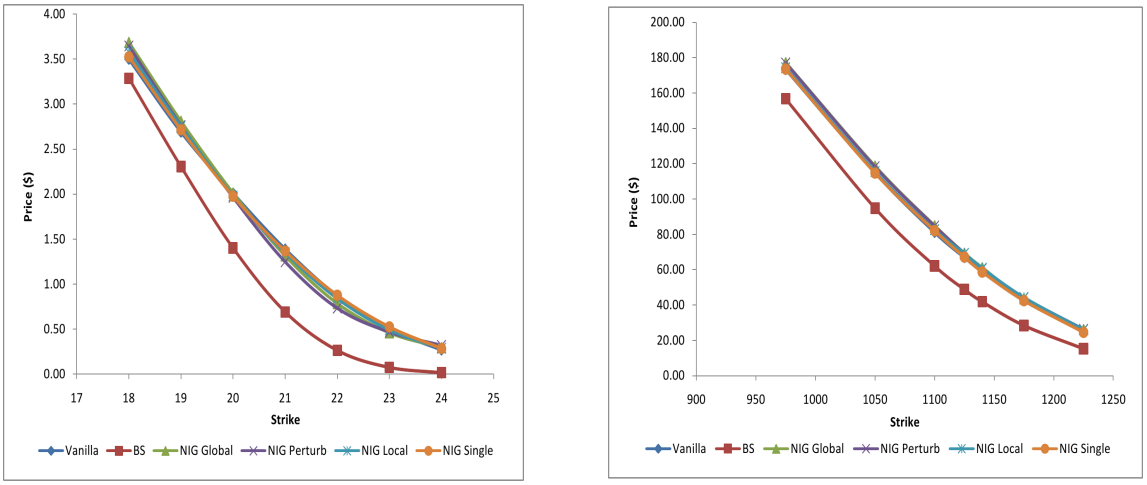


(a) INTC option prices

(b) S&P 500 option prices

**Figure 6.2.** Up-and-in call option prices for the NIG model computed using the four parameter sets. This is compared to those of the Black-Scholes model and the vanilla market prices.

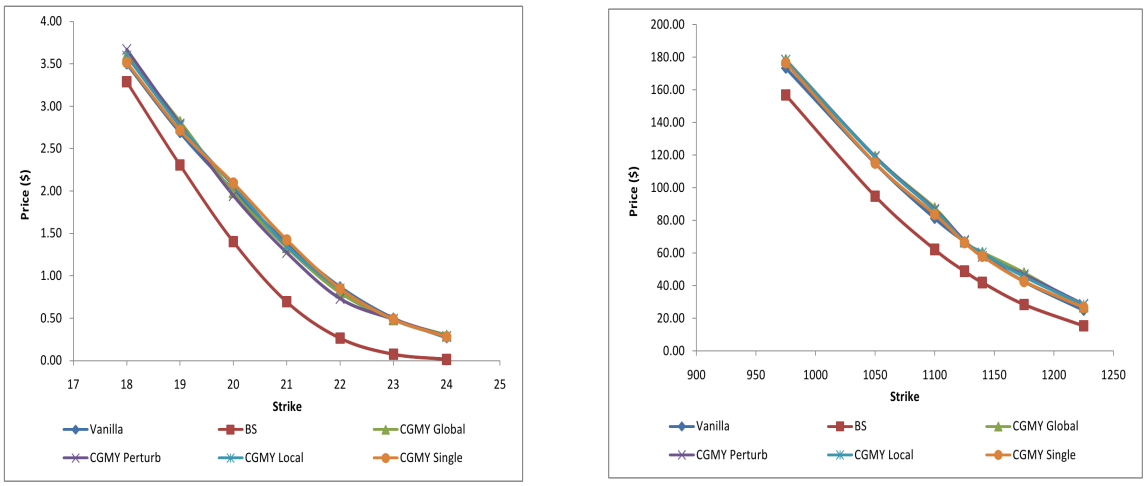


(a) INTC option prices

(b) S&P 500 option prices

**Figure 6.3.** Up-and-in call option prices for the CGMY model computed using the four parameter sets. This is compared to those of the Black-Scholes model and the vanilla market prices.

for the gamma random variables in almost all programming software. For the NIG model, the inverse Gaussian random variables need to be computed using Algorithm 3.4.2. The parameters for computing this random variable have varied amongst different authors, we followed that described in [8]. The CGMY model is more complicated as it does not only involve special functions (confluent hypergeometric function) which are difficult to find in programming software, but also, no exact simulation of its increments is known (see [73]).

### Results for Varying Barrier Levels

The prices computed here are for the strike prices 21 and 1125 for the INTC and S&P 500 data sets respectively. The barrier level is varied by 0.5 to 1.5 of the spot price, and a comparison plot with the Black-Scholes model prices is presented for each of the models. Another comparison is that between the prices of the Lévy models and these are also presented with the Black-Scholes model prices. These prices are for both the up-and-in and up-and-out call options, and are only computed for the global parameter sets.

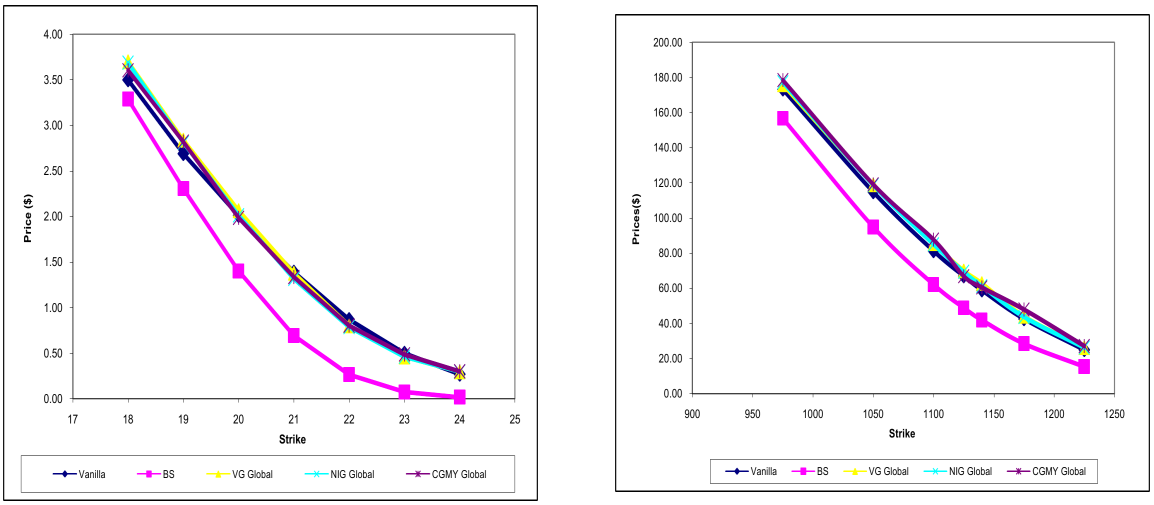


(a) INTC option prices (b) S&P 500 option prices

**Figure 6.4.** Up-and-in call option prices for all the models computed using the global parameter sets. This is compared to those of the Black-Scholes model and the vanilla market prices.

| Barrier | VG-In | VG-Out | NIG-In | NIG-Out | CGMY-In | CGMY-Out | BS-In | BS-Out |
|---|---|---|---|---|---|---|---|---|
| 10.6950 | 1.3790 | 0.0000 | 1.3155 | 0.0000 | 1.3366 | 0.0000 | 0.6930 | 0.0000 |
| 14.9730 | 1.3790 | 0.0000 | 1.3155 | 0.0000 | 1.3366 | 0.0000 | 0.6930 | 0.0000 |
| 19.2510 | 1.3790 | 0.0000 | 1.3155 | 0.0000 | 1.3366 | 0.0000 | 0.6930 | 0.0000 |
| 21.3900 | 1.3790 | 0.0000 | 1.3155 | 0.0000 | 1.3366 | 0.0000 | 0.6930 | 0.0000 |
| 23.5290 | 0.7971 | 0.5658 | 0.8470 | 0.4564 | 0.8027 | 0.5186 | 0.2821 | 0.4109 |
| 27.8070 | 0.2425 | 1.1138 | 0.2618 | 1.0493 | 0.2308 | 1.1614 | 0.0002 | 0.6928 |
| 32.0850 | 0.0869 | 1.2974 | 0.1041 | 1.1936 | 0.1161 | 1.2493 | 0.0000 | 0.6930 |

**Table 6.3.** INTC 'Up' call option prices for varying barrier levels. The barrier is varied by 0.5 to 1.5 of the spot price in each case.

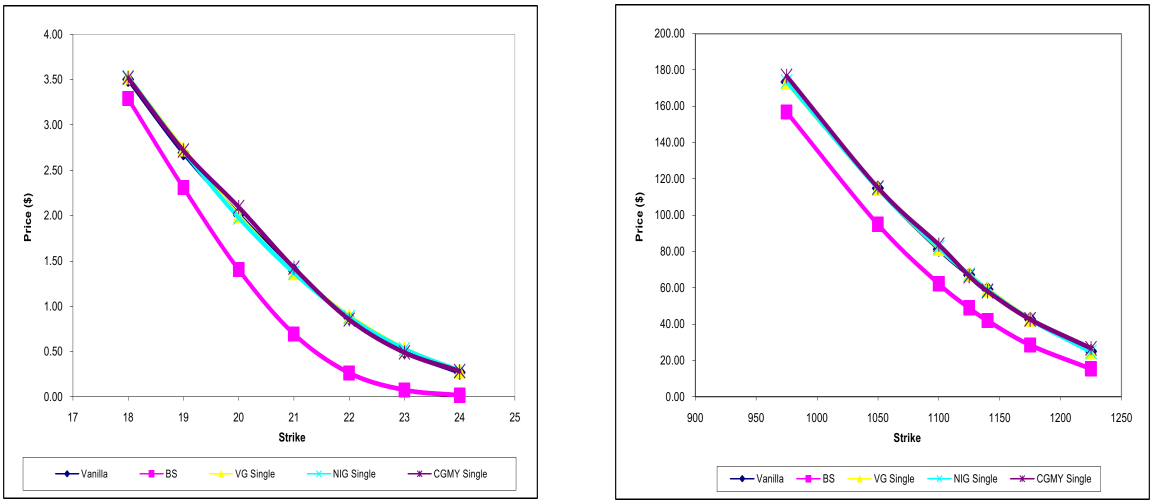


(a) INTC option prices

(b) S&P 500 option prices

**Figure 6.5.** Up-and-in call option prices for all the models computed using the single parameter sets. This is compared to those of the Black-Scholes model and the vanilla market prices.

| Barrier | VG-In | VG-Out | NIG-In | NIG-Out | CGMY-In | CGMY-Out | BS-In | BS-Out |
|---|---|---|---|---|---|---|---|---|
| 562.2350 | 69.9189 | 0.0000 | 69.3500 | 0.0000 | 66.8594 | 0.0000 | 48.7909 | 0.0000 |
| 787.1290 | 69.9189 | 0.0000 | 69.3500 | 0.0000 | 66.8594 | 0.0000 | 48.7909 | 0.0000 |
| 1012.0230 | 69.9189 | 0.0000 | 69.3500 | 0.0000 | 66.8594 | 0.0000 | 48.7909 | 0.0000 |
| 1124.4700 | 69.9189 | 0.0000 | 69.3500 | 0.0000 | 66.8594 | 0.0000 | 48.7909 | 0.0000 |
| 1236.9170 | 56.2563 | 14.1049 | 57.8757 | 12.3010 | 56.0166 | 13.0559 | 42.2983 | 6.4926 |
| 1461.8110 | 9.5882 | 61.0112 | 9.2598 | 60.4237 | 9.8063 | 58.1869 | 3.9600 | 44.8309 |
| 1686.7050 | 1.2931 | 68.9274 | 1.5410 | 68.4924 | 1.6252 | 63.6304 | 0.0567 | 48.7342 |

**Table 6.4.** S&P 500 index 'Up' call option for varying barrier levels. The barrier is varied by 0.5 to 1.5 of the spot price in each case.

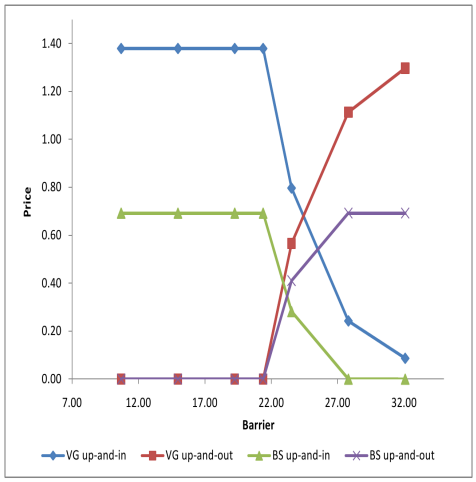


(a) INTC barrier option prices

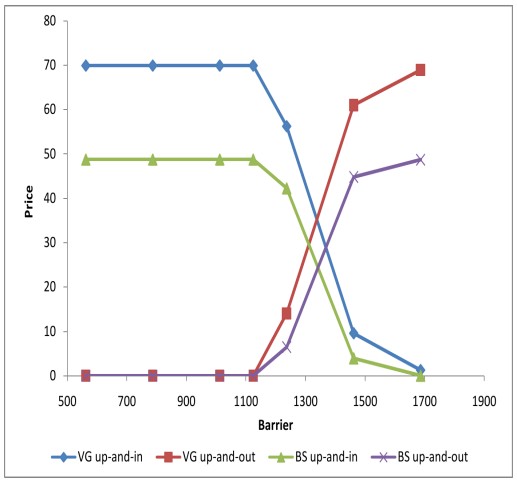


(b) S&P 500 barrier option prices

**Figure 6.6.** 'Up' barrier call option prices for the VG model computed using the global parameter sets. These are compared to those of the Black-Scholes model. The barrier is varied by 0.5 to 1.5 of the spot price in each case.

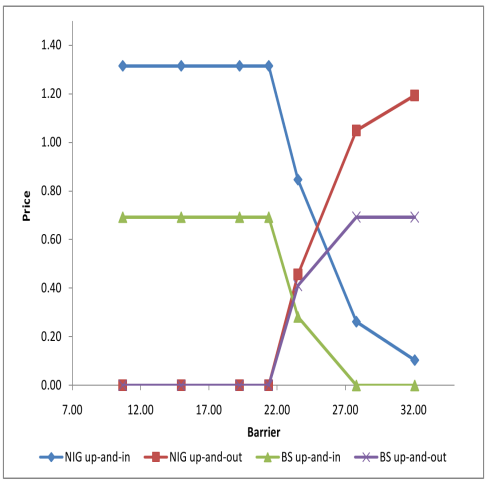


(a) INTC barrier option prices

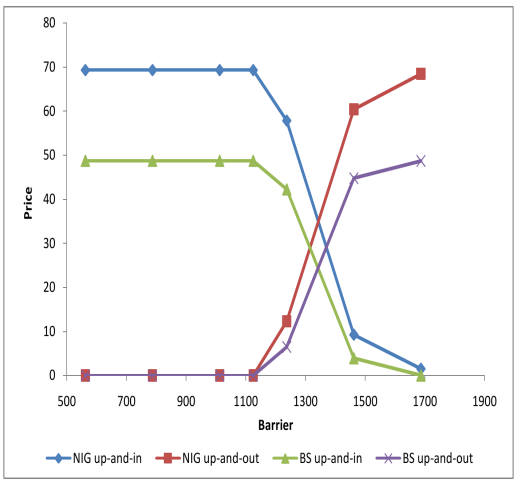


(b) S&P 500 barrier option prices

**Figure 6.7.** 'Up' barrier call option prices for the NIG model computed using the global parameter sets. These are compared to those of the Black-Scholes model. The barrier is varied by 0.5 to 1.5 of the spot price in each case.

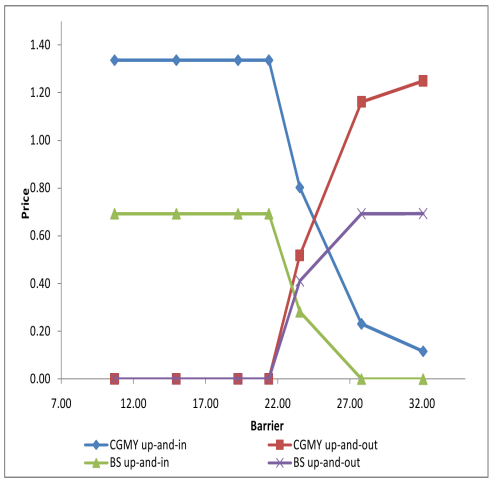


(a) INTC barrier option prices

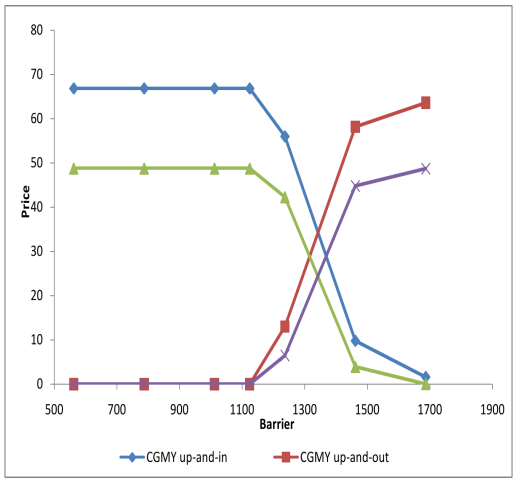


(b) S&P 500 barrier option prices

**Figure 6.8.** 'Up' barrier call option prices for the CGMY model computed using the global parameter sets. These are compared to those of the Black-Scholes model. The barrier is varied by 0.5 to 1.5 of the spot price in each case.

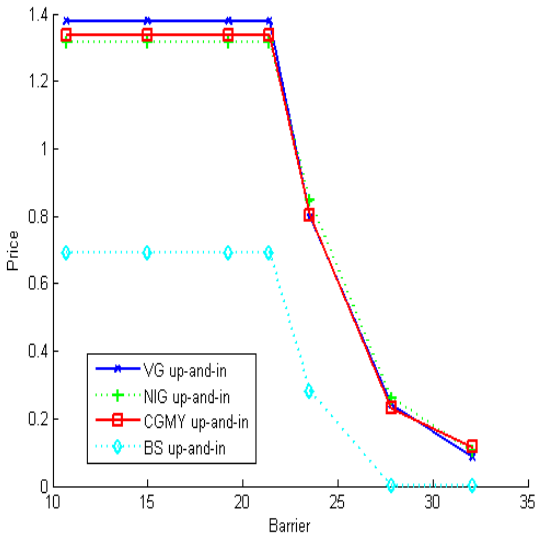


(a) INTC barrier option prices

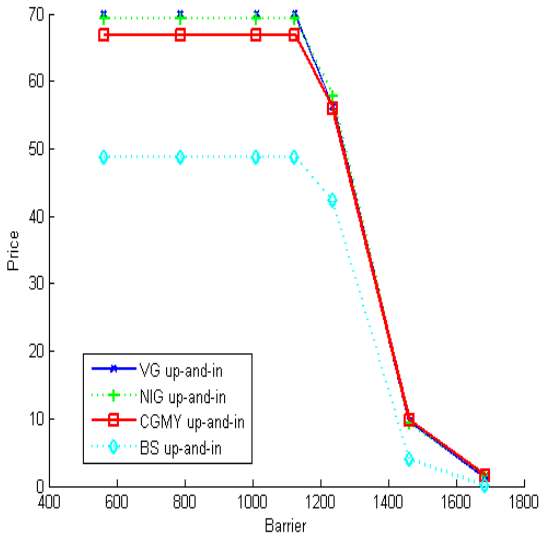


(b) S&P 500 barrier option prices

**Figure 6.9.** Up-and-in barrier call option prices for all the models computed using the global parameter sets. These are compared to those of the Black-Scholes model. The barrier is varied by 0.5 to 1.5 of the spot price in each case.

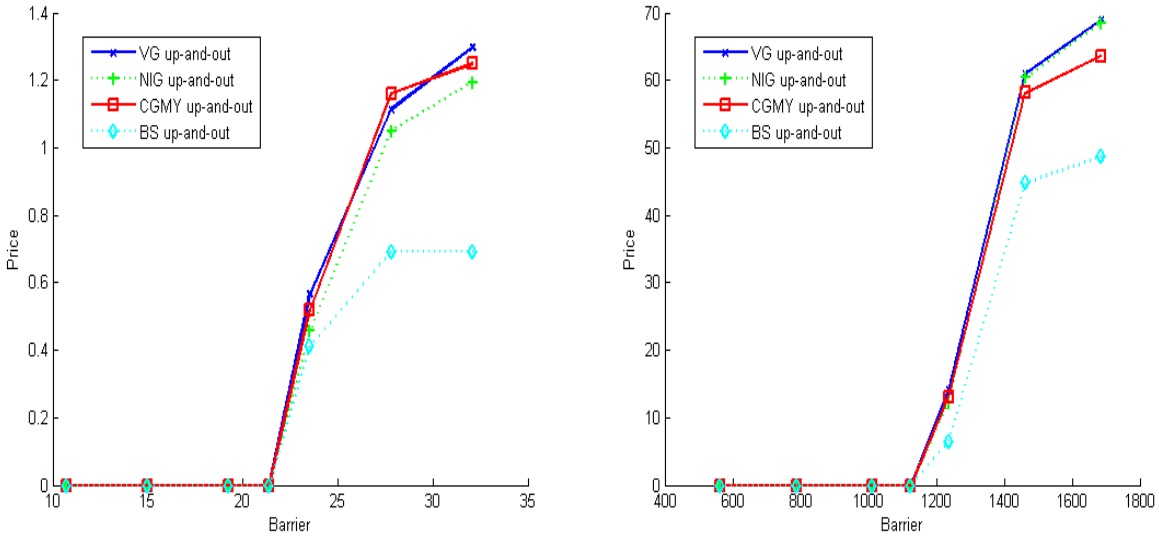


(a) INTC barrier option prices

(b) S&P 500 barrier option prices

**Figure 6.10.** Up-and-out barrier call option prices for all the models computed using the global parameter sets. These are compared to those of the Black-Scholes model. The barrier is varied by 0.5 to 1.5 of the spot price in each case.

Figures 6.6 - 6.8 show the prices of the up-and-in and up-and-out barrier call options when the barrier is varied by 0.5 to 1.5 of the spot price. The poor fit of the prices of the Black Scholes model is further highlighted again. This is in line with the trend we hoped to see. From Figures 6.9 and 6.10, we can notice the difference between the CGMY model and the other two Lévy models for the S&P 500 option prices. The price difference for the INTC is minimal (that is, VG is by 0.0635 and 0.0424 greater than the prices of the NIG and CGMY model for barrier = 10.6950), as shown by Table 6.3. On this note, we conclude this chapter by stating clearly that the ability of a model to calibrate vanilla option prices better than others does not necessary imply that it will also price exotic options better especially when other factors are placed into consideration as have been seen with the CGMY model.

# Chapter 7

# Conclusion

In this dissertation, we considered the model risks associated with pricing of barrier options under three different Lévy models. These models are the variance gamma, normal inverse Gaussian and CGMY models. We started by presenting the results obtained when we fit the densities of these models to the log returns of some major securities (INTC, IBM, DELL and S&P 500 Index). This procedure was carried out by inverting the characteristic function of the Lévy models using the fast Fourier transform method as presented by Carr and Madan [25]. It was observed that these models gave a very good fit when compared to the empirical densities.

A further analysis was conducted by calibrating these models to vanilla prices. It was discovered that the four-parameter model (CGMY) outperformed both the VG and NIG models when we compare the root-mean-squared error and the graphs of the calibration results. This was carried out for two different data sets (INTC and S&P 500 Index) and the calibration entailed all strikes and maturities. We went ahead to slightly perturb the data sets in order to see how different the parameters obtained would be from those of the initial calibration procedure. Our results show that there were instances where they were close, but in most cases, they were not similar. Finally on this aspect, we also calibrated to a single maturity across all strikes.

Our main task was to price barrier options using the parameter sets obtained from the calibration procedures. This we did, and a comparison was made to the Black-Scholes and vanilla prices. Since the prices of barrier options are not quoted on exchanges, we started

by computing the prices of the up-and-in call option when the barrier level is given by the spot price, knowing that this is equal to the price of the vanilla call option. Since the parameter sets were obtain from calibrating vanilla options, we expected our prices to be a good approximation of the market prices. Our results show that this is actually the case for the Lévy models and the prices from the four different parameter sets were very similar not just for the given model, but across all models.

In the course of pricing barrier options, we discovered some model risks which we will like to point out. They include:

- A very good knowledge of the range of the model parameters is very essential especially when calibrating to option prices. This is due to the fact that there were cases where we obtained lower values for the root-mean-squared error, but one of the parameters of the model will be reported as being negative, which should not be the case.

- In the simulation of these models, we discovered that the VG model had the simplest dynamics especially in terms of generating the random variables used in its simulation. This is no doubt the reason why this model has gained wide usage in the literature by several authors (see [84], [45], [24], [25], [22] and [83]). The NIG model involves simulating the inverse Gaussian random variable using Algorithm 3.4.2. Here, care needs to be applied in the choice of the parameters to ensure accuracy of the model simulation. The simulation of the CGMY process is quite tasking and there can be an introduction of bias resulting from the truncation of small jumps. This is not easy to quantify.

- Lastly, we want to mention that the ability of a model to fit vanilla option prices very well does not imply an automatic ability to price exotic options properly, especially where the dynamics involved in the two procedures are different. This we have seen in the case of the CGMY model where the calibration procedure was carried out via the FFT procedure using its characteristic function, and the pricing was carried out using Brownian subordination and the exact increment of the model is not known. This is reflected in the prices of the barrier options computed for this model especially for the S&P data. When time is to be considered, this model is time consuming as

it took about 28 seconds to run each simulation for the VG and NIG models, and it took a total of 38.45 minutes for the CGMY model.

In our work, we focused on just the pricing of barrier options and will therefore recommend a further study of the possible hedging strategies for models driven by Lévy dynamics. Considering the fact that these models are incomplete and replication of options in this framework is almost not possible, it will be great success to see that there are possible methods of hedging using these models. Another interesting aspect is to carry out similar analysis as have been presented in this work using Lévy models with stochastic volatility.

# Appendix A

# Call Option Prices

## A.1 INTC Call Option Prices

In the following table, we can find 38 call option prices on INTC stock at the close of the market on July 20th, 2010. The market closed at 21.39. We had values of $r = 1.13\%$ and $q = 3.00\%$ per year.

| Strike | Aug. 10 | Sept. 10 | Oct. 10 | Jan. 11 | Jan. 12 |
|---|---|---|---|---|---|
| 15 | 6.30 | | 6.40 | 6.55 | 7.10 |
| 16 | 5.20 | | 5.20 | | |
| 17 | 4.25 | | 4.46 | | |
| 18 | 3.45 | | 3.50 | | |
| 19 | 2.40 | 2.60 | 2.69 | 3.26 | |
| 20 | 1.58 | 1.78 | 2.01 | 2.60 | 3.85 |
| 21 | 0.79 | 1.08 | 1.39 | 2.00 | |
| 22 | 0.33 | 0.58 | 0.87 | | |
| 23 | 0.11 | 0.27 | 0.50 | | |
| 24 | 0.03 | 0.11 | 0.27 | 0.74 | |
| 25 | 0.02 | 0.05 | 0.15 | 0.52 | 1.73 |

**Table A.1.** The data set for INTC plain vanilla call option prices

## A.2 S&P 500 Call Option Prices

In the following table, we can find 75 call option prices on the S&P 500 Index at the close of the market on 18th April, 2002 [81]. The market closed at 1124.47. We had values of $r = 1.9\%$ and $q = 1.2\%$ per year.

| STRIKE | May 02 | Jun 02 | Sept 02 | Dec 02 | Mar 03 | Jun 03 | Dec 03 |
|---|---|---|---|---|---|---|---|
| 975 | | | 161.60 | 173.30 | | | |
| 995 | | | 144.80 | 157.00 | | 182.10 | |
| 1025 | | | 120.10 | 133.10 | 146.50 | | |
| 1050 | | 84.50 | 100.70 | 114.80 | | 143.00 | 171.40 |
| 1075 | | 64.30 | 82.50 | 97.60 | | | |
| 1090 | 43.10 | | | | | | |
| 1100 | 35.60 | | 65.50 | 81.20 | 96.20 | 111.30 | 140.40 |
| 1110 | | 39.50 | | | | | |
| 1120 | 22.90 | 33.50 | | | | | |
| 1125 | 20.20 | 30.70 | 51.00 | 66.90 | 81.70 | 97.00 | |
| 1130 | | 28.00 | | | | | |
| 1135 | | 25.60 | 45.50 | | | | |
| 1140 | 13.30 | 23.20 | | 58.90 | | | |
| 1150 | | 19.10 | 38.10 | 53.90 | 68.30 | 83.30 | 112.80 |
| 1160 | | 15.30 | | | | | |
| 1170 | | 12.10 | | | | | |
| 1175 | | 10.90 | 27.70 | 42.50 | 56.60 | | 99.80 |
| 1200 | | | 19.60 | 33.00 | 46.10 | 60.90 | |
| 1225 | | | 13.20 | 24.90 | 36.90 | 49.80 | |
| 1250 | | | | 18.30 | 29.30 | 41.20 | 66.90 |
| 1275 | | | | 13.20 | 22.50 | | |
| 1300 | | | | | 17.20 | 27.10 | 49.50 |
| 1325 | | | | | 12.80 | | |
| 1350 | | | | | | 17.10 | 35.70 |
| 1400 | | | | | | 10.10 | 25.20 |
| 1450 | | | | | | | 17.00 |
| 1500 | | | | | | | 12.20 |

**Table A.2.** The data set for S&P 500 plain vanilla call option prices

# Bibliography

[1] H. Albrecher and M. Predota. On Asian Option Pricing for NIG Lévy Processes. *J. Comput. Appl. Math.*, 172(1):153–168, 2004.

[2] A. Almendral. Numerical Valuation of American Options Under the CGMY Process. In: A. Kyprianou, W. Schoutens and P. Wilmott (Eds.): Exotic Option Pricing and Advanced Lévy Models. *John Wiley & Sons, Ltd.*, pages 154–198, 2005.

[3] K. Amin and J. Robert. Pricing Options on Risky Assets in a Stochastic Interest Rate Economy. *Mathematical Finance*, 2:217–237, 1992.

[4] D. Applebaum. Lévy Processes: From Probability to Finance and Quantum Groups. *Notices Amer. Math. Soc.*, 51(11):1336–1347, 2004.

[5] D. Applebaum. *Lévy Processes and Stochastic Calculus*. Cambridge University Press, Second edition, 2009.

[6] O.E. Barndorff-Nielsen. Normal Inverse Gaussian Distributions and Stochastic Volatility Models. *Research Report*, 300, 1995. Department of Theoretical Statistics, Aarhus University.

[7] O.E. Barndorff-Nielsen. Inverse Gaussian Distributions and Stochastic Volatility Modelling. *Scandinavian Journal of Statistics*, 24:1–13, 1997.

[8] O.E. Barndorff-Nielsen. Processes of Normal Inverse Gaussian Type. *Finance and Stochastics*, 2:41–68, 1998.

[9] E. Barndorff-Nielson, O.E.and Nicolata and N. Shephard. Some Recent Developments in Stochastic Volatility Modelling. *Quantitative Finance*, 2:11–23, 2002.

[10] O.E. Barndorff-Nielson and N. Shephard. Modelling by Lévy Processes for Financial Econometrics. In: O.E. Barndorff-Nielsen, T. Mikosch and S. Resnick (Eds.): Lévy Processes - Theory and Applications. *Birkhaáuser, Boston*, pages 283–318, 2000.

[11] O.E. Barndorff-Nielson and N. Shephard. Non-Gaussian Ornstein-Uhlenbeck-based Models and Some of Their Uses in Financial Economics. *Journal of the Royal Statistical Society, Series B*, 63:167–241, 2001.

[12] D. Bates. The Crash of 87: Was it expected? The Evidence from Option Markets. *Journal of Finance*, 46:1009–1044, 1991.

[13] D. Bates. Jumps and Stochastic Volatility: Exchange Rate Processes Implicit in Deutschemark Options. *Review of Financial Studies*, 9:69–108, 1996a.

[14] D. Bates. Post-87 Crash Fears in S&P 500 Futures Options. Working Paper, University of Iowa, 1996b.

[15] Z. Bing. A New Lévy Based Short-rate Model for the Fixed Income Market and its Estimation with Particle Filter. Thesis: University of Maryland, College Park, 2006.

[16] F. Black and M. Scholes. The Pricing of Options and Corporate Liabilities. *Journal of Political Economy*, 81(3):637–659, 1973.

[17] M. Broadie, P. Glasserman, and S.G. Kou. A Continuity Correction for Discrete Barrier Options. *Journal of Mathematical Finance*, 7(4):325–348, 1997.

[18] M. Brown. Least Squares Calibration. www.nezumi.demon.co.uk/consult/leastsq.htm, 1998.

[19] Y. Bu. Option Pricing Using Lévy Processes. Masterthesis, Chalmers University of Technology, Göteborg University Sweden, 2007.

[20] J. Bulla and I. Bulla. Stylized Facts of Financial Time Series and Hidden Semi-Markov Models. *Computational Statistics & Data Analysis*, 51(4):2192–2209, 2006.

[21] P. Carr. Two Extensions to Barrier Option Valuation. *Applied Mathematical Finance*, 2:173–209, 1995.

[22] P. Carr, E.C. Chang, and D.B. Madan. The Variance Gamma Process and Option Pricing. *European Finance Review*, 2:79–105, 1998.

[23] P. Carr, H. Geman, D.B. Madan, and M. Yor. The Fine Structure of Asset Returns: An Empirical Investigation. *Journal of Business*, 75(2):305–332, 2002.

[24] P. Carr, H. Geman, D.B. Madan, and M. Yor. Stochastic Volatility for Lévy Processes. *Journal of Mathematical Finance*, 13:345–382, 2003.

[25] P. Carr and D.B. Madan. Option Valuation Using the Fast Fourier Transform. *Journal of Computational Finance*, 2:61–73, 1998.

[26] K. Cheng. An Overview of Barrier Options. Global Derivatives Working Paper, 2003.

[27] R. Cont. Empirical Properties of Asset Returns: Stylized Facts and Statistical Issues. *Quantitative Finance*, 1:223–236, 2001.

[28] R. Cont and P. Tankov. Calibration of Jump-diffusion Option Pricing Models: A Robust Non-parametric. Centre de Mathematiques Appliquees, CNRS-Ecole Polytechnique, Palaiseau, France, 2002.

[29] R. Cont and P. Tankov. *Financial Modeling with Jumps Processes*. Chapman and Hall/CRC Press LLC, 2004.

[30] J. Cox, J. Ingersoll, and S. Ross. A Theory of the Term Structure of Interest Rates. *Econometrica*, 53:385–408, 1985.

[31] J. Cox and R. Stephen. The Valuation of Options for Alternative Stochastic Processes. *Journal of Financial Economics*, 3:145–166, 1976.

[32] S. David and Y.D. Christine. The Variance Gamma Distribution. http://cran.r-project.org/web/packages/VarianceGamma/VarianceGamma.pdf, 2010.

[33] NIST/SEMATECH e-book of Statistical Methods. Kolmogorov-Smirnov Goodness-of-Fit Test. Webpage: http://www.itl.nist.gov/div898/handbook/, 2010.

[34] E. Eberlein and K. Prause. The Generalized Hyperbolic Model: Financial Derivatives and Risk Measures. In *Mathematical Finance-Bachelier Congress, 2000 (Paris)*, pages 245–267. Springer, 2002.

[35] E.F Fama. The Behaviour of Stock-Market Prices. *Journal of Business*, 38(1):34–105, 1965.

[36] Filo Fiorani. Option Pricing Under the Variance Gamma Process. MPRA paper, University Library of Munich, Germany, 2004.

[37] H. Geman. Pure Jump Lévy Processes for Asset Price Modeling. *Journal of Banking & Finance*, 26:1297–1316, 2002.

[38] H. Geman, D.B. Madan, and M. Yor. Time Changes for Lévy Processes. *Mathematical Finance*, 11(1):79–96, 2001.

[39] P. Glasserman. *Monte Carlo Methods in Financial Engineering*. Springer, 2003.

[40] I.S. Gradshetyn and I.M. Ryzhink. *Tables of Integrals, Series and Products*. Academic Press, New York, Sixth edition, 1995.

[41] B.H. Hall. Notes on Generalized Method of Moments Estimation. http://www.nuffield.ox.ac.uk/users/hall/gmmnotes.pdf, 1996.

[42] L.P. Hansen. Large Sample Properties of Generalized Method of Moments Estimators. *Econometrica*, 50(4):1029–1054, 1982.

[43] V. Hatzivassiloglou. The Kolmogorov-Smirnov Test. Talk at University of Texas, Dallas.

[44] S. Heston. A Closed-form Solution for Options with Stochastic Volatility with Applications to Bond and Currency Options. *Review of Financial Studies*, 6:327–343, 1993.

[45] A. Hirsa, G. Courtadon, and D.B. Madan. The Effect of Model Risk on the Valuation of Barrier Options. *The Journal of Risk Finance*, 4(2):47 – 55, 2003.

[46] A. Hirsa and D.B. Madan. Pricing American Options Under Variance Gamma. *Journal of Computational Finance*, 7:63–80, 2004.

[47] J. Hull. *Options, Futures, and Other Derivatives*. Prentice Hall International, Inc., Sixth edition, 2006.

[48] J. Hull and W. Alan. The Pricing of Options with Stochastic Volatilities. *Journal of Finance*, 42:281–300, 1987.

[49] W.C. Hunter and D.W. Stowe. Path-dependent Options. In: R.W. Kolb: Practical Readings in Financial Derivatives. *Blackwell Publishers Inc.*, pages 30–80, 1998.

[50] H.T. Huynh, V.S. Lai, and I. Soumaré. *Stochastic Simulation and Applications in Finance with MATLAB Programs*. John Wiley & Sons, 2008.

[51] Myung I.J. Tutorial on Maximum Likelihood Estimation. *Journal of Mathematical Psychology*, 47:90–100, 2003.

[52] G.W. Imbens. Generalized Method of Moments and Empirical Likelihood. *Journal of Business and Economic Statistics*, 20:493–506, 2002.

[53] R.W. Iris, W. L. Justin, P. Wan, and A. Forsyth. Robust Numerical Valuation of European and American Options Under the CGMY Process, 2007.

[54] K. Itô. On Stochastic Processes 1 (Infinitely Divisible Laws of Probability). *Japan J. Math.*, 18:261–301, 1942.

[55] R. Jagannathan, G. Skoulakis, and Z. Wang. Generalized Method of Moments: Applications in Finance. *Journal of Business and Economic Statistics*, 20:470–481, 2002.

[56] T. Jaki. Kernel Density Based Parameter Estimation. Department of Mathematics and Statistics, Lancaster Univerisity, 2007.

[57] M. Jeanblanc, M. Yor, and M. Chesney. *Mathematical Methods for Financial Markets*. Springer-Verlag London Limited, 2009.

[58] A. John. R. A. Fisher and the Making of Maximum Likelihood 1912-1922. *Statistical Science*, 12:162–176, 1997.

[59] E. Jondeau, S. Poon, and M. Rockinger. *Financial Modeling Under Non-Gaussian Distribution*. Springer-Verlag London Limited, 2007.

[60] M. Krivoruchenko, E. Alessio, V. Frappietro, and L.J. Streckert. Modeling Stylized Facts for Financial Time Series. Quantitative Finance Papers, arXiv.org, 2004.

[61] P. Lévy. Sur les intégrales dont les éléments sont des variables aléatoires indépendantes. *Ann. Scuola Norm. Sup. Pisa*, 3.

[62] D.B. Madan. Purely Discontinuous Asset Price Processes. Working paper, Univeristy of Maryland, 1999.

[63] D.B. Madan and E. Seneta. The Variance Gamma (v.g.) Model for Share Market Returns. *Journal of Business*, 63(4):511–524, 1990.

[64] D.B. Madan and M. Yor. Cgmy and Meixner Subordinators are Absolutely Continuous with respect to One-sided Stable Subordinators. Prépublication du Laboratoire de Probabilités et Mod'eles Aléatoires, 2005.

[65] A.M. Matache and C. Schwab. Wavelet Galerkin Pricing of American Options on Lévy Driven Assets. *Quant. Finance*, 5:403–424, 2003.

[66] K. Matsuda. Inverse Gaussian Distribution. Department of Economics, The Graduate Center, The City University of New York, 2005.

[67] R. Merton. Theory of Rational Option Pricing. *Bell Journal of Economics*, 14:373–393, 1973.

[68] R. Merton. Option Pricing When the Underlying Stock Returns are Discontinuous. *Journal of Financial Economics*, 4:125–144, 1976.

[69] G.K. Mitov, S. Rachev, Y.S. Kim, and F.J. Fabozzi. Barrier Option Pricing by Branching Processes. *International Journal of Theoretical and Applied Finance*, 12(7):1055–1073, 2009.

[70] M. Nalholm and R. Poulsen. Static Hedging and Model Risk for Barrier Options. *Futures Markets*, 26:449–463, 2006.

[71] B. Otto. *Linear Algebra with Applications*. Upper Saddle River NJ Prentice Hall, Third edition, 1995.

[72] A. Papapantoleon. An Introduction to Lévy Processes with Applications in Finance. Lecture note: Universities of Piraeus and Athens, 2008.

[73] J. Poirot and P. Tankov. Monte Carlo Option Pricing for Tempered Stable (CGMY) Processes. *Asia Pacific Financial Markets*, 13:327–344, 2006.

[74] K. Prause. The Generalized Hyperbolic Model: Estimation, Financial Derivatives, and Risk Measures. PhD Thesis, Freiburg i. Br., 1999.

[75] E. Reiner and M. Rubinstein. Breaking Down the Barriers. *Risk*, 4:28–35, 1991.

[76] C. Ribeiro and N. Webber. Correcting for Simulation Bias in Monte Carlo Methods to Value Exotic Options in Models Driven by Lévy Processes. *Applied Math. Finance*, 13:333–352, 2006.

[77] J. Rosinki. Series Representations of Lévy Processes from the Perspective of Point Processes. In: O.E. Barndorff-nielsen, T. Mikosch and S.I. Resnick (Eds.): Lévy Processes - Theory and Application. *Birkhauser, Boston*, pages 401–415, 2001.

[78] J. Rosiński. Simulation of Lévy Processes. In: Encyclopedia of Statistics in Quality and Reliability. *Wiley*, 2008.

[79] T.H. Rydberg. The Normal Inverse Gaussian Lévy Process: Simulation and Approximation. *Stochastic Models*, 13:887 – 910, 1997.

[80] K. Sato. *Lévy Processes and Infinitely Divisible Distributions*. Cambridge University Press, Cambridge, 1999.

[81] W. Schoutens. *Lévy Processes in Finance*. John Wiley and Sons Ltd, 2003.

[82] W. Schoutens. Exotic Options Under Lévy Models: An Overview. *Journal of Computational and Applied Mathematics*, 189:526–538, 2006.

[83] W. Schoutens, E. Simons, and J. Tistaert. Model Risk for Exotic and Moment Derivatives. In: A. Kyprianou, W. Schoutens and P. Wilmott (Eds.): Exotic Option Pricing and Advanced Lévy Models. *John Wiley & Sons, Ltd.*, pages 67–98, 2005.

[84] W. Schoutens and S. Symens. The Pricing of Exotic Options by Monte Carlo Simulations in a Lévy Market with Stochastic Volatility. *International Journal for Theoretical and Applied Finance*, 6(8):839–864, 2002.

[85] W. Schoutens and J.L. Teugels. Lévy Processes, Polynomials and Martingales. *Commun. Statist.- Stochastic Models*, 14.

[86] L. Scott. Option Pricing when the Variance Changes Randomly: Theory, Estimators, and Applications. *Journal of Financial and Quantitative Analysis*, 22:419–438, 1987.

[87] L. Scott. Pricing Stock Options in a Jump-diffusion Model with Stochastic Volatility and Interest Rates: Application of Fourier inversion methods. *Mathematical Finance*, 7:413–424, 1997.

[88] B.W. Silverman. *Density Estimation for Statistics and Data Analysis*. Chapman and Hall, London, 1986.

[89] N.N. Taleb. *Dynamic Hedging: Managing Vanilla and Exotic Options*. John Wiley & Sons, Inc., 1997.

[90] B.A. Turlach. Bandwidth Selection in Kernel Density Estimation. In *A Review*. CORE and Institut de Statistique, 1993.

[91] Nick Webber and Claudia Ribeiro. A Monte Carlo Method for the Normal Inverse Gaussian Option Valuation Model Using an Inverse Gaussian Bridge. Computing in Economics and Finance 2003 5, Society for Computational Economics, 2003.

[92] F.D. Weert. *Exotic Options Trading*. John Wiley and Sons Ltd., 2008.

[93] P. Wilmott. *Derivatives: The Theory and Practice of Financial Engineering*. John Wiley and Sons, University edition, 1998.

[94] X. Wu. *Stochastic Volatility with Lévy Processes: Calibration and Pricing*. PhD thesis, University of Maryland, College Park, 2005.

[95] P.G. Zhang. *Exotic Options: A Guide to Second Generation Options*. World Scientific Publishing Co. Pty. Ltd., 1997.